

**MICRO- AND NANO- SCALE EXPERIMENTAL APPROACH TO
SURFACE ENGINEER METALS**

A Thesis

by

PRANAY ASTHANA

Submitted to the Office of Graduate Studies of
Texas A&M University
in partial fulfillment of the requirements for the degree of

MASTER OF SCIENCE

May 2006

Major Subject: Mechanical Engineering

**MICRO- AND NANO- SCALE EXPERIMENTAL APPROACH TO
SURFACE ENGINEER METALS**

A Thesis

by

PRANAY ASTHANA

Submitted to the Office of Graduate Studies of
Texas A&M University
in partial fulfillment of the requirements for the degree of

MASTER OF SCIENCE

Approved by:

Chair of Committee, Hong Liang
Committee Members, Terry Creasy
Richard Griffin
Andreas Holzenburg
Head of Department, Dennis O'Neal

May 2006

Major Subject: Mechanical Engineering

ABSTRACT

Micro- and Nano- Scale Experimental Approach to Surface Engineer Metals.

(May 2006)

Pranay Asthana, B.E., Osmania University, India

Chair of Advisory Committee: Dr. Hong Liang

This thesis includes two parts. The first part reviews the history and fundamentals of surface science and tribology. The second part presents the major research outcomes and contributions. This research explores the aspects of friction, wear, and surface modification for tribological augmentation of surfaces. An effort has been made to study these aspects through gaining insights by fundamental studies leading to specific practical applications in railroads. The basic idea was to surface engineer metals for enhanced surface properties. A micro- and nano- scale experimental approach has been used to achieve these objectives. Novel principles of nano technology are incorporated into the experiments. Friction has the potential to generate sufficient energy to cause surface reactions through high flash temperatures at the interface of two materials moving in relative motion. This allows surface modifications which can be tailored to be tribologically beneficial through a controlled process. The present work developed a novel methodology to generate a functional tribofilm that has combined properties of high hardness and high wear resistance. A novel methodology was implemented to distinguish sliding/rolling contact modes during experiments. Using this method, a super hard high-performance functional tribofilm with “regenerative”

properties was formed. The main instrument used in this research for laboratory experiments is a *tribometer*, using which friction, wear and phase transformation characteristics of railroad tribo-pairs have been experimentally studied. A variety of material characterization techniques have been used to study these characteristics at both micro and nano scale. Various characterization tools used include profilometer, scanning electron microscope, transmission electron microscope, atomic force microscope, X-ray diffractometer, nanoindenter, and X-ray photon spectroscope.

The regenerative tribofilms promise exciting applications in areas like gas turbines, automotive industry, compressors, and heavy industrial equipment. The outcome of this technology will be an economical and more productive utilization of resources, and a higher end performance.

DEDICATION

TO MY PARENTS, FRIENDS, & THE WONDERFUL AGGIELAND

ACKNOWLEDGEMENTS

First of all I would like to acknowledge Dr. Hong Liang for choosing to be my academic advisor and guiding me in my research pursuits at Texas A&M University. She has played an important role in advancing my technical and research skills by presenting many opportunities for career development. She has also supported my creativity by encouraging me to pursue multiple projects. I would also like to acknowledge all my committee members for having been co-operative all through my master's study. I would like to thank Dr. Holzenburg who taught me the fundamentals of microscopy which played an integral role in my research. Special thanks to Dr. Terry Creasy for letting me use his glove box needed for this project. The efforts of microscopists E. Ann Ellis, Dr. Zhiping Luo and Dr. Michael Pendleton are appreciated with regards to their valuable input in sample preparation techniques and general instrument operation of JEOL JSM 6400 SEM, JEOL JEM 2010 TEM and JEOL 1200 EX TEM. I acknowledge the Department of Mechanical Engineering, Material Characterization Facility, Microscopy and Imaging Center, the ECAE Laboratory, Surface and Interface Science Laboratory, Thin Film Materials Laboratory and the mechanical engineering machine shop of Texas A&M University for the generous use of the equipment at these facilities. I also thank Dr. Sudeep Ingole and Dr. Bo Ning for their support in my research. Constant support and encouragement from all my colleagues is appreciated.

The American Association of Railroads (AAR) and their research affiliate, Texas Transportation Institute (TTI), are appreciated for providing financial support for my research. I appreciate the Rocky Mountain Steels Company based in Colorado, for generously sending me rail samples and Griffin Inc. for sending the wheel samples. I am deeply indebted to all my course professors who have helped me gain the knowledge required to successfully carry out research at the master's level. Lastly, I want to thank my parents and family who have always been there to encourage and motivate me while I was away from them. The Aggieland has given me much more than just a quality education. Personally, coming here for studies has and will remain one of the best decisions of my life.

TABLE OF CONTENTS

	Page
ABSTRACT.....	iii
DEDICATION.....	v
ACKNOWLEDGEMENTS.....	vi
TABLE OF CONTENTS.....	viii
LIST OF FIGURES.....	xi
LIST OF TABLES.....	xiv
NOMENCLATURE.....	xv
 CHAPTER	
I INTRODUCTION TO SURFACE SCIENCE AND TRIBOLOGY.....	1
1.1. Definition.....	1
1.2. History and Background.....	2
1.3. Challenges in Tribology.....	12
1.4. Motivation of Research.....	14
II TOOLS OF TRIBOLOGY.....	16
2.1. Tribometer.....	16
2.2. Surface Characterization Techniques.....	19
2.2.1. Profilometry.....	22
2.2.2. Electron Microscopy.....	24
2.2.2.1. Scanning Electron Microscopy.....	24
2.2.2.2. Transmission Electron Microscopy.....	27
2.2.5. Atomic Force Microscopy.....	29
2.2.6. X-ray Photon Spectroscopy.....	31
2.2.7. X-ray Diffraction.....	33
2.2.8. Nanoindentation.....	36
III TRIBOLOGICAL PROBLEMS IN RAILROADS.....	38
3.1. Introduction.....	38

CHAPTER	Page
3.2. Problem Definition.....	40
3.3. Wear in Railroads.....	41
3.3.1. Wear Mechanisms of Railroad.....	41
3.4. Lubrication in Railroads.....	46
3.5. Proposed Solution.....	49
 IV REVIEW OF TRIBOFILMS.....	 51
4.1. Definition.....	51
4.2. Background.....	51
4.3. Tribofilm Generation and Mechanisms.....	52
4.4. Characterization of Tribofilms.....	55
4.5. Additive Chemistry.....	56
4.6. Summary.....	69
 V REGENERATIVE TRIBOFILMS.....	 70
5.1. Limitations of Pin-on-Disk Tribometer.....	70
5.2. Dynamic Wheel/Rail Contact Mode Simulator.....	70
5.3. Materials and Methods.....	73
5.3.1. Sample Preparation.....	73
5.3.2. Tribology Tests.....	74
5.3.2.1. Material Formulation.....	74
5.3.2.2. Sliding Test.....	75
5.3.2.3. Rolling Test.....	77
5.3.2.4. Scratch Test.....	79
5.4. Tribofilm Analysis.....	81
5.4.1. Surface Characterization.....	81
5.4.2. Mechanical Characterization.....	81
 VI RESULTS AND DISCUSSION.....	 82
6.1. Tribofilm Morphology.....	82
6.2. Frictional Behavior.....	88
6.3. Hardness of Tribofilm.....	89
6.4. Phase Transformation.....	90
6.5. Scratch Wear Resistance.....	91
6.6. Tribofilm Chemistry.....	92
6.7. Self Repairing Effects.....	101
6.8. Proposed Mechanism of Tribofilm Formation.....	102

CHAPTER	Page
6.8.1. Physical Mechanism.....	102
6.8.2. Chemical Mechanism.....	104
VII CONCLUSIONS AND FUTURE WORK.....	112
7.1. Conclusions.....	112
7.2. Future Work.....	113
REFERENCES.....	114
VITA.....	131

LIST OF FIGURES

FIGURE	Page
1. Classification of some important areas in Surface Science.....	8
2. Different test configurations. a) line contact b) point contact c) line contact d) circular flat contact e) point contact.....	17
3. Reciprocating module tribometer configuration.....	18
4. Different input signals used by the surface characterization tools.....	20
5. Dektak Profilometer at Materials Characterization Facility, Texas A&M University.....	23
6. Typical surface line profile on a rough sample.....	23
7. JEOL JSM 6400 Scanning Electron Microscope at Microscopy and Imaging Center, Texas A&M University.....	26
8. SEM image showing dry spores of <i>Bacillus subtilis</i>	27
9. JEOL JEM 6400 Transmission Electron Microscope at Microscopy and Imaging Center, Texas A&M University.....	28
10. TEM image of a crystalline boron particle showing lattice fringes.....	29
11. Nano-R™ Atomic Force Microscope (Pacific Nanotechnology Incorporated) at the Surface & Interface Science Lab, Texas A&M University.....	30
12. Working modes of the Atomic Force Microscope a) contact mode b) noncontact mode.....	31
13. Noncontact images of a polished pure Al surface. Topographic image (left) and phase image (right).....	31
14. Kratos Imaging X-ray Photoelectron Spectrometer at Materials Characterization Facility [39], Texas A&M University.....	33
15. XPS spectrum of the surface of steel rubbed with a vegetable oil based lubricant.....	33

FIGURE	Page
16. Bruker D8 Powder X-ray Diffractometer at X-ray Diffraction Laboratory, Department of Chemistry, Texas A&M University.....	35
17. X-ray spectrum of a steel surface showing distinct iron peaks at specific angles based on the crystal structure.....	35
18. Hysitron Nanoindenter at Materials Characterization Facility, Texas A&M University.....	37
19. Schematic of working principle of Nanoindenter.....	37
20. Nomenclature in railroads.....	39
21. Classification of rail road wear.....	40
22. Contact modes of a rail/wheel interface.....	42
23. Wear mechanisms of the rails.....	42
24. a) Surface wear: shelling, adhesive wear b) Flaking.....	44
25. a) Surface crack b) corrosion c) fatigue tache ovale d) fatigue failure.....	45
26. a) Undeformed rail b) Gage wear and plastic flow after service.....	45
27. Illustration of hypothesis depicting approach utilized in research.....	50
28. The rolling contact modification in the commercial pin-on-disc tribometer.....	71
29. Illustration of the modified sample holder assembly.....	72
30. Experimental contact modes showing lubricant application method.....	72
31. Schematic showing the locations in the rail from where the samples were cut.....	74
32. Tribometer illustration showing experimental conditions for the tribo-tests.....	77
33. Depiction of the micro scratch test.....	80

FIGURE	Page
34. Profilometer line scans: a) tribofilm formed at 25 °C ambient test temperature b) tribofilm formed at 100 °C ambient test temperature.....	83
35. Part of the rolling-sliding tribofilm shown contrasted against the substrate. Arrow shows the roll-slide direction of the wheel.....	84
36. Contact area region of the wheel showing distinct tribofilm formation.....	84
37. Wear scar of the sliding counter face ball showing abrasive grooves and transfer film remnants.....	85
38. Tribofilm morphology: a) 600 grit emery paper smoothed substrate b) sliding tribofilm at 100 °C c) rolling-sliding tribofilm at 60 °C.....	86
39. Sliding tribofilm produced during sliding at 25 °C.....	87
40. Etched cross-section showing film and substrate (left) and only the substrate (right).....	87
41. Layered tribofilm structure showing material build up and terrace features.....	88
42. Friction curve during the sliding test at 100 °C for 9 hours.....	89
43. Micro hardness along the cross-section of the film (under 30 mN load).....	90
44. Transmission Electron Micrograph of a fragment of the film showing small particles impregnated in the film. Inset shows selected area diffraction pattern on the film.....	91
45. Scratch test on the sliding (100 °C) wear track revealing the wear resistance of the film.....	92
46. Qualitative energy dispersive X-ray spectra of tribofilms a) sliding tribofilm (100 °C) b) rolling-sliding tribofilm (60 °C).....	93
47. XPS spectra plotted on a range of binding energies (1000 – 0 eV).....	97
48. Chemical area map of the sample cross-section showing self-repair.....	101
49. Physical mechanism model of tribofilm formation.....	103

LIST OF TABLES

TABLE	Page
1. Classification of some characterization techniques based on input/output signals	21
2. Lubricants vs. friction modifiers.....	48
3. Molecular structures of different additives.....	59
4. Classification of different acid and base species	63
5. Composition of samples in weight percent of individual elements.....	73
6. Interpretation of XPS data obtained for the tribofilm and the reference substrate.....	94

NOMENCLATURE

AFM	Atomic Force Microscopy
SPM	Scanning Probe Microscopy
SEM	Scanning Electron Microscopy
TEM	Transmission Electron Microscopy
STEM	Scanning Transmission Electron Microscopy
LEED	Low Energy Electron Diffraction
RHEED	Reflection High Energy Electron Diffraction
ILEED	Inelastic Low Energy Electron Diffraction
EELS	Electron Energy Loss Spectroscopy
LEELS	Low Energy Electron Energy Loss Spectroscopy
HREELS	High Resolution Electron Energy Loss Spectroscopy
REELS	Reflected Electron Energy Loss Spectroscopy
AES	Auger Electron Spectroscopy
CL	Cathodluminescence
CIS	Characteristic Isochromat Spectroscopy
APS	Appearance Potential Spectroscopy
SXAPS	Surface X-ray Appearance Potential Spectroscopy
XES	X-ray Emission Spectroscopy
SXES	Soft X-ray Emission Spectroscopy
EIID	Electron Impact Ion Desorption
EPSMS	Electron Probe Surface Mass Spectrometry

EID	Electron Induced Desorption
SDMM	Surface Desorption Molecule Microscopy
EDX	Electron Dispersive X-ray
WDX	Wavelength Dispersive X-ray
EPMA	Electron Probe X-ray MicroAnalysis
INS	Ion Neutralization Spectroscopy
IIR	Ion Infra Red
PIX	Photon Induced X-ray
TOF-SIMS	Time of Flight Secondary Ion Mass Spectroscopy
SIMS	Secondary Ion Mass Spectroscopy
ISS	Ion Scattering Spectroscopy
RBS	Rutherford Backscattering Spectrometry
UPS	Ultraviolet Photoelectron Spectroscopy
IR	Infra Red
ELL	Ellipsometry
OM	Optical Microscopy
RS	Reflective Spectroscopy
XPS (ESCA)	X-ray Photoelectron Spectroscopy (Electron Spectroscopy for Chemical Analysis)
XRD	X-ray Diffraction
SAXS	Small Angle X-ray Scattering
TXRF	Total Reflection X-ray Fluorescence

XAFS	X-Ray Absorption Fine Structure
SEXAFS	Surface Extended X-Ray Absorption Fine Structure
EXAFS	Extended X-Ray Absorption Fine Structure
NEXAFS	Near Edge X-ray Absorption Fine Structure
XANES	X-ray Absorption Near Edge Structure
ESR	Electron Spin Resonance
NMR	Solid State Nuclear Magnetic Resonance
FIM	Field Ion Microscopy
SPM	Scanning Probe Microscopy
TA	Thermal Absorption
TDS	Thermal Desorption Spectroscopy

CHAPTER I

INTRODUCTION TO SURFACE SCIENCE AND TRIBOLOGY

1.1. Definition

A *surface* can be described in simple terms to be the outermost layer of an entity. An *interface* can be defined to be the transition layer between two or more entities which differ either chemically or physically or in both aspects. J.B. Hudson in his book [1] defines a surface or interface to exist in any system which has a sudden change of system properties like density, crystal structure and orientation, chemical composition, and ferro- or para-magnetic ordering.

It is common knowledge now that any surface/interface can be examined closely using the high resolution microscopy and chemical characterization tools available. However it is wrongly assumed that this is the definition of surface science. It is wise to say that these tools have rather been built by humans to sate their innate curiosity of surface and interface interaction phenomena. They are now the arms and legs of surface science. In the author's perspective, the branch of science dealing with any type and any level of surface and interface interactions between two or more entities is called *Surface Science*. These interactions could be physical, chemical, electrical, mechanical, thermal, biological, geological, astronomical and maybe even emotional.

This thesis follows the style of Surface Science Reports.

Thus this field encompasses all other fields of science and everything related to the Universe. It in essence forms a basis for life. *Tribology* started out as the specific case of surface science dealing with mechanical interactions concerning mostly industrial applications. It is the study of surface phenomena of moving and interacting bodies in relative motion. It has now come to include physical and chemical interactions with those aspects widely recognized as *tribophysics* and *tribochemistry* respectively, and which are now in themselves full fledged sciences.

1.2. History and Background

It is said that one cannot appreciate the beauty of a science without proper reference to its history and epic efforts of earlier people. An effort is made in this chapter to give the reader an overall idea of the origin and scope of the field of surface science. Surface interaction phenomena have growing importance in a multitude of engineering and biological situations. As a result there are a number of sources of literature that contribute to our knowledge in this vast area of surface science [2]. The birth of surface science could perhaps be attributed to the first few moments of the Big Bang with all the complex surface interactions following the birth of the Universe. Scientific studies of different surfaces date back to the early days of physics and chemistry. Independent work in both these areas of science created two specialized fields within surface science called *surface physics* and *surface chemistry* respectively. Much later, *biological surface science* was explored. Surfaces are integral in medicine and biology as most biological reactions occur at the surfaces and interfaces [3]. However, the gap between all these

fields has bridged in the past few decades with science foraying into studies at the atomistic scale which seems to present an ultimate culmination point for all sciences.

Perhaps the earliest known documented record of observations of surface physical phenomena are the inscriptions of the Babylonian cuneiform dating back to the time of Hammurabi (1758 B.C) which talk about a certain practice called *Babylonian Lecanomancy* [4] dealing with prophesies based on oil spreading on water. Caius Plinius Secundus, also known as Pliny the Elder (Roman Officer and Encyclopedist AD 23-79) had first mentioned in his encyclopedic work, *Natural History*, his observations about how oil smoothed the rough sea waters [5,6]. Manuscripts like *De Proprietatibus Rerum* (The Properties of Things) written by Franciscan Bartholomeus Anglicus dated 1250 A.D outline the importance of surfaces by describing surface preparation techniques to achieve metal-metal bonding [7]. Plinys' idea on oil water interaction was investigated by the great Benjamin Franklin (1706-1790) during one of his visits to London, England. He used a simple bamboo cane with a hollow top for storing oil as his experimental apparatus. He aptly credited Pliny for his discovery thus starting the respectful tradition of giving credit to honorable people of original research. An extract from one of Franklins' original letters [8] talking about his experiments with oil and water is stated below:

At length being at Clapham, where there is on the common a large pond which I observed one day to be very rough with the wind, I fetched out a cruet of oil and dropped a little of it on the water. I saw it spread

itself with surprising swiftness upon the surface; but the effect of smoothing the waves was not produced; for I had applied it first on the leeward side of the pond where the waves were greatest; and the wind drove my oil back upon the shore. I then went to the windward side where they began to form; and there the oil, though not more than a teaspoonful, produced an instant calm over a space several yards square which spread amazingly and extended itself gradually till it reached the lee side, making all that quarter of the pond, perhaps half an acre, as smooth as a looking glass.

It is now known that the oil actually spreads out on water to the extent that a single uniform molecular layer is left. A century later, it was Lord Rayleigh (Nobel laureate in Physics, 1904) and Agnes Pockels (a German *hausfrau*) who investigated the surface properties of water. Infact Agnes Pockels discovered surface tension while doing experiments in her kitchen sink. She developed the apparatus for making measurements on surface films and some of her methods are still used as standard techniques. In her recognition, the minimum area occupied by a monolayer film is called *Pockels point*. Her work was recognized by Lord Rayleigh who helped her publish her first ever research in *Nature* in 1891 [9]. She followed this up a number of publications through 1936, the citations of which can be found in the reference [10].

First knowledge about membranes, which are so critical to biology, interestingly came through the study of lipids, chemistry, and interactions of oils with water pioneered

by the above people. At about the same time as Lord Rayleighs' experiments with oil films, it was Charles Ernest Overton (1865-1933) who when working on his doctoral degree in Botany (1889) at the University of Zurich, discovered important properties of cell membranes and their similarities with lipids [11,12]. The concept of membrane permeability and osmosis is a classic case of biological surface and interface interactions. Infact, biomedical surface science has emerged as one of the fastest thriving areas in the modern times.

One of the key concepts in surface science is adsorption in gas-liquid, liquid-solid and gas-solid systems. Although the study of adsorption dates back to ancient times, the first quantitative observations were reported by Scheele [13] and Fontana [14] in independent studies. First Systematic efforts in this field were carried out in the early 19th century by Saussure [15]. An excellent review dealing with interactions due to adsorption and its historical perspective can be found in the reference [16].

In 1833 Michael Faraday was curious about a phenomenon observed by Dobereiner (1780-1849) a decade earlier. He observed that in the presence of platinum, the reaction between hydrogen and oxygen occurred far below their combustion temperature [17]. His astonishing insight into this mechanism of reaction at surfaces led him to put forth a theory on catalytic action (a name given by Berzelius in 1836) based on his experiments and it remains valid to this day. This was the first noteworthy event for the future of surface science, specifically surface chemistry. Two other key events central to the development of surface science were as follows: In 1874, Karl Ferdinand Braun (Nobel Laureate in Physics, 1909) discovered a phenomenon now called

rectification which solved one of the greatest problems for wireless technology [18]. In 1877, J. William Gibbs laid down the mathematical foundations for statistical mechanics and thermodynamics. In this effort he completely described the thermodynamics of surface phases [19,20].

Then came Irving Langmuir (Nobel Laureate in Chemistry, 1932) who made major contributions in knowledge of surface phenomena and whose stupendous efforts led to the recognition of surface science as a significant research field [21]. He developed the first quantitative theory of adsorption in 1915 and also did research on oil films, lipids, biofilms and molecular mono layers while working in the laboratories of General Electric at Schenectady, N.Y [12]. He also carried out fundamental research on work function of metals and came out with a detailed model on thermionic emission [21]. A comprehensive collection of his multidisciplinary research pursuits is found in the classic historical reference [22].

Surface physics was in a nascent stage since the discovery of the electron and the atom, and it wasn't until the 1960's that surface physics actually progressed to be an independent field. This was made possible by the ultra-high vacuum technology, newly developed sophisticated surface analysis tools and digital age computers which allowed for comparisons of actual theoretical calculations with available reliable experimental data [21].

Earlier events that had a direct impact on surface physics development were the work on thermionic emission by Irving Langmuir, the explanation of photoelectric effect by Albert Einstein (Nobel Laureate in Physics, 1921) and the confirmation of the De Broglies' assertion of wave nature of quantum mechanical particles through electron diffraction by Clinton Davisson and Lester Germer [21]. Davisson shared the Nobel Prize for Physics in 1937 with G.P. Thompson. The next two decades produced intensive theoretical research in this field.

The invention of the transistor in 1947 marked a milestone in the lineage of surface physics. Reckoning work in solid state physics and semiconductors picked up pace after the war and since then surface physics has been moving along at a steady pace with new theories being put forward and contributions from several rewarding researchers. The study of surface science received a big thrust with the invention of newer and more powerful surface characterization tools in the mid 20th century which allowed for both sophisticated physical and chemical analyses. A classification of some of the important areas in the different fields of surface science is shown as an illustration in Figure 1.

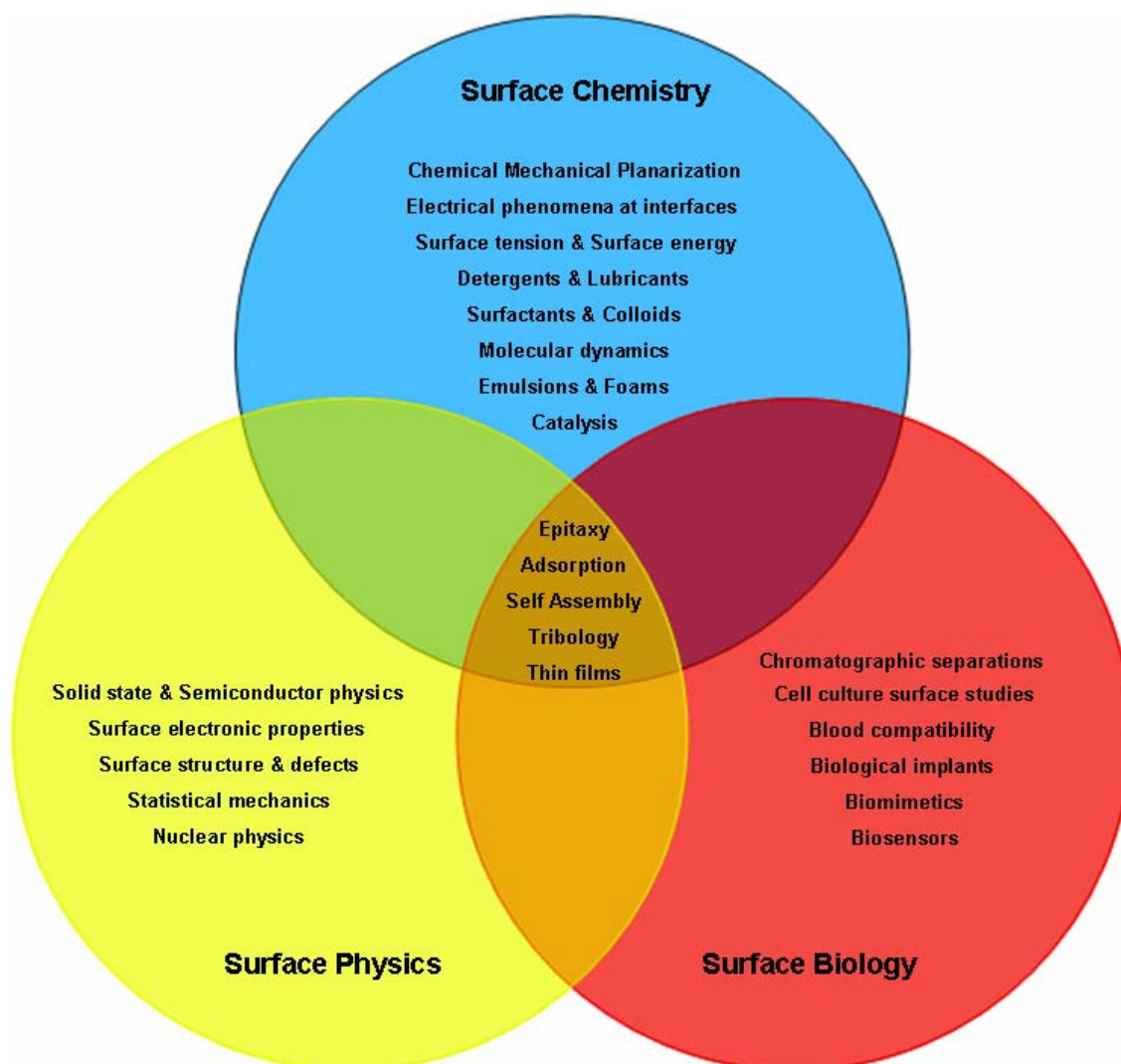


Figure 1: Classification of some important areas in Surface Science

Tribology has an interesting tale to tell about its own remarkable history. The mechanical manifestations of surface interactions like friction and wear have been known in some form right from pre-history. These attributes along with the study of lubricants and lubrication theory, additives, and bearings form the core of Tribology [23]. This science has attained a great deal of technological and economical importance

very quickly due to its deep focus on industrial and day to day device applications. The word Tribology is derived from the Greek root “*tribos*” which means rubbing and “*logos*” which means to study. The word was coined in the late 1960’s by the Jost report [24] which advised the then British government to look into the severe economic loss caused due to the mechanical surface interactions.

Tribology has much longer roots longer than what meets the eye. Evidence suggests that the Stone Age which covered a period of about a million years had early man taking interest in devices which required plain bearings. His requirement of tools for various purposes instinctively involved Tribology. There are reports of stone and wooden door sockets, boring tools and hand held bearings on drill spindles being developed in this age. The six earliest civilizations of the world located in Mesopotamia, Egypt, India, China, Central America and South America each had significant tribological contributions to make to the world. Among the more important ones are the potter’s wheel, simple bearings, drill tools, wheeled vehicles, use of lubricants (water, bitumen, vegetable and animal based oils), sledges, metals and porcelain. The advantages of rolling over sliding were recognized in the Greek and Roman period with the development of rolling-element bearings and other developments of machinery around the world. Though the tribological development during the middle ages was slow, the importance of combating wear was recognized as evidenced by the use of hard pebbles in carts and ploughs in the later period of this era. Scientific recognition of Tribology emerged in the Renaissance period which had geniuses like Leonardo da Vinci, who made significant contributions in studies of friction, wear, bearing elements,

rolling-element bearings, plain bearings, lubrication, gears, and screw-jacks to name a few. There were many other notable contributions by people in this period which truly set the stage for steady development of Tribology in the time to follow. The 17th and 18th centuries and the Industrial Revolution saw progress in this field leading to the current knowledge that we have in this widely explored but still largely unfathomed field. [23]

It is interesting to note the historical applications of friction in the flow of time. Friction is perhaps the oldest phenomenon that presented utility to man. The first applications of friction date back to the prehistoric times, the first being lighting a fire through frictional rubbing and the second, in easing transportation of heavy goods by developing rollers, wheels and sleds about three millennia ago through an understanding of frictional phenomena [2]. As noted earlier, the scientific study of friction perhaps was started by Italian genius Leonardo da Vinci (1452-1519) who had an astonishing curiosity and foresight in both science and art alike. The two basic tenets of friction that the resistance offered by friction is directly proportional to load and that it is independent of the area of sliding have been long known and were experimentally verified by Leonardo da Vinci in the 15th century [25]. French engineer Guillaume Amontons [26] restated these laws in 1699 followed by Charles Augustin Coulomb, who verified the laws in 1781. Coulomb demarcated static friction from kinetic friction and published his work in 1785 [27]. This was followed by friction studies of Morin during the early 1830's [28]. It must also be recalled that Leonhard Euler (1707-1783), a great mathematician, had important contributions to the mathematical formulations of friction which he reported through his three landmark papers [29-31]. The analytical

approach to friction and the well-known symbol μ used to represent coefficient of friction are his gifts to this field.

These early efforts essentially described friction in terms of what is called the “roughness hypothesis” which states that friction is due to tangential resistance offered by the interlocking of the asperities and protuberances of the two surfaces in relative motion. This was sufficient to support the experimental observations that frictional force is proportional to the load and independent of the area of contact [2]. However, work by the Hardy duo [32] and Tomlinson [33] bolstered the “adhesion hypothesis” which presented a better model of friction as shown later by Holm [34], Ernst and Merchant [35], and Bowden and Tabor [25]. This hypothesis was based on the premise that friction is a result of adhesive forces between the contact surfaces. This approach could also explain the variable frictional behavior on contaminated surfaces.

The shearing, deformation and plucking away of the metallic junctions formed by adhesion and welding together of surface asperities constitute surface damage recognized as *physical wear* of materials [25]. A generally accepted broad classification of wear is as follows: adhesive, abrasive, erosive, corrosive delamination, surface fatigue, fretting, and three body wear [2]. Detailed history and theories of friction, adhesion and wear can be found in the references [2,23]. An experimental study of the physical and chemical processes during frictional sliding, lubrication and wear phenomena is found in the famous book by Bowden and Tabor [25] which is a must-read for all tribologists. However, it was John Frederick Archard (1918-1989) who pursued study of wear and lubrication enthusiastically in the 1950's and 1960's. His work

advanced the modeling of adhesive wear and he developed the famous “Archard wear law” [23]. It should be pointed out here that the development of the hydrodynamic theory by Osborne Reynolds [36] in 1886 set the pace for the future of lubrication research. Further developments like the elastohydrodynamic theory (EHL), which is one of the tribological milestones of the 20th century spurred extensive studies in bearings and gear lubrication. Another area of development in surface science was surface coatings technology with the advent of advanced deposition coating methods like Chemical Vapor Deposition (CVD) and Physical Vapor Deposition (PVD) in the later part of the century [37].

1.3. Challenges in Tribology

Surface science is a truly multi-disciplinary field and offers integration of knowledge in all sciences in its research pursuits. The industrial relevance of the area called tribology has motivated enthusiastic research in many practical and real life applications. A fundamental understanding of friction, wear, and lubrication has yet to satisfy the needs of technology development. Interesting issues are, for example, the changing material properties during friction; strengthening of engineering materials and surfaces; new methodology of modifying surfaces; and innovative methods to protect, repair, and maintain engineering surfaces. Obtaining understanding of fundamental aspects of friction and wear and developing new methods for surface engineering and materials protection have significant impacts on surface science and tribology. The importance of improving surfaces of materials cannot be underestimated as major issues

related to surface from a practical application point of view remain unexplored. Issues such as failure of machinery and wear of transportation systems such as railroads are some reckoning problems. There is a need for high performance coatings, economical methods of producing such coatings, as well as fundamental understanding in tribosystems, tribochemical interactions and surface properties, etc. Recent development has lead the tribological research toward environment friendly and more energy efficient approaches while striving for higher reliability and consumer satisfaction. New emerging areas like biotribology and micro and nano tribology for MEMS and NEMS devices have attracted great attention. The study of lubricants will press for more biofriendly and biodegradable formulations. The limited oil resources of the world call for extended research in self-lubricated and controlled friction devices. Tribology in extreme environments will become important as the demand for performance increases in industry. Tribology of space components is an interesting and challenging field for the future. Study of friction and wear at the atomic scale can reveal the underlying cause for these basic phenomena. A few of industrially important but neglected areas of tribology are the study of friction and wear in railroads, grease lubrication and seals [37]. Friction induced phase transformation and nanostructures are an attractive area in surface engineering. A holistic approach in formulating methods to determine reliability and better predict the lifetime of machines and products is imminent. This would require synergistic expert systems and condition monitoring in tribology. On an ending note, perhaps a unified theory on friction, wear and lubrication will allow for enhanced and efficient assimilation of the current fragmental knowledge in the field [37].

1.4. Motivation of Research

There are two major objectives in this research. One is to obtain basic understanding in fundamental effects of friction on material properties. The second is to develop a novel methodology to engineer material surfaces to suit the relevant tribological application. This research uses experimental approaches to investigate tribological behavior of metallic materials leading to a novel technology to surface engineer railroads for tribological augmentation.

A fundamental study of friction and wear in different materials was undertaken leading to a basic understanding of these surface phenomena. This knowledge was combined with lubrication theory and applied to known tribological problems in railroads. Tribological problems in the railroad industry are significant in terms of the amount of annual loss incurred due to wear alone around the world. The cost of repair and replacement runs into several billions of dollars in the United States alone. A one percent reduction in the overall wear can result in the saving of a few billion dollars. There has been some notable work to improve the wear resistance through metallurgical improvement of the rail steels. However, with increasing axle loads and user demand, this approach has now reached its limit and no longer offers a feasible solution. Now the focus has changed to improve the lubrication systems used in the industry with an effort to reduce wear. Another approach explored has been the use surface coatings. The rail industry offers an open ended challenge to any tribologist.

A new approach of producing a wear resistant tribofilm coating during normal operation of the trains using nanotechnology has been explored in this research. This

technology is derived from a synergistic combination of fundamental principles of energy at the nano-scale and lubricant chemistry, externally stimulated by mechanical activation.

CHAPTER II

TOOLS OF TRIBOLOGY

2.1. Tribometer

The tribometer is an instrument which is widely used to study the friction and wear of different materials. Friction and wear has been a subject of study since the early human times. However the first quantitative work in friction is widely attributed to Leonardo da Vinci in the 15th century as discussed in the last chapter. Scientific studies of wear though had little development until the mid 20th century. The tribometer is basically a machine which enables two materials surfaces to move in relative motion to each other in different contact modes. Parameters like normal load, speed of motion, temperature, pressure etc. can be controlled to simulate the real wear processes of industrial machinery parts or any other application involving a tribological pair. One of the first reported wear testing machines was developed by Mr. Charles Hatchett [38] during the reign of King George III (1760-1820) of the United Kingdom. The King had commissioned two fellows of the Royal Society, Mr. Charles Hatchet and Mr. Henry Cavendish in February 1798 to inquire into the considerable loss which the state gold coins seem to have sustained by wear within a certain period. This reciprocating wear-testing machine was remarkable in that it was designed to have a continuous change of rubbing direction to avoid the formation of wear grooves in a particular place which would accelerate the wear in the coins [23]. Thus the wear data would be more representative and practicable. Ironically, most modern tribometers have ignored this

important design aspect and have wear tracks running over the same wear path repeatedly as will be seen further in this section.

Various contact mode configurations have been devised to simulate the different tribological pairs occurring in life. Some of the important configurations are illustrated in Figure 2. All these basic tribo pairs enable a point, line or flat contact at the interface between the two test surfaces (as per ASTM standards).

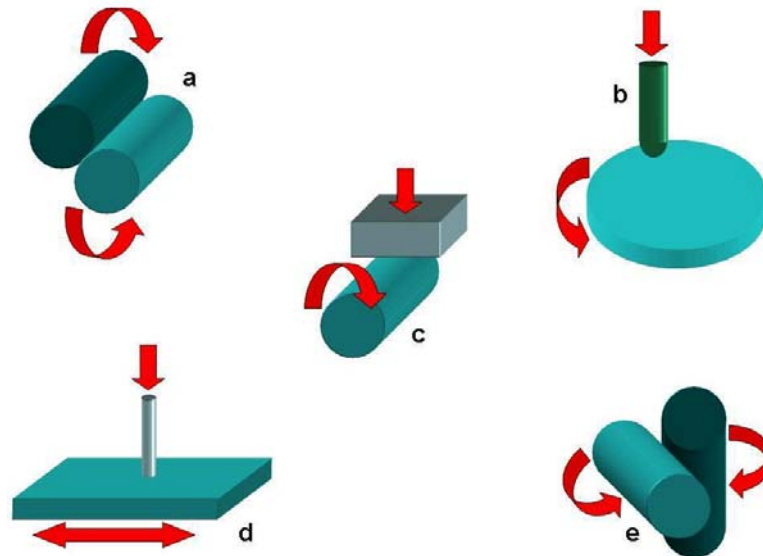


Figure 2: Different test configurations. a) line contact b) point contact c) line contact d) circular flat contact e) point contact

Figure 3 shows a modern day commercial reciprocating pin-on-disc configuration tribometer. Here a flat sample is moved across the counter face slider (static friction partner or tribometer pin) by means of a linear reciprocating stage. The

sample and the counter face can be made of same or different materials as per the test specifications. A desired normal load is applied over the tribometer pin and the linear speed of the reciprocating stage can be controlled. The tribometer arm measures the tangential force (friction force) through the lateral movement when the sample is reciprocating against the counter face. The sensors transmit the force signal to the controller. The controller directly presents the output data on a computer screen as a plot of coefficient of friction versus time. The experiment can be performed in a controlled environment (specific temperature, vacuum etc.) using specially designed sealing chambers and heating stage accessories. Other types of relative motion (e.g. circular) between the sample and the counter face (contact partner) can be achieved by replacing the reciprocating stage with a rotating cup mounted on the cam shaft.

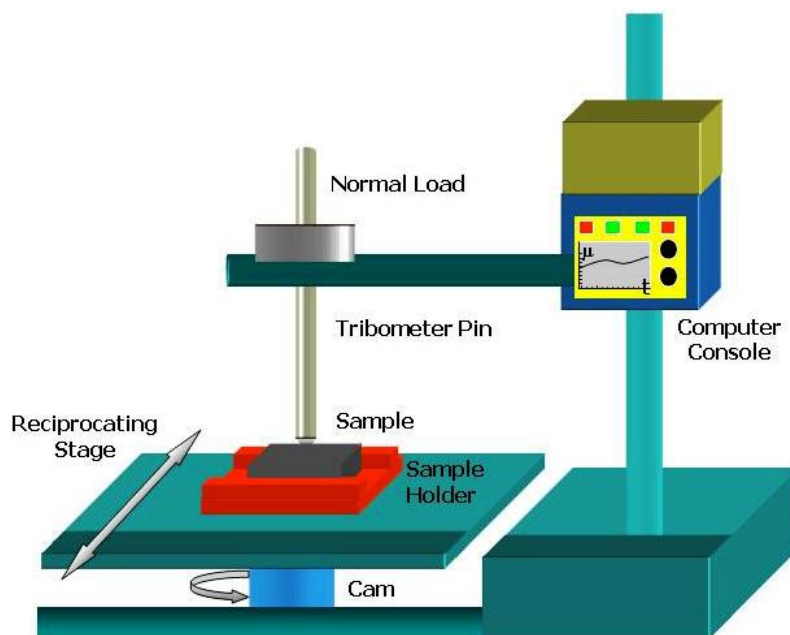


Figure 3: Reciprocating module Tribometer configuration

2.2. Surface Characterization Techniques

There is a need for surface analysis both before and after conducting tribometer experiments to understand mechanisms of the tribological process. Various sophisticated surface characterization tools are available today to study the details of the surface like morphology, surface parameters, and surface physical and chemical properties. The underlying general principle of most such instruments is stimulus of a sample surface by means of a source signal and analysis of the resultant signal generated from the sample. Bombarding a surface with high energy particles or providing an energy stimulus by different means results in emission of different type of particles from the surface. Different tools use a combination of one or more of these output signals to derive meaningful data. Figure 4 shows an illustration of different input signals. Table 1 summarizes typical input/output signals and the instruments that use these signals (Acronyms are expanded in Nomenclature). A few such important surface tools extensively used by the author in his research are briefly discussed below.

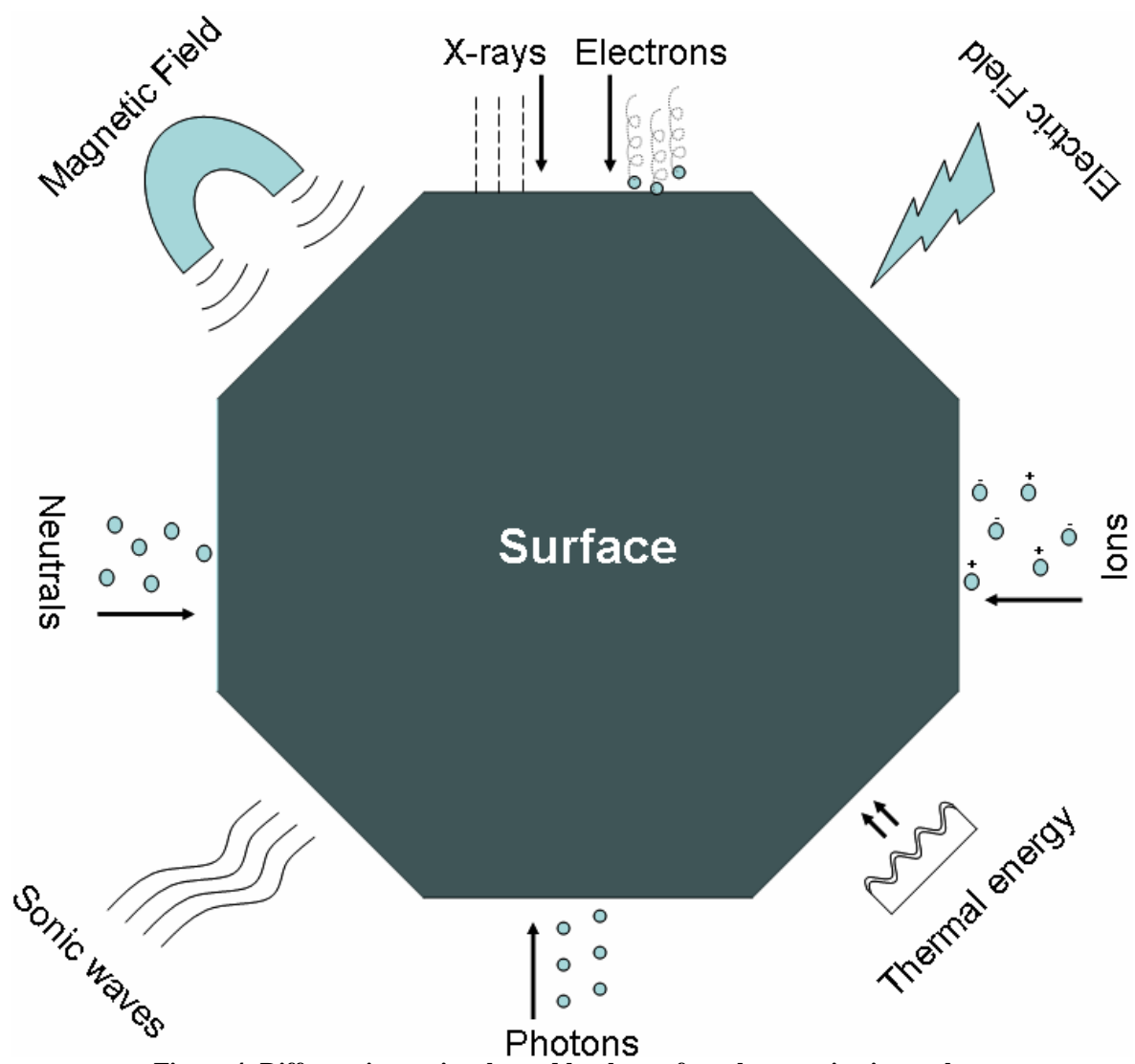


Figure 4: Different input signals used by the surface characterization tools

Table 1: Classification of some characterization techniques based on input/output signals

Input Signal	Output Signal	Characterization Technique
Electrons	Electrons	LEED RHEED ILEED EELS REELS HREELS STEM TEM SEM AES
	Photons	CL CIS APS SXAPS XES SXES
	Ions	EIID EPSMS
	Neutrals	EID SDMM
	X-rays	EDX WDX EPMA
Ions	Electrons	INS
	Photons	IIR PIX
	Ions	TOF-SIMS SIMS ISS RBS
	Neutrals	Sputtering
Photons	Electrons	UPS
	Photons	IR ELL OM RS
	Neutrals	Photo Desorption

(Table 1 continued)

Input Signal	Output Signal	Characterization Technique
X-rays	Electrons	XPS (ESCA)
	X-rays	XRD SAXS TXRF XAFS EXAFS SEXAFS NEXAFS XANES
Magnetic field	Electromagnetic wave	ESR NMR
Neutral + Electric field	Ion	FIM
Electric field	Tunneling current	SPM
Thermal energy	Heat dissipation	TA
	Desorbed atoms and molecules	TDS

2.2.1. Profilometry

The profilometer is an instrument which maps a sample surface morphology. There are two types: contact mode and non-contact mode. The contact mode tip has a very sensitive probe which is traversed slowly along a surface. The probe is generally made of a hard material like diamond and is somewhat rounded at the tip. The movement of this tip in the lateral and vertical directions is monitored by a controller which transmits the output signal to a computer. The screen displays a line profile of the traversed path. The sensitivity of this instrument is a few microns depending on the radius of the probe. The profilometer also measures the roughness and waviness parameters of the surface using one of the standard methods available. Figure 5 shows a

modern day contact mode profilometer. An illustration of the typical output from a profilometer is shown in Figure 6.



Figure 5: Dektet Profilometer at Materials Characterization Facility [39], Texas A&M University

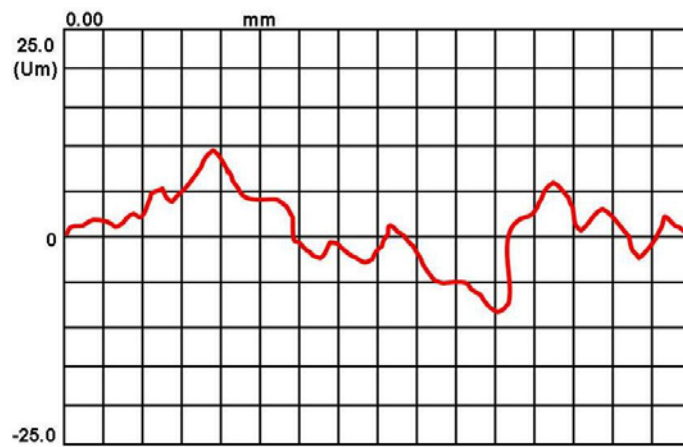


Figure 6: Typical surface line profile on a rough sample

2.2.2. Electron Microscopy

After the discovery of the electron by J.J. Thompson in 1897, it was Debroglie [40] who in 1929 proved that electrons have properties of waves. Busch [41] first demonstrated that the path of electrons can be deflected by magnetic lenses just like light could be deflected by an optical lens. This discovery eventually led to the invention of the electron microscopes in early 1930's. The Scanning Electron Microscope (SEM) and the Transmission Electron Microscope (TEM) are two classes of the electron microscope. These microscopes take advantage of the much shorter wavelength of the electrons when compared to light which is used in light microscopy. This results in a much higher magnification and improved resolution making it possible to view the molecular structure. Chemical investigation is possible in these microscopes using techniques like Electron Dispersive Spectrometry (EDS), Wavelength Dispersive Spectrometry (WDS), Electron energy Loss Spectroscopy (EELS) and Electron diffraction. The TEM and SEM complement each other very well with the information that can be derived from analysis of a sample. Both these microscopes are now used for research in almost all fields of science.

2.2.2.1. Scanning Electron Microscopy

The Scanning Electron Microscope (SEM) is one of the most powerful and versatile present day material characterization tools available. It is applied to study a wide range of materials including metals, non-metals, semiconductors and biological specimens. The capabilities of the SEM and its variants extend from high resolution topographic imaging to both qualitative and quantitative chemical analysis. The three

dimensional feel of an SEM image has opened up new possibilities in the field of microscopy. The SEM provides a fast and easy way of analyzing a given sample with its relatively simple sample preparation techniques when compared to the TEM. The earliest reported work describing the theoretical feasibility of an SEM was in 1927 by H. Stintzing who later filed a German patent in 1929 [42]. The first scanned electron image was produced by Max Knoll in 1935 [43]. However the potential of the SEM remained dormant due to the parallel rapid development of the Transmission Electron Microscope (TEM). It wasn't until 1942 when the first SEM used to study thick specimens was described by Zworykin et. al. [44]. In the next few years, C.W. Oatley and his student D. McMullan developed their first SEM with a resolution of 50 nm [45]. Subsequently, crucial work by many others [46-51] over the years has improved the capabilities of the microscope to the most current configuration. The first SEM's were commercialized in the mid 1960's. A lateral resolution of 1-5 nm and a depth resolution of 1-10 nm have been achieved in the modern SEM [52]. In the SEM, a finely focused electron beam is rastered across the surface of the specimen to form images using electron detectors and cathode ray tubes. The two major imaging modes of the SEM use secondary electrons and the backscattered electrons respectively as input signals. For the purpose of chemical characterization using X-ray analysis (EDS), the beam can be maintained static to do point analysis. In the modern day SEM, the electron beam can be rastered during chemical analysis to generate chemical area maps of the specimen. This is often a very useful tool in material, biological and forensic sciences. For a detailed review on the history and working of SEM, please refer to [52,53]. An illustration of the SEM is

shown in Figure 7. A typical scanning electron micrograph is shown in Figure 8. The depth of field or vertical resolution is clear in this picture which shows a stack of spores of *Bacillus subtilis*.



Figure 7: JEOL JSM 6400 Scanning Electron Microscope at Microscopy and Imaging Center [54], Texas A&M University

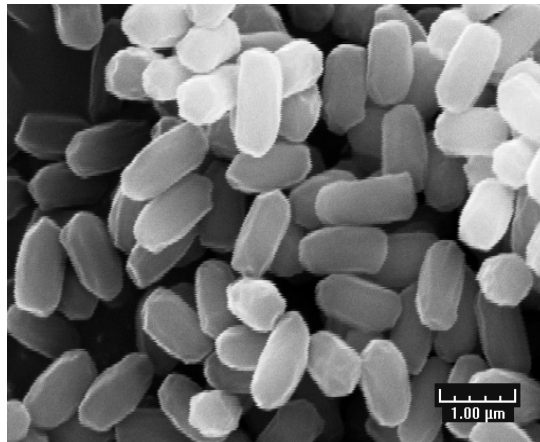


Figure 8: SEM image showing dry spores of *Bacillus subtilis*

2.2.2.2. Transmission Electron Microscopy

The Transmission Electron Microscope (TEM) was the first type of electron microscope to be introduced in 1932 by the work of Knoll and Ruska in Germany [55]. The SEM development by the creators of TEM followed shortly. During the early period of electron microscopy, the efforts of developing the TEM far exceeded the ones for SEM with the TEM's being commercially available as early as 1940's. The TEM has a much higher resolution than the SEM. Typical resolution of the modern TEM is $< 2 \text{ \AA}$. The best resolution achieved so far is 0.6 \AA . The TEM for the first time presented the biologists with a view of the cell structure and the very macromolecules that made up the cells. The materials scientists could perceive the atomic structure and crystal lattice using high resolution transmission electron microscopy (HRTEM) and electron diffraction. However the specimen preparation techniques for TEM are quite tedious and time consuming. The TEM is fundamentally different from the SEM in its operation.

Both imaging and chemical characterization of the specimen can be done in the TEM. The TEM projects electrons through a very thin slice of specimen onto a phosphorescent screen creating a two dimensional image. The image has bright and dark areas which are proportional to the number of electrons that are transmitted through different density areas of the specimen. Elemental characterization is possible by analyzing the X-rays generated by the specimen (EDS) and EELS. The TEM is a very useful analytical tool and can give accurate quantitative results. Modifications of the TEM have produced the scanning transmission electron microscope (STEM) which combines the features of the SEM and TEM. Further information on the development and operation of the TEM can be found in reference [56]. An illustration of the TEM is shown in Figure 9. A typical TEM image is shown in Figure 10. This picture shows the lattice fringes of a crystalline boron particle against the background of amorphous carbon.



Figure 9: JEOL JEM 6400 Transmission Electron Microscope at Microscopy and Imaging Center [54], Texas A&M University

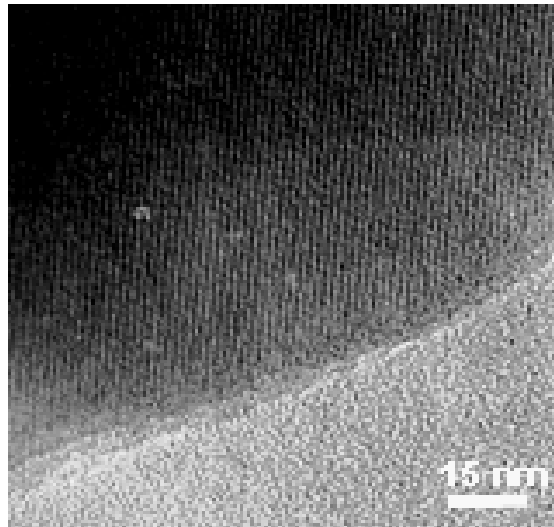


Figure 10: TEM image of a crystalline boron particle showing lattice fringes

2.2.3. Atomic Force Microscopy

The field of Nanotechnology took a dramatic turn with the introduction of the Atomic Force Microscope (AFM) in 1986. This invention was pioneered by G. Binnig and C. F. Quate [57] who built the AFM based on the underlying principles of Scanning Tunneling Microscope (STM) and the stylus profilometer. Using an AFM, one can create a highly magnified three dimensional surface topographic map of a specimen. It is possible to measure surface features with dimensions of the order of a few nanometers through a magnification of up to 1,000,000x [58]. The AFM works by raster scanning an atomically sharp probe on a surface to map the morphology. The probe is usually grown out of single crystal silicon. This probe is mounted on a cantilever which deflects an incident laser beam on to a photo detector based on the movement of the probe. The

physical interaction of the probe with the surface enables measurement of surface properties like friction, phase difference, adhesion force and hardness. Figure 11 shows a commercial AFM. The scanning can be done in two modes namely the contact mode and the noncontact mode respectively. An illustration of the two modes is shown in Figure 12. In contact mode, the tip follows the surface profile while in noncontact mode, the change in the vibration amplitude or phase of the cantilever is monitored. Both modes give a topographic image of the surface. The phase difference is measured in noncontact mode and the friction behavior is monitored in contact mode scanning. Typical noncontact mode topographic and phase images are shown in Figure 13.



Figure 11: Nano-R™ Atomic Force Microscope (Pacific Nanotechnology Incorporated) at the Surface & Interface Science Lab, Texas A&M University

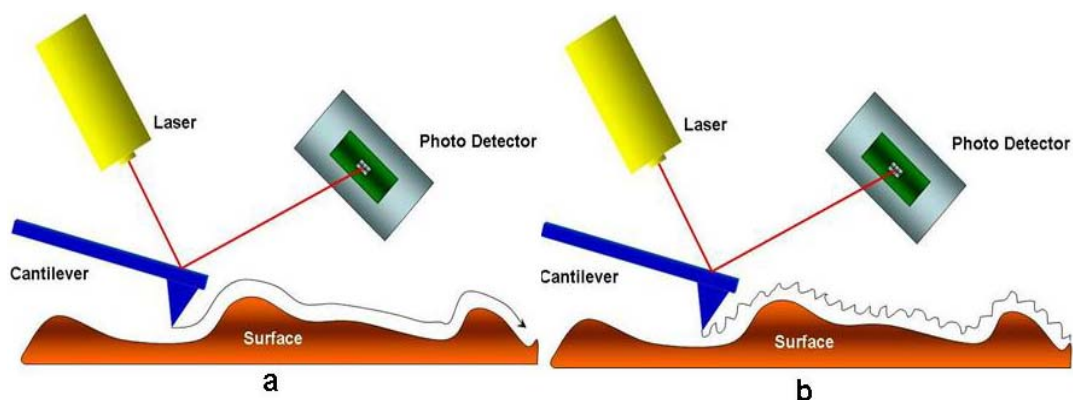


Figure 12: Working modes of the Atomic Force Microscope a) contact mode b) noncontact mode

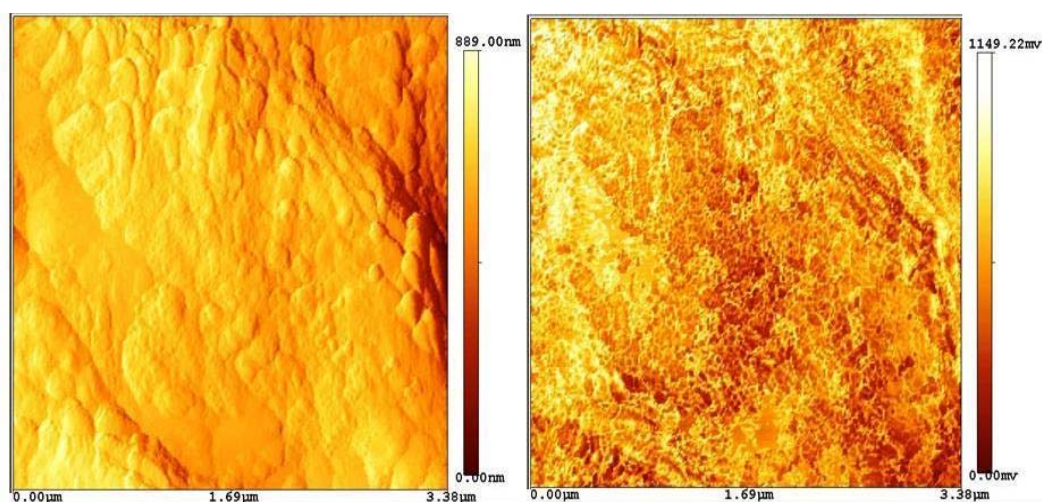


Figure 13: Noncontact images of a polished pure Al surface. Topographic image (left) and phase image (right)

2.2.4. X-ray Photoelectron Spectroscopy

X-Ray Photoelectron Spectroscopy (XPS) is a very sensitive tool for surface analysis of a wide variety of materials including metals, ceramics, polymers, biological materials, and semiconductors. The specimens can be solid, liquid or gaseous [37]. The first work reported in literature about the X-ray Photoelectron Spectrometer was by R.G.

Steinhardt et. al. who in 1953 studied the influence of chemical and physical properties of a surface on the emitted photoelectrons [59]. This technique was also known as Electron Spectroscopy for Chemical Analysis (ESCA), which was the popular acronym given by Kai Siegbahn who made significant contributions to the development of XPS [60,61]. He was later awarded a Nobel Prize for Physics in 1981 for his work. The top few atomic layers can be studied using this technique. The working principle of XPS involves irradiating a solid with mono-energetic soft X-rays under high vacuum, and analyzing the emitted electrons based on energy [62]. The output signal is plotted showing the number of detected electrons as a function of their kinetic or binding energies. Every element has a unique spectrum showing specific peaks like a fingerprint. A combination of elements will show a peak which may be approximated to the sum of the individual peaks. Peak positions from various elements have been standardized in the handbooks. It is possible to identify the chemical states present from the exact measurements of peak positions and separations. Quantitative data can be obtained by measuring the peak heights or peak areas. A comprehensive study of history of photoemission and the principles of XPS can be found in the references [62,63]. An illustration of XPS is shown in Figure 14. A sample spectrum from XPS is shown in Figure 15. A conjugate tool called Auger Electron Spectroscopy (AES) provides an effective method to study thin films and interfaces. It has high lateral resolution and very good sensitivity to analyze the top few nm of specimen surface. Detailed information on AES can be found in the reference [1].



Figure 14: Kratos Imaging X-ray Photoelectron Spectrometer at Materials Characterization Facility [39], Texas A&M University

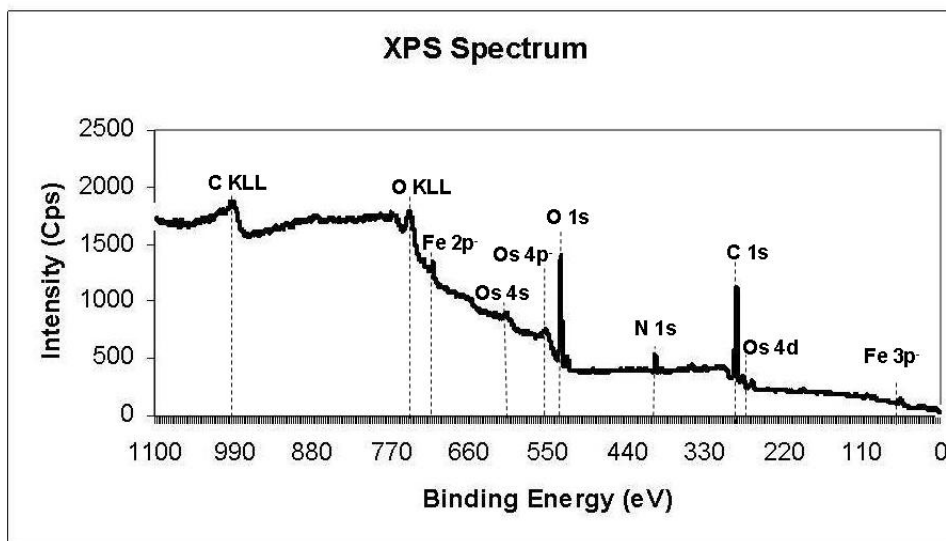


Figure 15: XPS spectrum of the surface of steel rubbed with a vegetable oil based lubricant

2.2.5. X-ray Diffraction

This is a very powerful characterization tool for nondestructive qualitative and quantitative analysis of crystalline materials. X-ray diffraction (XRD) is utilized to

identify the chemical constituents of the bulk crystalline substances. It can also give information about the crystallinity of a specimen, different grain orientations, strain states and defect structure. The underlying principle is that of Bragg's law of diffraction. This technique is very sensitive to the lattice spacing and crystal structure. A monochromatic X-ray source is used to irradiate the surface of the specimen.

These X-rays are diffracted to different angles by the atomic lattice which acts like a three dimensional grating, giving a diffraction pattern that includes the positions and intensities of the diffracted beam [64]. Different chemical phases and compounds can be identified due to the uniqueness of peaks defined by the positions and intensities for each compound. A comprehensive database of currently identified powder diffraction patterns exists in the International Centre for Diffraction Data (ICDD®). Figure 16 shows a modern day X-ray Diffractometer. X-ray spectrum of steel is shown in Figure 17.

Some other commonly used surface sensitive non destructive techniques based on the principle of diffraction are Low-energy electron diffraction (LEED) and reflection high-energy electron diffraction (RHEED). These techniques use electrons in high vacuum in place of X-rays which are used in XRD. They can provide surface crystallographic information in contrast to the bulk information provided by XRD. They are mostly used to study surfaces, interfaces and thin films. More information on the functions of LEED and RHEED can be found in the reference [1].



Figure 16: Bruker D8 Powder X-ray Diffractometer at X-ray Diffraction Laboratory [65], Department of Chemistry, Texas A&M University

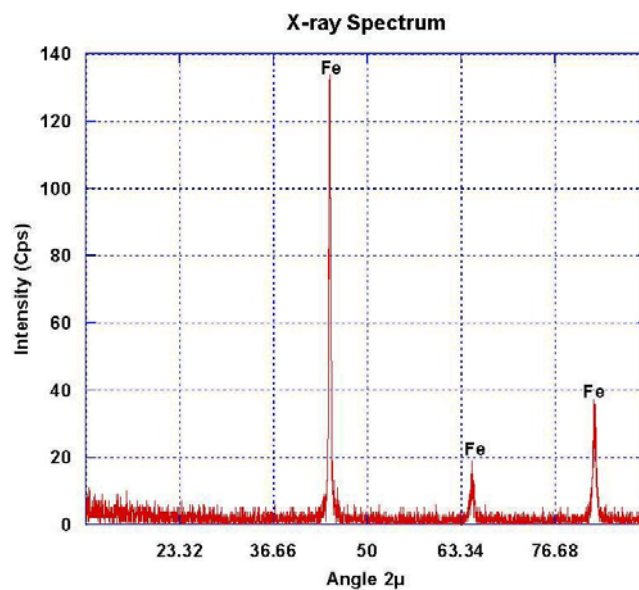


Figure 17: X-ray spectrum of a steel surface showing distinct iron peaks at specific angles based on the crystal structure

2.2.6. Nanoindentation

The nanomechanical properties of submicron regions of a flat specimen can be directly evaluated using a technique called Nanoindentation. The indentation resolution is of the order of a few nano meters and the load used can be controlled to the order of a few μN [66]. The nano-scale properties such as hardness and young's modulus of thin film materials can be determined using this method. The indentation tips are made of diamond and have different geometries depending on the application. The piezo sensors track the vertical movement of the tip at each increment of the changing normal force. The output data is plotted as a loading/unloading curve showing normal force versus depth of penetration [67]. Various relationships have been developed to estimate the hardness and modulus using this data. Figure 18 shows a commercially available Nanoindenter. An illustration of the working principle is shown in Figure 19. Modern Nanoindenters have a built in optics and AFM system which allows for easy location of the indents with both pre and post scanning ability.

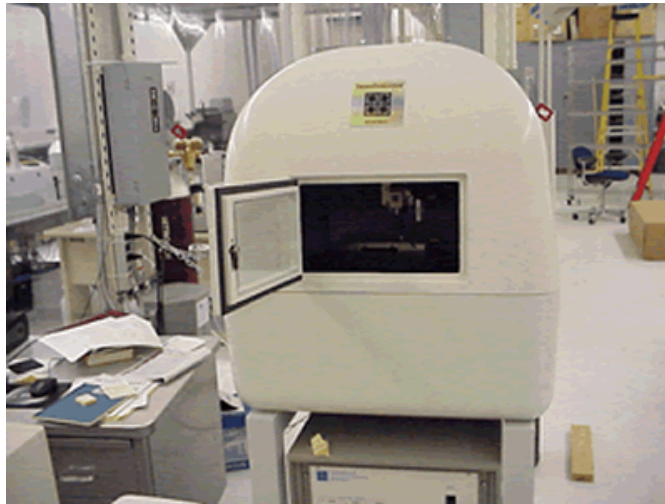


Figure 18: Hysitron Nanoindenter at Materials Characterization Facility [39], Texas A&M University

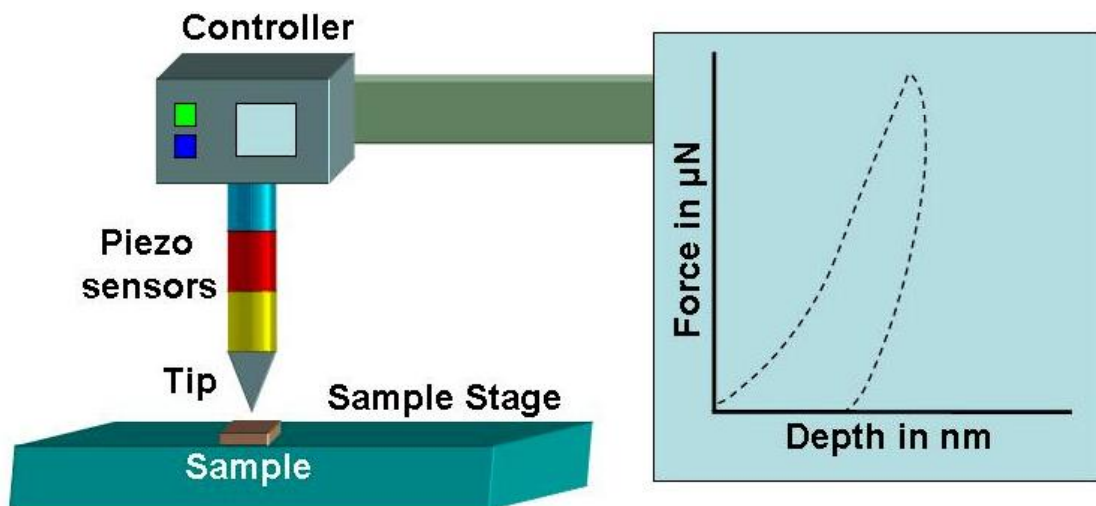


Figure 19: Schematic of working principle of Nanoindenter

CHAPTER III

TRIBOLOGICAL PROBLEMS IN RAILROADS

3.1. Introduction

The railroad industry presents some of the most interesting but challenging tribological problems to the researcher. This chapter introduces the typical wear behavior found in the railroads and some current prevalent measures to combat this problem. The author outlines his approach to the given problem as a closing note to the chapter.

Figure 20 illustrates a train wheel set showing the important railroad nomenclature. Rail wear is a complex phenomenon and has been an ever-growing problem in the rail industry, especially with the increasing axle loads and rail traffic. Several efforts are on around the world in search of ways to delay the failure of rails through wear. A summary of the different forms of rail wear is shown in Figure 21. Various sophisticated and bulky machines have been designed to study the rail wear in laboratories. The most popular ones used almost exclusively are the ball-on-disc tribometer for studying the rail/ wheel flange sliding wear and the twin disc rolling-sliding machine for simulating the top of the rail wear [68-77]. However, these machines cannot be used for testing both sliding and rolling-sliding wear. A disadvantage of the twin disc machine is that it provides a line contact between the two discs [78]. The real rail/wheel contact is generally a point or a small elliptical area. Certain modifications of these configurations have been employed to better simulate the real conditions but this

brings in higher cost and more sophistication. The pin-on-disc machine can effectively simulate the sliding wear. However, the uni-directional sliding generates a circular wear track that can be used to study the wear under normal loading conditions only. Recently, the study of wear under reversal loading has gained importance. This calls for further modifications of the existing apparatus. Various research groups have studied the operative rail wear mechanisms under lubricated and dry conditions. Standards like ASTM D4172 and DIN 51834 are used as a measure of lubricant effectiveness in preventing wear [79-81]. Currently a range of lubricants and lubricating systems exist in the rail industry.

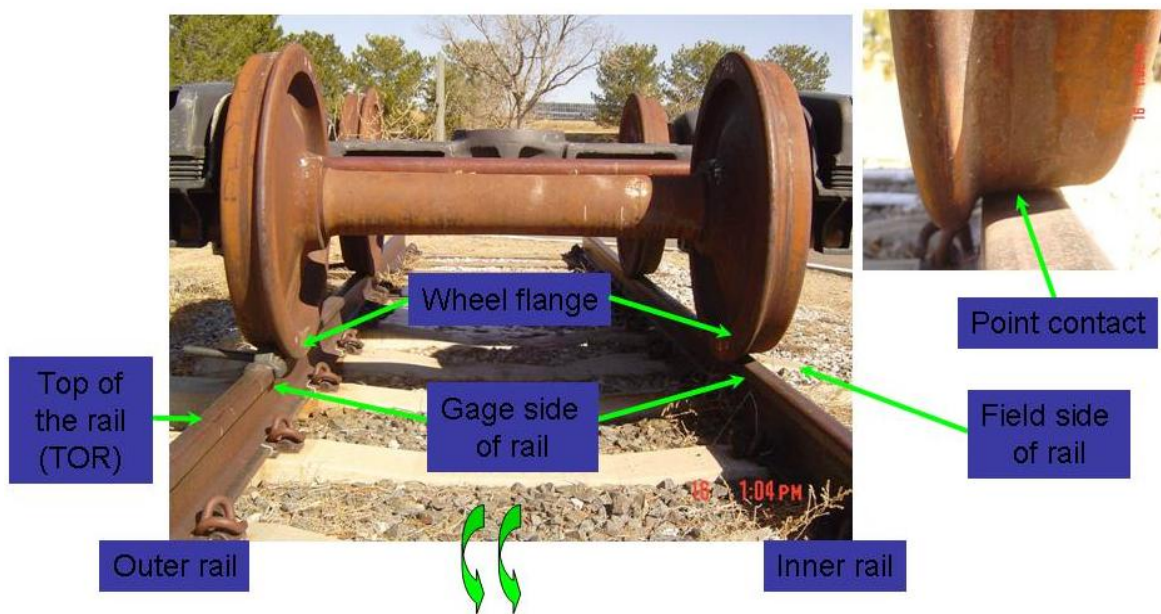


Figure 20: Nomenclature in railroads

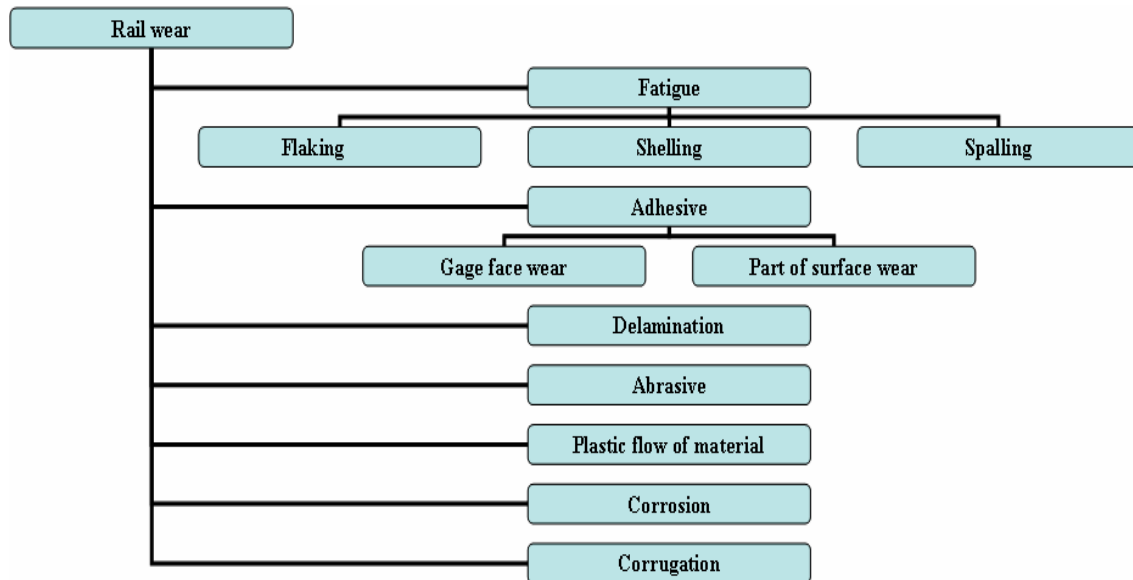


Figure 21: Classification of rail road wear

3.2. Problem Definition

The task of this project is to develop a method for tribological augmentation of railroad surface to reduce the occurrence of chemical and mechanical wear. To prove economical, this method should incorporate functionality during regular track operation thus reducing downtime. The scope of the project involves study of operative friction and wear mechanisms at the rail/wheel interface.

3.3. Wear in Railroads

3.3.1. Wear Mechanisms of Railroad

The wear mechanisms of the railroad typically involve multiple contact modes which are depicted in Figure 22. Wear behavior can have both direct and indirect effects upon the stress within the rail, and therefore is a factor of prime importance in assessing the serviceability of the rail. The serviceability of a rail is a reflection of how well the rail meets the requirements by resisting structural failure and excessive wear. The upper limit on serviceability is structural integrity. Excessive wear is one of the most prominent reasons for rail removal. The macroscopic crack growth rate in most metals responds to approximately the fourth power of stress. Therefore a relatively small decrease in section modulus can result in a very large increase in crack growth rate. It is reported however that modest wear may be something of an advantage, since rails with moderate wear have shown a lower service induced defect occurrence rate [82-84]. The different wear mechanisms pertaining to the wheel/rail interface are shown in Figure 23.

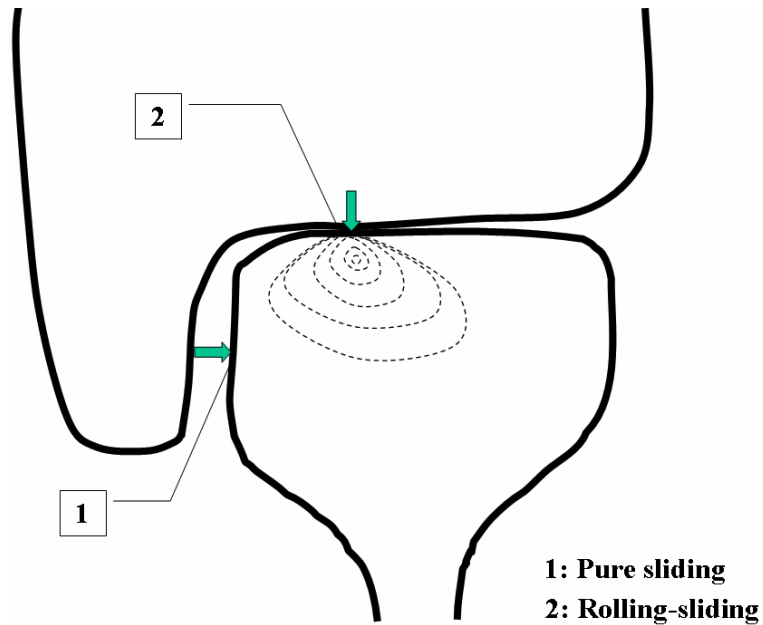


Figure 22: Contact modes of a rail/wheel interface

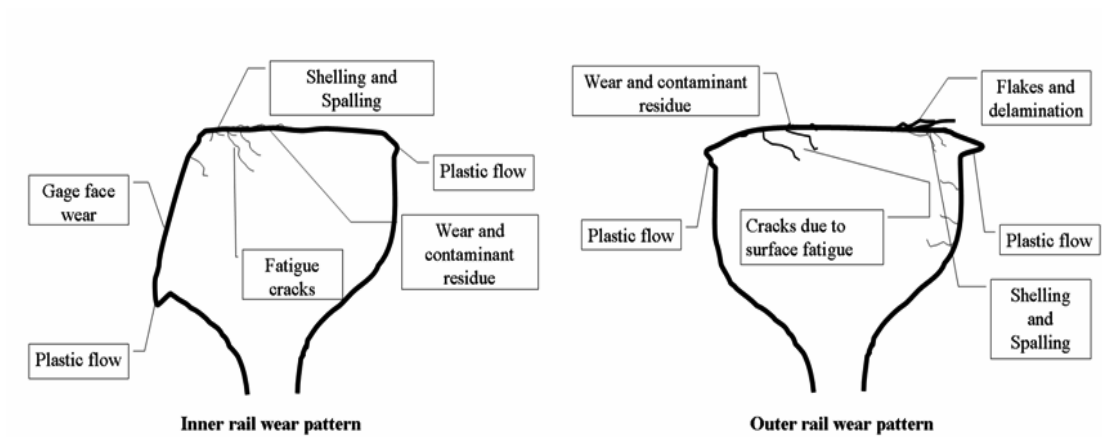


Figure 23: Wear mechanisms of the rails

The contact region between rail and the wheel is normally located as a single point contact on the railhead and includes an adhesion zone and a slip zone (in tangent tracks and curves with big radii). In sharp curves, two-point contact can occur

depending on wheel/rail profiles and dynamics. The flange contact encounters pure slip, as compared to the railhead contact. The curve radius and track elevation give wear or rolling contact fatigue (RCF) damage which is a major concern in the rail industry. In general, small curve radii result in flange wear while more moderate radii result in RCF damage [85]. Squats, shelling and head checks are classified under RCF. Head checks which are observed in curves and switches because of flange rail contact at the gauge corner are caused due to increased slip and decreased wheel-rail contact area. These can ultimately lead to rail failure. A major environmental concern is the high noise emission due to the stick-slip at the wheel-rail interface. The INFRA-STAR project focused on developing a surface coating to be applied on the rail head in order to prevent RCF and reduce noise emissions in small radius curved rail [86].

High axle loads (HAL) cause rail head shelling in operational rails. Shelling begins about 4 to 6 mm below the running surface of the rails. Also called fatigue ruptures, these are caused by the long-term fatigue strength of the rail being exceeded [87]. Rail wear is broadly classified into fatigue wear and adhesive wear. Flaking, shelling and spalling are fatigue forms of wear. Gage face wear and a portion of surface wear on the outer rail are predominantly adhesive forms of wear. Delamination and some abrasive types of wear are also present. It is observed that the inner rail in curves usually experiences substantial plastic flow of metal towards the field side. Another mechanical form of wear called corrugation exists in railroads. The characteristic of a sinusoidal run in rail heads is the main cause of corrugation. Although both vertical and lateral wear could be attributed to a plastic deformation and fracture mechanism, there

are two factors which complicate the vertical wear of rails [88]. First, there is the influence of atmospheric corrosion on the fracture process. Second, the rolling/sliding action of the wheel tread gives rise to surface phase transformations in the rail commonly observed with ferrous materials which have experienced rubbing contact [89]. This does not occur with flange/rail contact on curves. Corrosion can be a problem in unlubricated tracks. When a train passes over the track, the corroded material is removed by the wheels. This is a type of wear by way of material loss over time. Some real life examples of rail wear are depicted in Figures 24 - 26. These pictures were taken at TTCI, Pueblo, Colorado by the author.

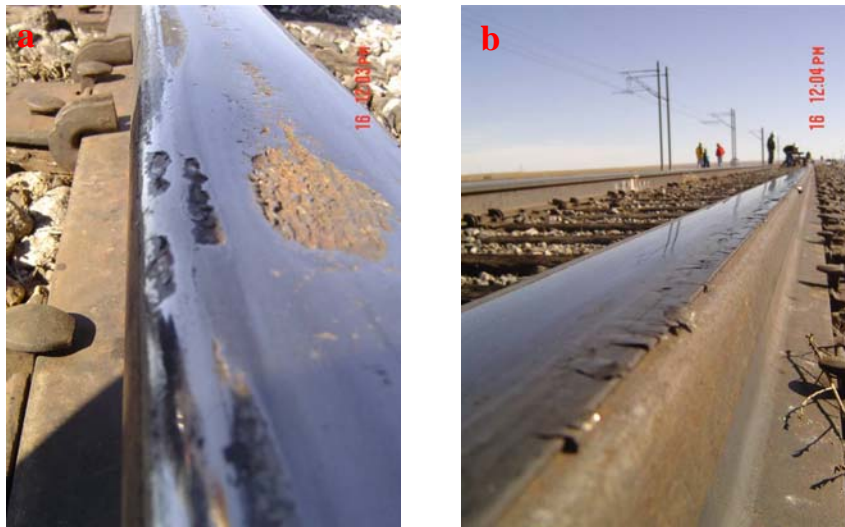


Figure 24: a) Surface wear: shelling, adhesive wear b) Flaking

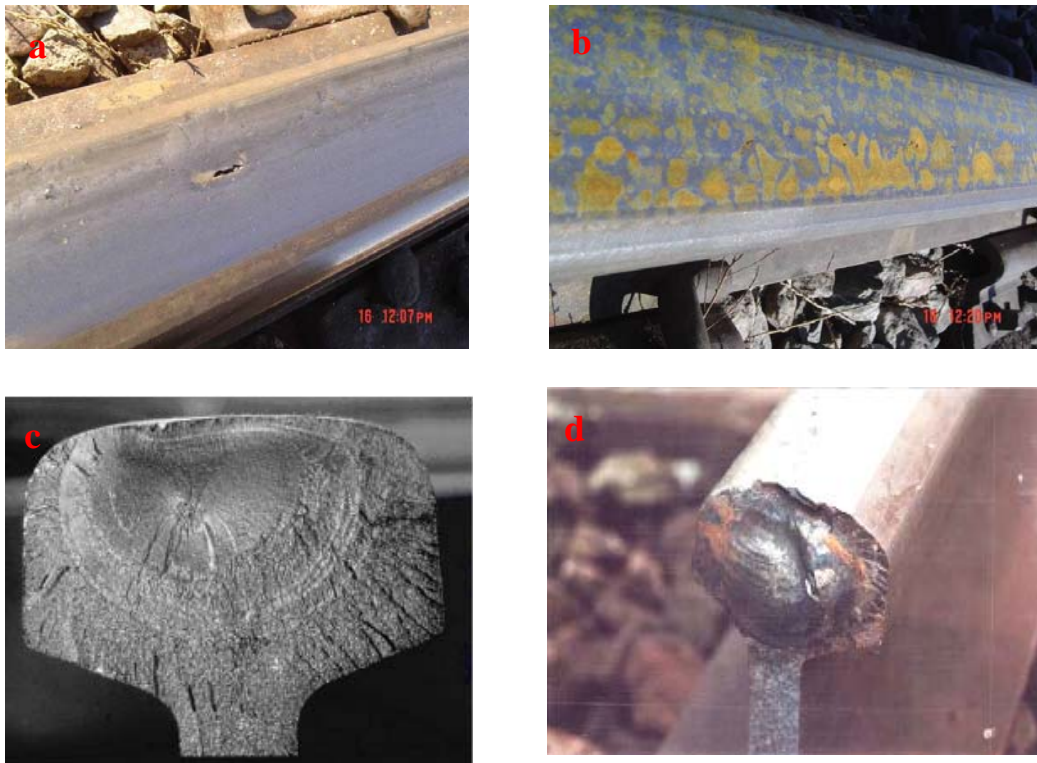


Figure 25: a) Surface crack b) corrosion c) fatigue tache ovale [90] d) fatigue failure [90]



Figure 26: a) Undeformed rail b) Gage wear and plastic flow after service

The fact that the rails are always in a state of plastic deformation coupled with the high temperatures involved, allow for structural transformation of the surface layers. The phase transformation process can be explained as follows. Under operating conditions, the rail steel plasticizes resulting in work-hardening. Because of this phenomenon and the fact that there is high slippage between the wheel and the rail, very high temperatures (flash temperature) appear briefly in the contact area. These temperatures can lie above the transformation point of steel. There is extremely rapid cooling due to the large heat capacity of the bulk. This drastic quenching of the momentarily heated points results in the formation of martensite (phase transformation). This is termed as “friction martensite” [91].

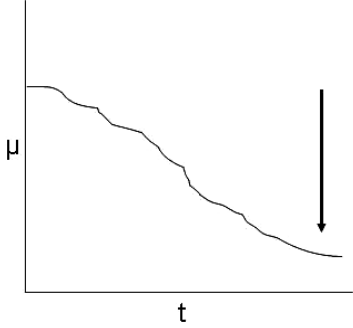
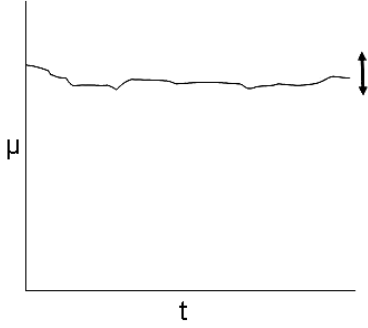
The gage/flange wear is amplified when the train is traveling at high speeds or traversing steep curves. At higher speeds, there is instability introduced into the course of the wheel set. This instability or an occurrence of resonance cause the wheel-set to strike hard against the rail, which results in the higher wear of the wheel flange. An elaborate study of rail wear can be found in work done by Kalousek et al [92].

3.4. Lubrication in Railroads

Lubrication has been sought as a long term solution to the rail road wear problems. It is found that lubrication in fact significantly reduces the rail gage wear and drastically decreases the squeal and noise in railroads. It also helps reduce the lateral forces which cause the flange wear and a part of top of the rail wear due to high friction and hence directly help reduce energy and fuel consumption. This is an effective method

for the problems at the gage/flange interface. The top of the rail lubrication (TOR) has gained focus over the past decade or so. Here a new family of materials called friction modifiers (FM) has been investigated for top of the rail application. These materials have distinctly different behavior from the conventional lubricants and display different performance characteristics. FM's can hit a plateau of target friction with time and this is crucial to the railroads since friction is important for traction and braking on the top of the rails. The regular lubricants will tend to reduce the friction coefficient with time. Different commercial manufacturers design their custom friction modifiers for different target friction values based on their experience and research. A typical target value for the top of the rail friction value is 0.15-0.45. Kelsan Technologies Corp. designs FM with a target friction range between 0.30 and 0.35. A Chicago based manufacturer, Friction Management Services LLC has designed a product called TracGlide which provides a coefficient of friction (COF) of 0.15 under normal rolling conditions and 0.5 under traction or braking conditions. Table 2 summarizes the important differences between these two classes of materials [93-95]. There are lubrication systems in place for delivering both these materials to the target areas of application. Typical systems include computer controlled on board train systems, intelligent way side systems and hi-rail systems.

Table 2: Lubricants vs. friction modifiers

Lubricants	Friction Modifiers
Low coefficient of friction	Intermediate coefficient of friction
Negative friction behavior: COF decreases with increased sliding velocity and creep	Positive friction behavior
	
Types: Solid, liquid, petroleum based, bio degradable, organic	Types: Solid, water based, petroleum based, bio degradable
Examples: oils, greases, synthetic polymers	Examples: engineered dry composite solid water soluble suspensions, polymer based matrix
Possible additives: anti wear, low friction, high pressure	Possible additives: anti wear, controlled friction, high pressure
Application region: gage/flange	Application region: top of the rail (TOR)
Application methods: on board	Application methods: on board, wayside, hi- rail
Track retentivity: low	Track retentivity: high
Potential uses: lateral force reduction, wear reduction, prevention of crack initiation, energy and fuel savings	Potential uses: noise and squeal reduction, lateral force reduction, wear reduction, prevention of crack initiation, prevention of crack propagation, energy and fuel savings

3.5. Proposed Solution

This research proposes an innovative method to generate a *functional tribofilm* that exhibits high-wear and corrosion resistance, high strength and toughness, and controlled friction properties. The hypothesis proposed to achieve the final objectives is illustrated in Figure 27. The principal idea was to use potential nano and micro sized particles of specially chosen elements to be used as functional additives in a carefully designed custom lubricant formulation. The target was to generate a tribofilm with identified properties as shown in Figure 27. A tribofilm in simple terms is a protective layer formed over the surfaces of bodies in relative motion. The next chapter provides a detailed overview of tribofilms.

This work utilizes a cost effective and simple ball-on-flat tribometer, which was modified to simulate both sliding and rolling-sliding motion at the rail/wheel interface in a laboratory. Further, this tribometer was also used for conducting micro scratch tests. A novel lubricant formulation showed promise of repairing the damaged surfaces and improving the tribological properties during operating conditions. This could be achieved by the formation of a wear resistant and durable tribofilm on the sample surface. This can reduce cost of maintenance caused due to downtime while providing desired surface properties. The multi purpose tribometer offers a simple and cheap way to study rail wear in the laboratory.

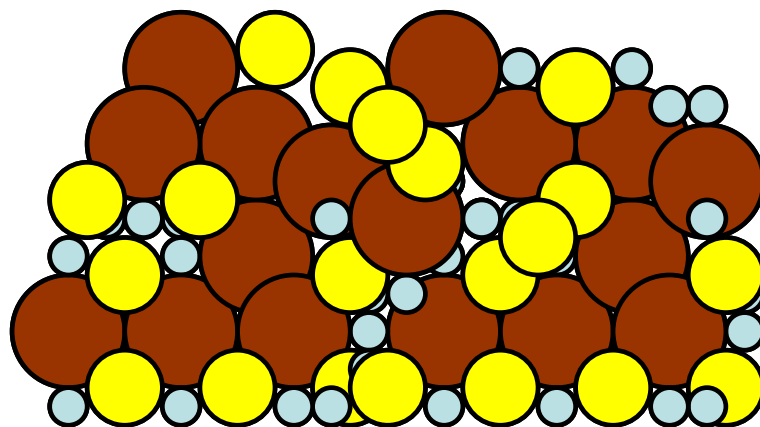
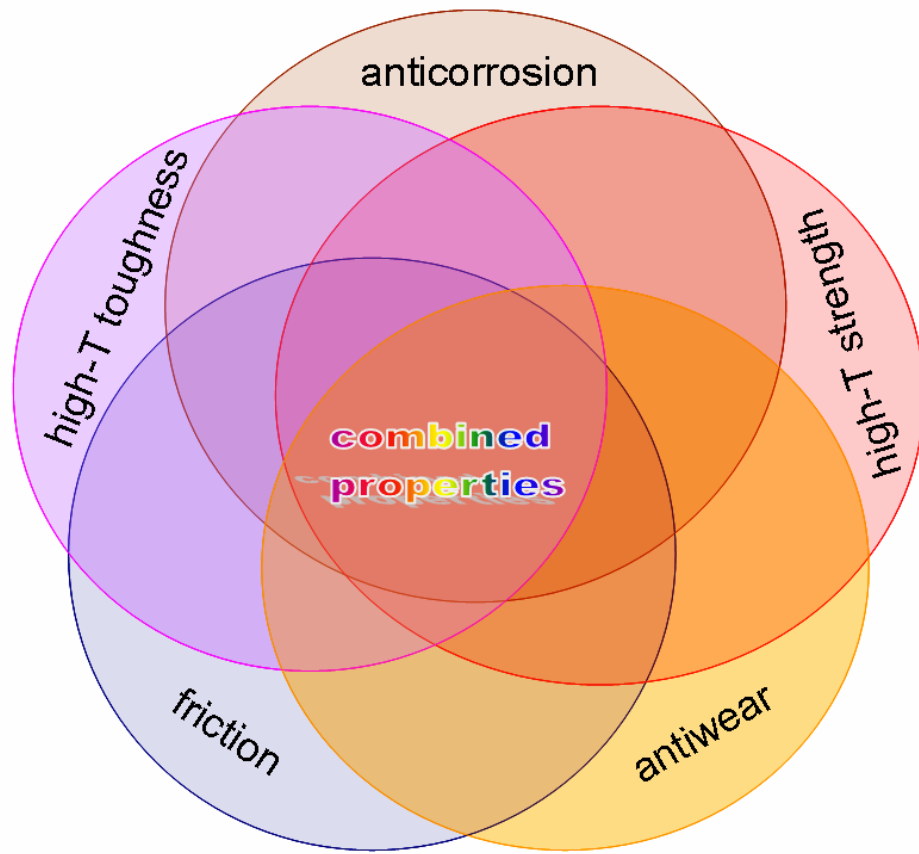


Figure 27: Illustration of hypothesis depicting approach utilized in research

CHAPTER IV

REVIEW OF TRIBOFILMS

4.1. Definition

A “tribofilm” is a protective layer that is generated during sliding or rolling in a frictional contact between two surfaces, generally in the presence of a lubricant which contains some special additives which form “*antiwear*” pads that act as load bearing surfaces and prevent metal-to-metal contact.

4.2. Background

Tribofilm generation proceeds usually under boundary lubrication regime where the friction modifier and the antiwear agents undergo tribochemical interactions resulting in the formation of chemically bonded films [96-98]. In ceramics, tribofilms are found to form in both dry and wet sliding. The tribofilms are known to reduce the friction between the contact bodies and in general enhance the wear resistance. However, tribofilms may be protective or tribologically deleterious. The tribofilms can be formed by mechanical mixing, tribochemical interactions or thermal activation [99]. In the mechanically generated tribofilm, the mechanically mixed particles have the same physical structure and chemical composition as those of the base sliding pair. Another class of tribofilms, where the microstructure of the film constituents is different from that of the base pair is the much discussed white layer formed during the sliding of ferrous material where the base material is suggested to undergo a phase transformation

to fine grain martensite [99]. The chemically generated tribofilms are a result of tribochemical interactions occurring at the sliding interfaces under the presence of active additives. Thermally produced tribofilms are a result of temperature activation in the presence of additives. This section focuses primarily on tribochemically generated tribofilms and the various additives used in lubrication.

4.3. Tribofilm Generation and Mechanisms

A “tribofilm” is a protective layer that is generated during sliding or rolling in a frictional contact between two surfaces, generally in the presence of a lubricant which contains some special additives which form “*antiwear*” pads that act as load bearing surfaces and prevent metal-to-metal contact.

The research so far on tribofilms formed in lubricated contacts due to tribochemical reactions has formed a basis for the synthesis of more efficient additives and lubricants [100]. The thickness and composition of the chemical tribofilms depends on the type and concentration of the additive used in the base oil [101] and the applied load [102]. It also depends on environmental factors such as humidity, and test parameters like interface temperature, contact pressure, sliding/rolling speed and total time of test. The thickness is a key attribute for anti wear performance, since the film acts as a sacrificial layer between the two sliding surfaces by reducing the asperity contact [103]. The antiwear pads that form during the sliding process (tribofilm) act as load bearing areas reducing the metal to metal contact and thus minimizing plowing, abrasive and adhesive wear. The increase of interfacial temperature resultant upon

frictional heating affects the reactivity and adsorption of additive molecules on sliding metal surfaces [104,105]. During the frictional sliding process, the tribofilm ruptures locally due to sliding and micro asperity contacts and is continuously replenished by the tribochemical reaction products. The rate of additive reactions is high at elevated interface temperatures thus allowing for faster tribofilm formation and replenishment. K. Komvopoulos et.al [106] reported that tribofilms maintain their integrity even under relatively low sliding temperatures where the lower rates of tribochemical reactions may retard tribofilm replenishment.

The regenerative capacity and the stability of these tribofilms under high temperatures and high loads make them efficient antiwear films which help in reducing the plowing, abrasive, adhesive and scuffing wear by hard asperities and wear debris in boundary lubrication. The properties of the tribofilms depend on chemisorption, decomposition, and the chemical interactions between the most reactive decomposition products and the sliding interfaces [106]. Tribology and in particular tribochemistry deals with a large parameter space [102], since the friction, wear and tribochemical reactions of a given tribological system depend strongly on the applied conditions (e.g. relative velocity, contact pressure, sliding time, and temperature) [107]. Various tribosystems have been investigated in the past to study the tribofilm formation mechanisms, properties of the protective layer, which are characteristic to the specific test and tribosystem. Various additives have been used for different lubricant formulations to give different properties of the generated tribofilms.

“Transfer films” are obtained by tribochemical reactions between tribofilm, native oxide film and nascent metal surfaces produced by friction. The chemistry of transfer films is modeled using the hard and soft acids and bases principle (HSAB) which was proposed by Pearson [108] and is explained later in this chapter. The transfer film is produced due to transfer of additive reaction products onto the counter face tribochemically from the sliding surface. Transfer films play an important role in modifying the friction behavior of a tribosystem. The molecular scale transfer mechanisms may govern the frictional response of the tribosystem in the presence of additives under boundary lubrication [109]. External electrical and magnetic fields seem to affect friction transfer direction and kinetics by changing the growth rate and composition of transfer films. “Selective transfer” is a specific case of transfer films where certain lubricants exhibit both surface and chemical activity providing generation of colloidal particles of wear and simultaneous tribochemical reactions resulting in the formation of a low shear porous film [110].

Inorganic tribofilms are generally thought to consist of metal oxides, sulphides, phosphates and borates, with compositions depending on the additives used to generate them. These films are ionic insulating solids. Antiwear tribofilms formed from P- and B-containing additives are thought to be phosphate and borate glasses respectively. They have resistivities similar to that of oxides. Sulphides may be semiconductors and possess much lower resistivities, depending on the tribofilm composition and formation temperature [106]. Sulphide dominated tribofilms produce lower friction while borate and phosphate dominated tribofilms are more effective in increasing the wear resistance

of steel surfaces. Some sulfur containing lubricant additives like sulfurized olefin, perform better as friction modifiers rather than antiwear agents. The efficacy of sulfurized lubricants to reduce friction is related to their ability to form sulphide layers. J.H. Petersen et.al. [111] investigated the tribological properties of sulphur-implanted steel. They reported that sulfur implantation at high doses amorphized the steel surface and formed nanocrystallites of the hexagonal FeS compound, which is known to have very good lubricating properties. FeS, also known as troilite, has a layered hexagonal structure with low shear strength and a high melting point (1100 °C). Hence it is a very effective solid lubricant like graphite and MoS₂.

4.4. Characterization of Tribofilms

The tribofilms and the reaction products are characterized using a wide variety of surface-analytical methods. X-ray photoelectron spectroscopy (XPS), scanning auger microscopy (SAM), time-of-flight secondary ion mass spectroscopy (ToF-SIMS) and X-ray absorption near-edge structure (XANES) are the usual methods for the chemical characterization of tribochemical reaction films [102]. Most of these methods can combine imaging and spectroscopy. Scanning auger electron microscopy (SAM) has been used to map elemental distribution of a contact area [109] and recently imaging XPS (i-XPS) has shown promise in investigating the distribution of chemical species according to their chemical state [112,113]. Auger electron spectroscopy (AES) and transmission electron microscopy (TEM) have also been used for study of tribofilms. Atomic force microscopy (AFM) has also been used to characterize the tribofilms.

Contact and non contact modes in the AFM provide useful topographic information while phase imaging with non contact mode and frictional imaging using contact mode (FFM) provide some chemical information. X-ray photo electron emission microscopy (X-PEEM) gives sub micron local resolution of a particular species in a thin film and has been used recently to study tribofilms [114-117]. A number of other surface analyzing tools have been investigated for chemical characterization and imaging. Nano indentation technique has been utilized to characterize the mechanical properties of the tribofilms [117,118]. K. Komvopoulos et al. used electrical contact resistance (ECR) measurements between the sliding surfaces in the presence of the lubricant to study the initiation, formation, rupture and replenishment of tribofilms [106]. ECR is proportional to the measured voltage and hence provides an effective measure to detect the presence of an insulating tribofilm [101]. During the past two decades new quantum mechanical/quantum chemistry (QM/QC) methods like the density functional theory (DFT) simulations have been developed to explore and understand the basic tribochemical interactions and additive chemistry at the atomic level. This method has shown potential to tribo-engineers to be able to design tribo coatings in the future and find alternative additives which will form more durable, efficient and environmental friendly tribofilms [119].

4.5. Additive Chemistry

Lubricating oils generally contain antiwear (AW) and extreme pressure (EP) additives. As the name suggests, the AW additives work by forming protective

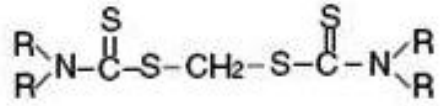
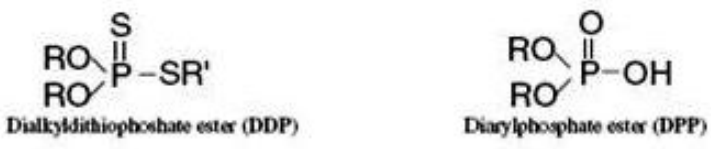
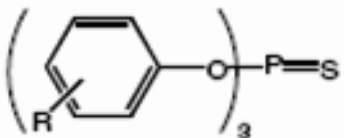
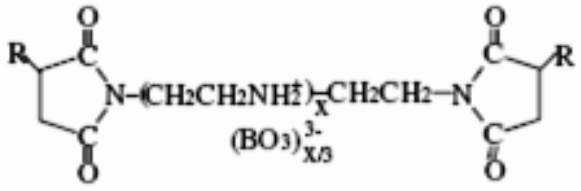
tribofilms through tribochemical interactions occurring at the friction interfaces. EP additives are active organic molecules, which adsorb in the boundary layer and eventually decompose under high frictional heating, thus releasing active elements such as B, P, Cl or S which can react directly with the surface metal atoms (forming sulphides, chlorides etc.) or catalyze the formation of protective boundary films [111]. The most common additives used in lubrication can be classified into organic and inorganic types. The most vastly studied organic additives are metallic alkyl and aryl thiophosphates. Among these zinc dialkyl dithiophosphate (ZDDP) and Zinc dithiophosphate (ZnDTP/ ZDTP, which is a C₃/C₆ secondary ZDDP) additives have been the center of focus for around 50 years because of their good anti wear properties. Ashless di alkyl thiophosphates (DTP) and triaryl monothiophosphates (MTP) have also been studied as eco compatible alternatives to ZDDP [120]. Dialkyldithiophosphate esters (DDP), diarylphosphate ester (DPP) exhibit some useful properties. DPP works well as an AW agent under medium stress [121]. It has been reported that ashless methylene-bis (di-n-butylthiocarbamate), DTC is an excellent AW additive with good antioxidant properties [122,123]. It is used in gear oils and lubricant greases. Apart from these, organo molybdenum compounds are being used because of their good antiwear and friction-reducing properties, among which Molybdenum dithiophosphates (MoDTP) have been extensively investigated [124]. Molybdenum dialkyl thiocarbamate (MoDTC, a friction modifier) and combinations of ZDDP and MoDTC have also been studied. Organo borates have been investigated for antiwear performance [125].

Various inorganic additives like Molybdenum disulphide, alkali borates, phosphorus-sulphur compounds and calcium borates have also been investigated. Other than the AW/EP agents, additives like detergents and dispersants play an important role especially in engine lubrication for smooth operation. Both of these are long chain hydrocarbons with polar ends. The detergents have a metal ion contained in the polar end while a dispersant does not contain a metal ion but utilizes oxygen and/or nitrogen-containing moieties for polarity [126]. The detergents help in keeping the engine clean while also preventing deposition of harmful sludge and carbon. In addition to cleaning, detergents also neutralize acidic combustion and oxidation products, thereby, minimizing corrosion, rust and deposit formation in the engine [127]. An important class of detergents is metal sulphonates. Calcium sulphonate is a known detergent which also possesses good AW and anti-scuffing properties [128-130]. Detergent-dispersant additives like polyisobutenyl succinimide (PIBSI) and polyisobutenylacetylamine (PIB-Amine) are well known surfactants [131]. Additive packages containing dispersants and ZDDP, dispersants and dialkyldithiophosphate esters (DDP), dispersants and diarylphosphate ester (DPP), or dispersant and DTC combinations are used extensively in gear oils, transmission oils, and engine oils [132]. The molecular structures of the important additives are shown in Table 3.

Table 3: Molecular structures of different additives

Additive	Type	Molecular structure	Reference
ZDDP	AW/EP		[133]
ZnDTP	AW/EP	<p>Zndtp</p> <p>where R is an alkyl group.</p>	[109]
MoDTP	AW	<p>R = $\text{CH}_3\text{-CH(CH}_3\text{)-CH}_2\text{-CH(CH}_3\text{)-CH}_3$</p>	[124]
MoDTC	AW/ friction modifier	<p>Modtc</p> <p>where R is an alkyl group.</p>	[109]

(Table 3 continued)

Additive	Type	Molecular structure	Reference
DTC	EP	 <p>Methylene Bis(dialkyldithiocarbamate) (DTC)</p>	[132]
DDP & DPP	AW/EP	 <p>Dialkyldithiophosphate ester (DDP) Diarylphosphate ester (DPP)</p>	[132]
MTP	AW		[134]
B-PIBSI	Dispersant	 <p>R = Polyisobutylene, X ≥ 3 Borated polyisobutylene succinic anhydride/polyamine</p>	[132]

proposed by Pearson [108]. In particular, the HSAB principle states that the phosphates prefer to react with the oxides while the sulphides prefer to react with metals [124,137]. The phosphate anions (PO_4^{3-}) are hard bases and will prefer to react with iron or molybdenum cations (Fe^{3+} and Mo^{6+}) which are hard acids. The soft bases such as sulphides prefer to react with pure metals (Fe^0) which is a typical soft acid. Fe^{3+} and Mo^{6+} are harder Lewis acids than Zn^{2+} [109]. The Pearsons' classification of the different species into HSAB is shown in Table 4. The formation and interactions of tribofilms from ZnDTP and ZDDP have been studied extensively by several authors and an extended review can be found elsewhere [137]. It is widely accepted that the tribofilm is composed of an amorphous inorganic polyphosphate glass containing some embedded sulphide species, covered by a ZnDTP rich zone which regenerates the film removed under friction and wear [124]. Tribological films from ZnDTP have been reported to be polyphosphate films having a layered structure [107,136]. They are formed under pure thermal or combined thermal and tribological stress [138]. Tribologically derived ZDDP antiwear films are slightly different from their thermal counterparts. The tribological films have a layered structure whereas the thermal films lack a layered structure, though they have similar composition. It is reported that ZDDP starts to decompose at temperatures below 150 °C [139]. At temperatures above 100 °C, tribofilms with a thickness of a few tens of nanometers are found, while at lower temperatures thinner films are reported [140]. However, environmental implications of using ZDDP have emerged and now the focus is on finding suitable alternative additives which are more environment friendly [141,142].

Table 4: Classification of different acid and base species

	Acid	Base
Hard	$H^+, Fe^{3+}, Mo^{6+}, Ca^{2+}, RPO^{2+}$ $, RSO^{2+}, CO_2$	$H_2O, OH^-, CO_3^{2-}, O^{2-}, PO_4^{3-}$ $, ROH, RO^-, SO_4^{2-}$
Borderline	$Fe^{2+}, NO^+, SO^2, Zn^{2+}$	$BO_3^{3-}, N^{3-}, N_2, SO_3^{2-}$
Soft	$Cu^+, Fe^0, RH^3, RO^+, Mo^{4+}$ metal atoms, bulk metals	$R_2S, S^{2-}, RNC, S_2O_3^{2-}$

Ashless thiophosphate oil additives are a possible replacement to ZDDP. They work in a similar way and provide wear protection comparable to ZDDP, outperforming them in some cases. Studies by Sarin et.al. [143] on the anti wear properties of the tribofilms formed by dialkylphosphorodithioic acids revealed that the performance was similar to that of ZDDP and that the additive was not affected by the exclusion of Zn which is encouraging. Further the antioxidative properties of the ashless additives were also similar to that of ZDDP. M.N. Najman et.al. [134] correlated the micro chemical properties to the antiwear (AW) performance in ashless thiophosphate oil additives. They conclude that an ideal AW film is comprised of a thick film with pad-like structures that are wider in area and micro chemically heterogeneous, with areas of varying polyphosphate chain length.

The importance of Al-Si alloys as revolutionary engine component materials has led researchers to study the effect of ZDDP enriched lubrication in an effort to understand the tribochemical interactions and the possible formation of antiwear tribofilms on Al-Si alloy surfaces [144,145]. It was found that the tribofilms formed comprised polyphosphates similar to that on steel. The length of the polyphosphate chain depends on the time and temperature [144]. Many authors have reported that in the presence of additives, a reduced friction layer, soap or polymer forms from a reaction between aluminum and the additive or from an additive by product [146-150]. However, Mark A. Nicholls et.al. [137] document that ZDDP does not perform well as an anti wear additive on Al-Si alloys.

Many previous studies have examined the effects of combining neutral and overbased detergents with AW/EP additives like ZDDP's [127]. A few studies have reported that detergents have a deleterious effect on the antiwear tribofilm formation and the performance of ZDDP [151-153]. On the other hand, Ramakumar et.al. [154] showed that overbased detergents in combination with ZDDP provided substantial wear protection. kasper et.al. [155] reported that when neutral calcium sulphonate was combined with ZDDP, the presence of the detergent only had a minor effect on the AW properties of the tribofilm. It was reported that dispersants in general enhance the wear performance by speeding up the decomposition of ZDDP [156-159]. Calcium borate overbased salicylate detergents were recognized as a multi functional class of anti corrosive/anti wear additives [160]. This CB micelles additive acts as an antiwear agent by the formation of an iron borate glass tribofilm material [161]. K Varlot et.al. [162]

reported that when ZDDP and Calcium Borate (CB) additives are used together in the lubricant used in the sliding test, long chain calcium and zinc borophosphate glass tribofilm is formed. They suggest that the role of viscous flow of the magma state glass tribofilm above its glass transition temperature seems to be a main contribution to the antiwear mechanism under mild wear conditions. They reported that the combination of ZDDP with CB additive did not exhibit good antiwear properties. They propose that the presence of borate core seemed to have had a negative effect on the antiwear properties of the additive. The antiwear properties were worse than that exhibited by the combination of ZDDP and calcium sulphonate detergent. Phosphorus- sulphur (P-S) additive based oils have been used for generating tribofilms for protection against high wear, especially in gears [106]. It was reported that a dispersed borate (B) additive in mineral oil produced much higher wear resistance and load bearing capacity than the conventional P-S lubricants [163]. Borate additive-enriched oil lubricants produce durable tribofilms that improve both friction and particularly the wear properties of sliding steel surfaces at elevated temperatures [164]. The alkali borates result in the formation of tribofilms containing borate glass which produce the high load bearing ability and these tribofilms have a faster rate of formation and replenishment [106]. Due to the electrical charging of the sliding interfaces, there may be migration of the charged borate particles at the surface. This causes the formation of a protective borate rich layer by electrophoresis and this layer is many times thicker than the tribofilms formed by traditional P-S lubricants [165]. The relatively higher wear resistance and endurance of the borate-enriched lubricants is attributed to a hard borate glass phase [106] and the

strong attachment of the tribofilms to the steel surfaces through hydrogen bonds between borate hydroxyl groups and the hydrated iron oxide layer [165]. The good mechanical properties and strong adhesion of borate tribofilms to metal surfaces make them ideal for boundary lubricated mechanical components operating at elevated temperatures. A critical B concentration and an elevated temperature (100 °C) are required for the formation of antiwear borate tribofilms [101]. Many other borate enhanced additives have been studied for enhancing tribofilm resistance [137,166,167]. It was reported that sulfurized and nonsulfurized organo borates combined with dibutyl-tin-dilaurate exhibit excellent antiwear synergism [125]. Other studies showed that borate sulphonates degrade the wear performance [168].

Jeng et.al. reported that the incorporation of molybdenum dithiocarbamate (MoDTC) into P-S gear oil reduced friction between the steel surfaces sliding in the mixed and boundary lubrication regimes due to the formation of a boundary film containing molybdenum-sulfur compounds [169]. Other people [170] have shown that equi-molar concentration of ZDDP and MoDTC in base oil yields optimum reduced friction, while M.I. De Barros et.al [171] report that MoDTC + ZnDTP containing oil produces mainly shorter chain metal polyphosphate tribofilms in addition to ZnS and MoS₂. They confirm that the formation of MoS₂ is enhanced by the presence of ZnDTP due to the synergistic effect of ZnDTP on the decomposition of MoDTC molecule. C. Grossiord et.al. [124] studied the friction-reduction mechanism of MoDTP additives by performing ultra high vacuum (UHV) tests on a previously formed MoDTP tribofilm. They observed centirange friction which was attributed to a very thin MoS₂ rich transfer

film and concluded that a few sheets of MoS₂ are sufficient to produce very low friction. Super low friction ($\mu < 0.01$) is observed with a MoS₂ film of very high purity. A study on interaction between MoDTP and succinimide (dispersant) additives reported that amine plays a fundamental role in inhibiting the MoDTP tribofilm formation [131]. J.M Martin et.al. [109] studied transfer films and friction under boundary lubrication for organo molybdenum compounds. They reported that the reduction in friction was associated with the transfer of highly dispersed MoS₂ as isolated sheets from the tribofilm to the slider.

Ceramics are known to display chemical inertness in most aggressive environments. But in tribological dry contacts, the ceramic friction surfaces reach interface temperatures much higher than those obtained in metallic-metallic sliding contacts which makes the ceramic sliding interfaces vulnerable to chemical reactions, phase transitions and other reactions [172]. Thus a suitable environment for generation of tribofilms is created without the need of any lubricant or additives. It has been established that the effect of loose wear debris and the solid surface layers formed during sliding on wear resistance is more significant than the bulk material [173-177]. Therefore the solid layer tribofilms play an important role in tribology applications. In the case of ceramic tribosystems it has been shown that the wear debris generated during dry sliding remains between the surfaces and facilitates tribofilm formation which plays a decisive role in wear resistance in the severe wear regime of ceramics [178,179]. Adam Blomberg et. al. [172] have studied the wear and tribofilm formation for different ceramic pairs. It was reported that the presence of water in ceramic sliding interfaces

reduces the friction and wear, probably due to tribochemical formation of hydrated layers which act as solid lubricant [180]. But water may also promote rapid crack growth on some ceramics, therefore leading to accelerated wear [181]. T. Aizawa et.al. [182] studied the self lubrication mechanism in titanium based ceramic coatings (TiN, TiC) on cutting tools. They report the formation of robust and lubricious oxide tribofilms in the presence of chlorine atoms which promote the in situ formation of intermediate titanium oxides to preserve the friction and wear properties.

In a study on ceramic hip joints, Jun Kusaka et.al. [183] reported smooth surfaces covered with a tribofilm for alumina, silicon carbide and silicon nitride tribo pairs. In case of alumina, the tribofilm was proposed to be composed of aluminum hydroxide [184] produced by tribochemical reaction, while that of silicon carbide and silicon nitride was thought to be composed of silicon dioxide hydrate produced by different tribochemical reactions in each case [185]. P. Larsson et. al. [181] reported that B_4C forms tribofilms even under tough test conditions which results in relatively smooth tribosurfaces. In other studies Rabinowicz and Imai [186] investigated the frictional properties of B_4C . They report the formation of a boron oxide (B_2O_3) layer during sliding which becomes lubricious above 650 °C and produces a low friction value.

Diamond like carbon coatings (DLC) are known to exhibit good wear resistance and low friction in dry sliding conditions. H. Ronkainen et.al. [187] investigated the wear behavior of hydrogenated and hydrogen free carbon coatings deposited on stainless steel substrates by conducting pin-on-disk sliding tests. They report the formation of a rather thick tribofilm on the pin wear surface in both the cases. The tribofilm effectively

reduced the coefficient of friction in both the cases and wear of the pin significantly in the case of hydrogenated coatings and to a very small extent in the case of hydrogen free carbon coatings. The tribofilms formed on the pin consisted of pin material, carbon, oxygen and hydrogen. Previous studies on DLC coatings [188,189] reported that addition of commercial AW or EP additives to poly-alpha-olefin (PAO) oil significantly improved the tribological properties by the formation of a tribofilm which was composed of coating material constituents and additive reaction products. B. Podgornik et.al. [190] reported that the concentration of additive has a major influence on the tribological behavior of DLC coated steel surfaces. They suggest that a lower EP additive concentration may give better wear performance contrary to the general rule for steel/steel surfaces.

4.5. Summary

In this section, we have reviewed some basic concepts of tribofilm generation and discussed in detail about the various additives used in lubrication today. The different tools of tribofilm characterization have been briefed. The tribofilms have been classified and an in-depth study of previous research carried out on tribochemically formed films has been reported. The various useful properties of the tribofilms have been summarized and the different tribosystems which potentially develop tribofilms have been looked at in brief. The mechanisms of tribofilm formation in certain tribosystems have been studied. The various factors affecting the growth kinetics and anti-wear properties of tribofilms have been detailed.

CHAPTER V

REGENERATIVE TRIBOFILMS

5.1. Limitations of Pin-on-Disk Tribometer

It has already been seen that rail wear involves various contact modes. The reciprocating module tribometer can realistically simulate the sliding contact of the rail gage/flange in the laboratory. However, to study the top-of-the-rail contact, i.e. a rolling-sliding mode, this configuration cannot be used. Therefore a new contact mode has to be designed which can impart the facility of a rolling-sliding contact with control on parameters like slip ratio. This would facilitate an apparatus for studying the total rail wear process in laboratory simulated conditions.

5.2. Dynamic Wheel/Rail Contact Mode Simulator

The approach used in this research was to apply the principles of friction, wear, and lubrication to devise a method to produce regenerative super-hard and wear-resistant tribofilms. This was achieved through formulation of special lubricants with functional nanoparticles and experimental simulation of the rail wear in laboratory using a modified tribometer and the custom designed lubricants.

An illustration of the novel rolling-sliding modification incorporated into the commercial reciprocating tribometer is shown in Figure 28. A wheel (made from rail wheel material) is mounted on an axle in a tight fit by a locking key way. The axle is supported on two precision roller bearings at the ends which provide a free rolling

condition for the wheel. The slip-ratio can be controlled by using the two set screws provided on either sides of the wheel. A desired normal load could be applied along the axis of the wheel. A modified sample holder (Figure 29) was also designed to allow more vertical clearance for the rolling contact and a greater horizontal traverse distance for the wheel. Figure 30 shows the lubricant application method and a comparison of the experimental sliding and the rolling-sliding contact modes.

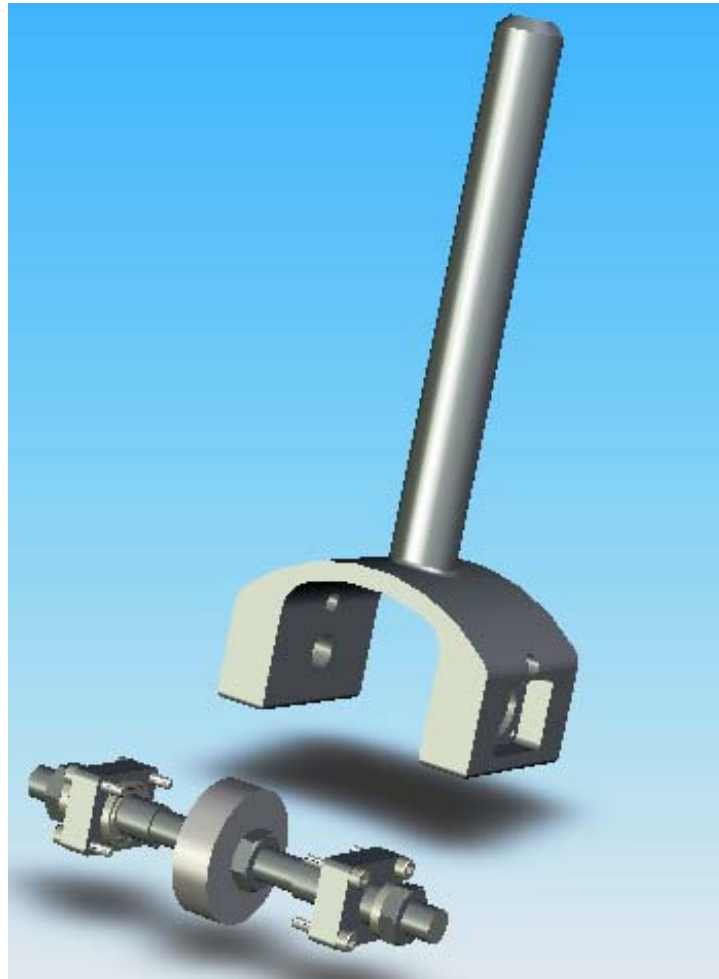


Figure 28: The rolling contact modification in the commercial pin-on-disc tribometer.

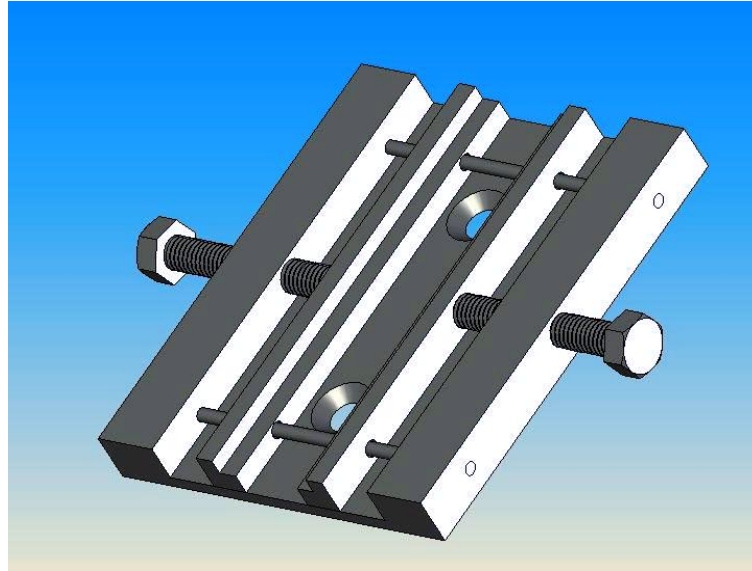


Figure 29: Illustration of the modified sample holder assembly

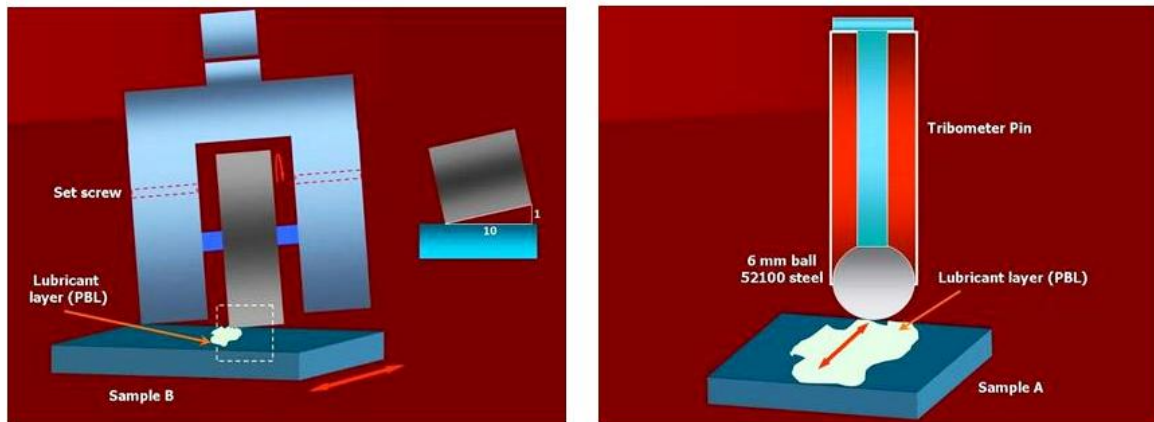


Figure 30: Experimental contact modes showing lubricant application method

5.3. Materials and Methods

5.3.1. Sample Preparation

The samples used for this study were made of rail grade steels supplied by Rocky Mountain Steels (Colorado). The as-received samples were cut from two different parts of the rail, the top of the rail (rail head) where the wheel/rail contact mode is rolling with or without slip; and the rail gage flange, where the wheel/rail contact mode is pure sliding. Figure 31 shows the locations in the rail from where the samples were cut. The wear test samples were prepared by cutting small rectangular sections from the as-received samples. All processed samples were smoothed with 600 grit emery paper to obtain a consistent surface finish of 0.144 μm average roughness. The average Vickers hardness of the polished substrates was 446 ± 20 HVN. The composition of some major elements (in wt %) of the samples used in sliding and rolling tests are shown in. Sample A was used for sliding tests and sample B was used for rolling tests.

Table 5: Composition of samples in weight percent of individual elements

	C	Mn	P	S	Si	Cu	Ni	Cr	Fe
A	0.81	0.98	0.012	0.013	0.28	0.30	0.11	0.23	balance
B	0.80	0.98	0.016	0.012	0.29	0.24	0.08	0.23	balance

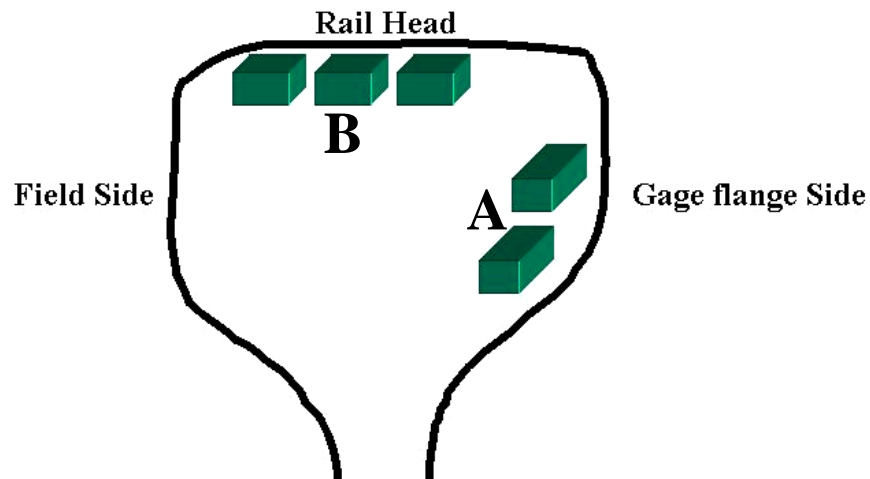


Figure 31: Schematic showing the locations in the rail from where the samples were cut

5.3.2. Tribology Tests

Tribofilms were generated under sliding and rolling conditions using a modified ball-on-flat tribometer (CSM Instruments). Friction and wear tests were carried out in lubricated conditions. A boundary lubrication regime was maintained. The general experimental setup illustration is shown in Figure 32. Samples A and B were used for pure sliding and rolling tests respectively. Dry scratch tests were performed on the sliding tribofilm to assess the wear resistance. The different tribo-tests are discussed in detail below.

5.3.2.1. Material Formulation

Additives were selected for making a lubricant. This custom-named chemical compound mix or lubricant was trade marked as PBL. Different particles in micro to

nano-sizes were mixed in an organic matrix. The major elements are Al, Si, and Fe. Additional information is withheld for patentable reasons.

5.3.2.2. Sliding Test

The sliding contact mode of the rail/wheel interface was simulated in the lab by using the reciprocating module of the tribometer. An illustration is shown in Figure 30. The static sliding partner was an AISI 52100 chrome steel ball of 6mm diameter. Pure sliding is achieved when the ball is fixed rigidly in the tribometer pin and has only one degree of freedom, to slide on the sample. An initial dry pre-test was carried out on a standard steel sample mirror polished with 1200 grit emery paper and smoothed with 0.05 μ m alumina slurry on a microcloth® from Buehler. The purpose of the pre-test was to generate an initial wear scar on the ball to control the initial normal contact stress for the real wear test. The conditions used for the pre-test were: 5N normal load, 1min sliding time, 5 cm/s sliding speed. The average wear scar thus produced was measured as 245.38 μ m which corresponds to an initial nominal Hertzian stress of 0.423 GPa under the conditions used for the real test. This stress is representative of the contact stress condition in the rail/wheel flange. The test sample A, and the contact partner were cleaned with isopropyl alcohol before starting the wear test. 0.1 ml of the lubricant (PBL) was applied as a layer on the sample/contact partner interface before the test.

The sample was heated to a stable temperature of 100 ± 1 °C using a pre-calibrated heating apparatus before starting the test. The humidity was maintained at $55 \pm 5\%$. A normal load of 20 N was applied to generate an initial contact stress of 0.423 GPa. The total duration of the test was 9 hours. The sliding test was paused every three hours to add lubricant (0.1 ml PBL) in order to maintain a lubricating layer. Friction coefficient was measured against time for all tests. A distance of 1031.33m was traversed in the total process. Tribofilms were formed in course of time and a layered tribofilm was generated due to periodic change of lubricant. Multiple tests were carried out to check repeatability of the tribofilm formation. A distinct advantage of using the pin-on-flat configuration is that wear and deformation process can be studied under both normal and reversal load conditions. At both ends of the wear track formed due to the reciprocating pin, the sliding direction is reversed. Hence the subsurface and surface studies at the cross-section of a wear track can reveal insights into operative wear mechanisms.

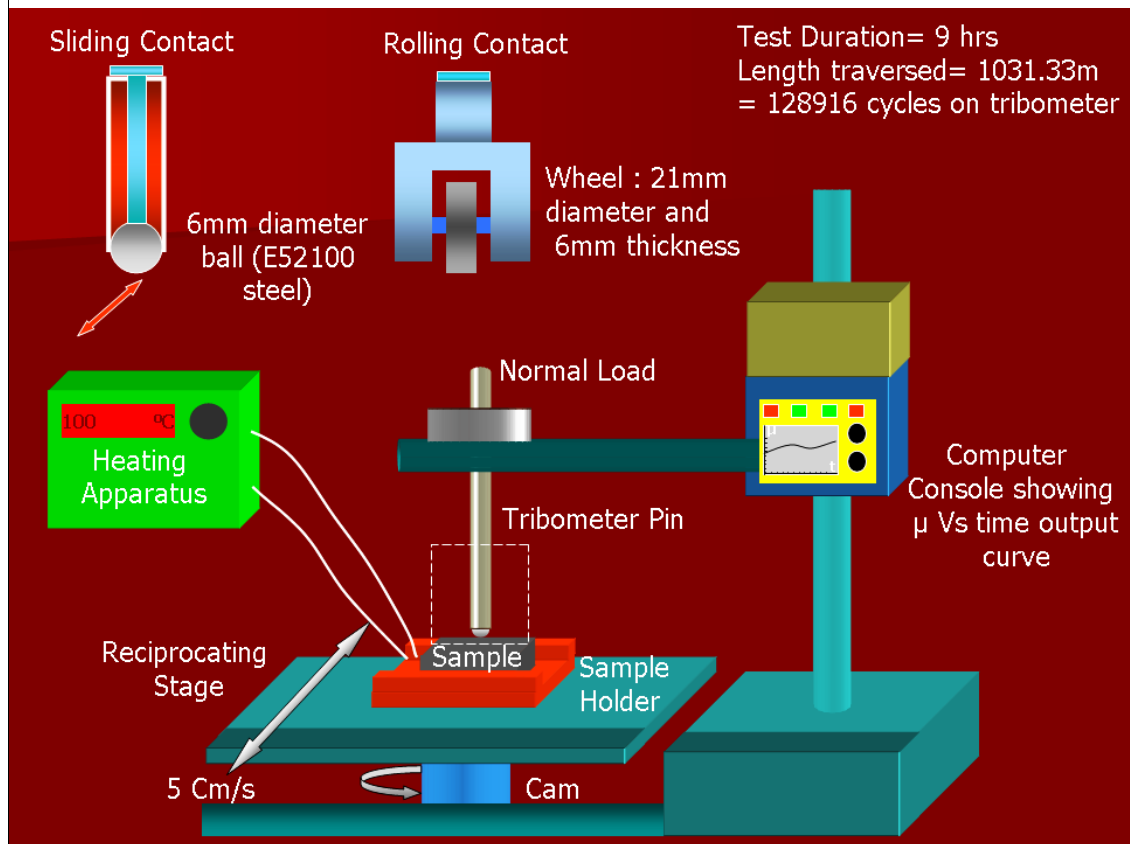


Figure 32: Tribometer illustration showing experimental conditions for the tribo-tests

Apart from this, the tribofilm formation mechanisms and properties can be investigated by connecting a resistance or capacitance circuit between the sample and the counter face partner. The output resistance or capacitance signal will give information on the formation and local rupture of the tribofilm with time.

5.3.2.3. Rolling Test

The rolling contact mode of the wheel/rail interface on the top of the rails was simulated in the lab by using a specially designed wheel contact that could be used with

the tribometer in place of the tribometer pin to generate pure rolling and rolling-sliding motion. Sample B was used for the rolling test. The wheel was made of high chromium steel with the following composition in weight per cent: Si 0.58 %, Cr 1.26 %, Ni 2.56 %, balance iron. The wheel was smoothed with a 600 grit emery paper. The wheel had dimensions of 6mm in thickness and 21 mm in diameter. The wheel was mounted rigidly on a central axle supported on two precision bearings at the ends of the frame, to minimize friction. This enabled a pure rolling condition to be achieved. A setscrew on either side of the frame could be used for controlling the slip. An illustration of the experimental contact mode is shown in Figure 28. The slip was calculated using the following formula (1)

$$S(\%) = \frac{(C - L)}{C} \times 100 \quad (1)$$

Where S is the slip factor, C is the total horizontal distance traveled by a point on the circumference of the wheel in pure rolling condition in one complete revolution (i.e. here equal to the circumference of the wheel). L is the actual horizontal distance covered by a point on the wheel circumference under the experimental conditions for one revolution of the wheel. The creepage in case of the twin disc machine is set by maintaining a difference between the rotating speeds of both rollers. Using the new rolling contact, slip can be easily varied in between the test to study the effect of varying slip on wear characteristics.

The wheel frame was fixed in the tribometer in such a way that the wheel contacted the sample surface at a single point. A slope of 1:10 between the wheel and the sample was realized in the final contact. In the real conditions also, the rail and wheel are made to have an inclination, usually 1:15 to 1:30 to account for conformity and achieve a point contact between the conical tapered wheel and the rail surface. Rolling motion was generated because of the back and forth motion of reciprocating stage on which the sample was fixed. The wheel was calibrated for pure rolling condition before the wear test. However, it was noted that there was a small amount of slip induced into the system due to the high contact stress condition and internal friction in the bearings. This slip was not estimated. The samples and the wheel were cleaned with isopropyl alcohol before the test. The test conditions used for the rolling test were the same as in the sliding case except for the following changes: stable temperature 59 ± 2 ° C and normal load 43.25 N which resulted in an initial nominal Hertzian stress of 1.003 GPa. 0.1 ml of PBL was applied as a layer on the sample/wheel interface before the test. The lubricant was replaced every 3 hours as in the case of sliding test. Higher contact stresses can be easily achieved by varying the dimensions of the wheel used (lower diameter and thickness). Thus, a range of normal stress conditions is possible using this rolling contact.

5.3.2.4. Scratch Test

Scratch tests were performed perpendicular to the sliding tribofilm to test the wear resistance of the film relative to the substrate. The tribometer was modified to

perform the scratch tests. A sharp steel pin with a nominal tip diameter of $74\ \mu\text{m}$ was used as the static sliding partner for the scratch test. The experimental conditions used for the scratch test were: 1 N normal load generating an initial nominal Hertzian stress of 0.123 GPa, 0.3 mm/s sliding speed, scratch time 41 sec. An illustration of the scratch test is shown in Figure 33.

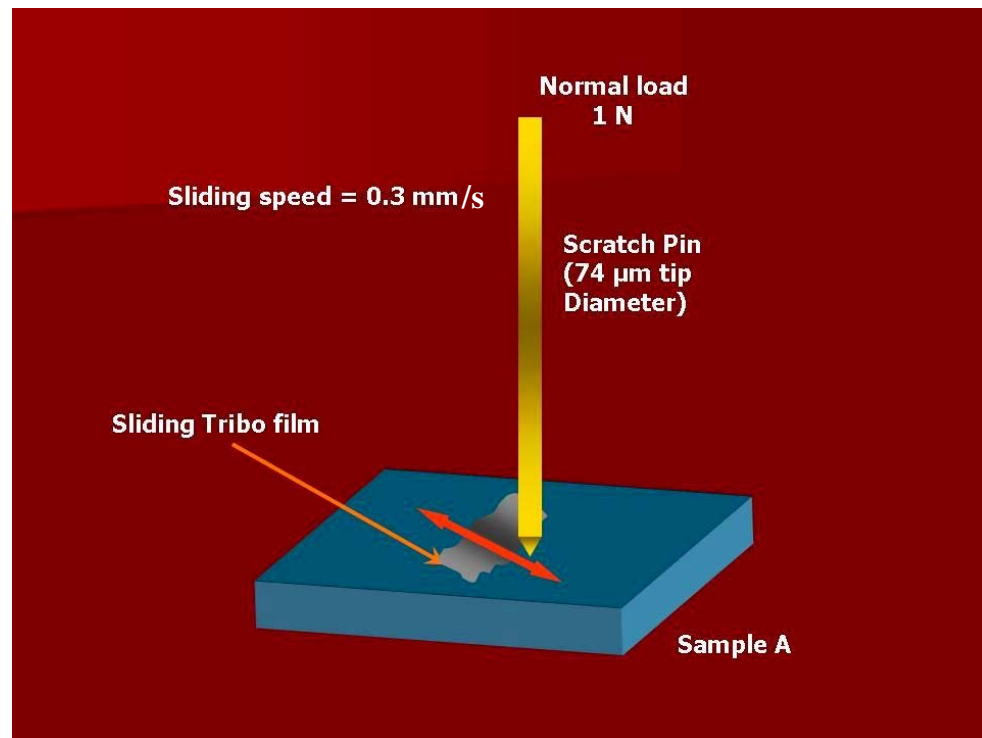


Figure 33: Depiction of the micro scratch test

5.4. Tribofilm Analysis

5.4.1. Surface Characterization

The surface and cross-sectional morphology of the tribo films were characterized using a JEOL-JSM 6400 scanning electron microscope (SEM) and a JEOL 2010 transmission electron microscope (TEM). Secondary electron acquisition mode (SEI) was used for all SEM micrographs. Bright field imaging was used for all TEM micrographs. The TEM sample was prepared by using the standard ultramicrotomy process with the sample embedded in a very hard epoxy formulation. The scratch wear track was also examined using the SEM. Chemical characterization of the tribofilm was done using X-ray photoelectron spectroscopy (XPS) and Energy dispersive X-ray (EDX). All samples were cleaned thoroughly in an ultrasonicator using isopropyl alcohol before the post-test analysis.

5.4.2. Mechanical Characterization

Micro hardness tests were carried out on the cross-section of the sliding tribofilm. The cross-section sample was made by embedding the sample with tribofilm in an epoxy mould using the sandwich technique. The cross-sectioned sample was smoothed with 1200 grit emery paper and polished to a mirror finish using slurry of 0.05 μm sized alumina particles on a on a microcloth[®] from Buehler. The average surface roughness was around 0.02 μm . The Vickers micro hardness was tested using a Fischer scope HM 2000 hardness tester. A Federal[®] Surfanalyzer 5000 was used to measure the average roughness and surface line profile of the tribofilm.

CHAPTER VI

RESULTS AND DISCUSSION*

6.1. Tribofilm Morphology

The generated tribofilms were typically rough ($\sim 0.635 \mu\text{m}$) with certain smooth areas. It was observed that the roughness decreased with the increase of ambient test temperature signifying the higher reaction energies involved in the latter case. Figure 34 shows a profilometer line scan of the sliding tribofilm at 25 °C and 100 °C ambient temperatures. However, the film covered almost the whole wear track in both the sliding and rolling cases, an example of which is shown in Figure 35. In case of rolling-sliding, the film also formed appreciably on the contact area of wheel as depicted in Figure 36. In the case of sliding, the effect of the substrate tribofilm was to wear out the counter face pin significantly as seen by the grooves on the wear scar of the ball illustrated in Figure 37. Remnants of a transfer film are also seen in the zoom inset. A closer look at the rolling-sliding and sliding tribofilm morphology in comparison to the bare substrate is shown in Figure 38. Compare the incomplete tribofilm generated at 25 °C (Figure 39) to the complete one developed during sliding at 100 °C. The reasons underlying this drastic improvement in morphological quality are explained later. The cross-sectional morphology of the film was analyzed by preparing transverse sections of substrate along with the film. Figure 40 shows etched cross-sectional SEM micrographs clearly showing

* Technology developed from this research has been filed for US Patent.

the different microstructure of the film versus the substrate, which has a typical pearlitic micro structure. Tilt SEM micrographs revealed a layered tribofilm structure as shown in Figure 41. The reason for this is explained later in the proposed mechanism section.

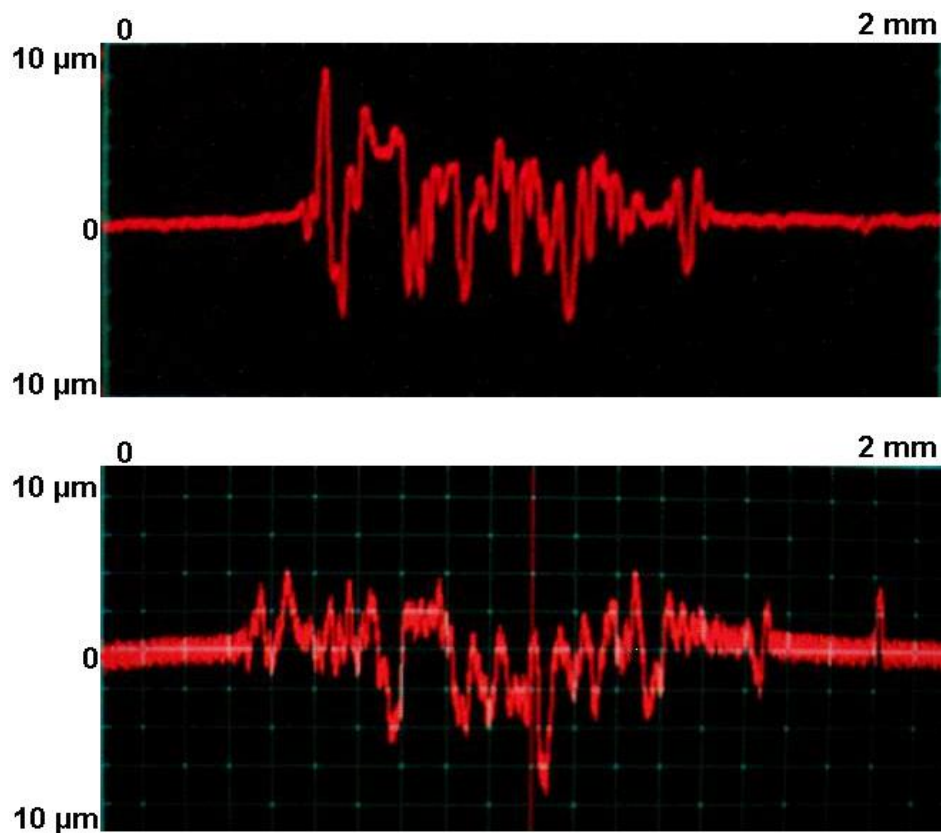


Figure 34: Profilometer line scans: a) tribofilm formed at 25 °C ambient test temperature b) tribofilm formed at 100 °C ambient test temperature

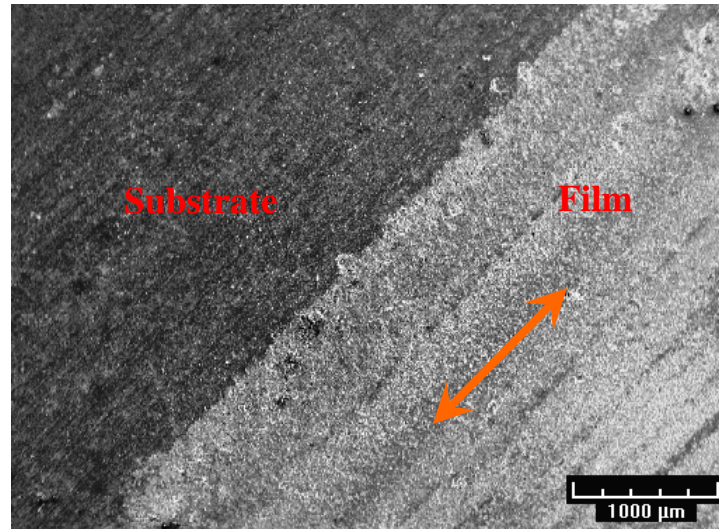


Figure 35: Part of the rolling-sliding tribofilm shown contrasted against the substrate. Arrow shows the roll-slide direction of the wheel

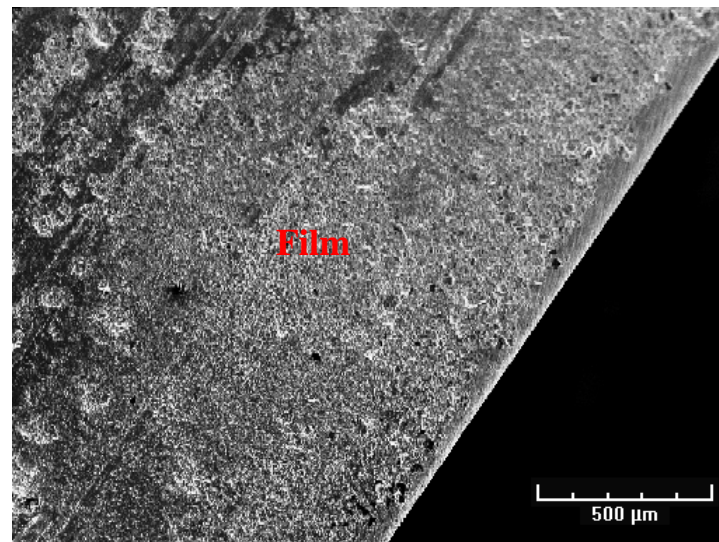


Figure 36: Contact area region of the wheel showing distinct tribofilm formation

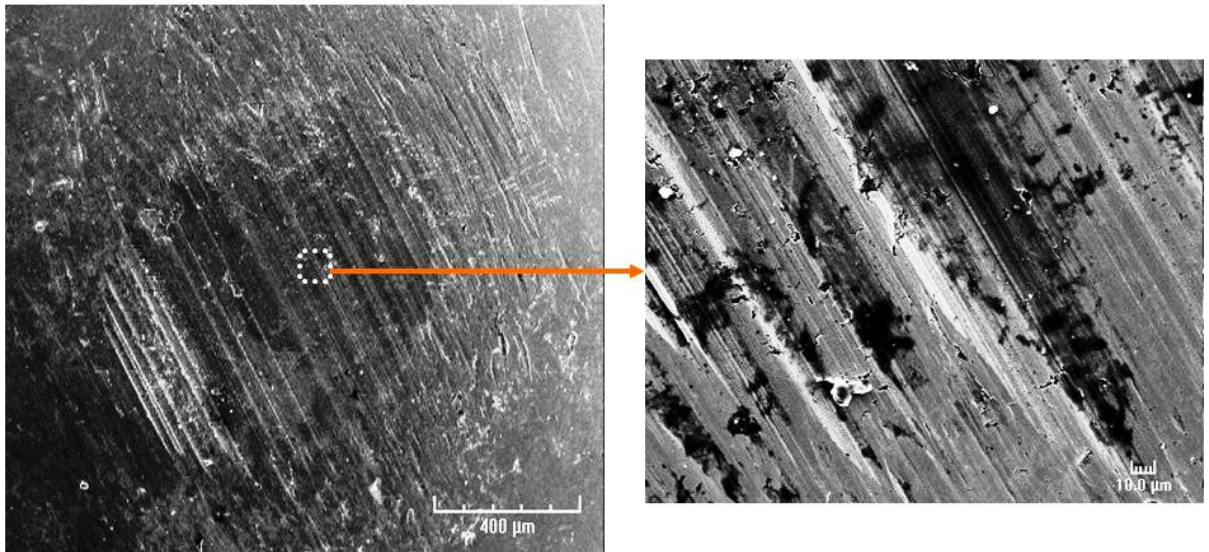


Figure 37: Wear scar of the sliding counter face ball showing abrasive grooves and transfer film remnants

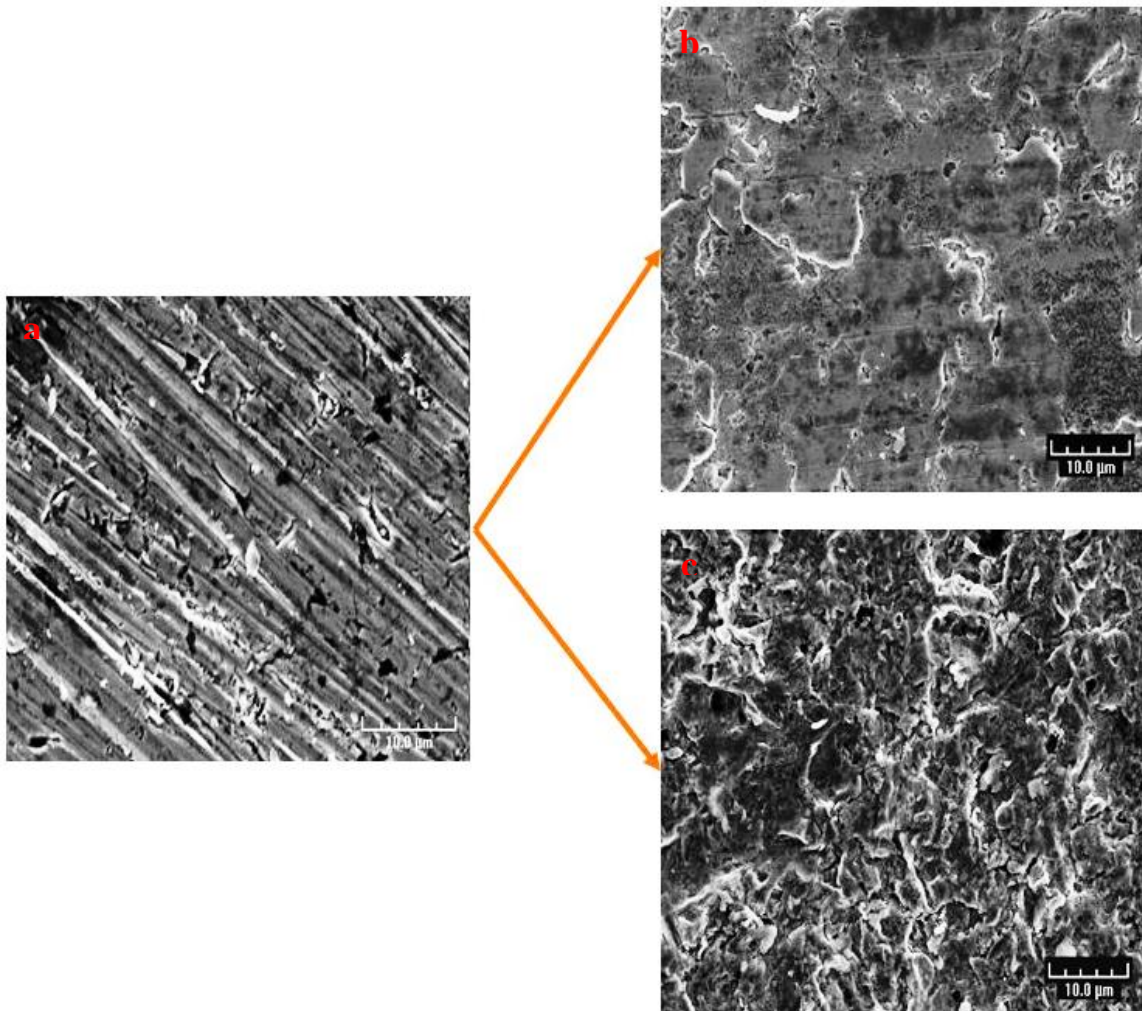


Figure 38: Tribefilm morphology: a) 600 grit emery paper smoothed substrate b) sliding tribefilm at 100 °C c) rolling-sliding tribefilm at 60 °C

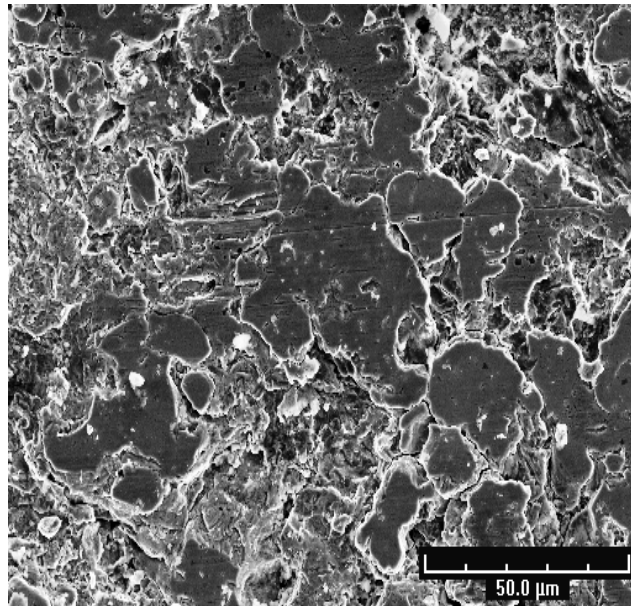


Figure 39: Sliding tribofilm produced during sliding at 25 °C

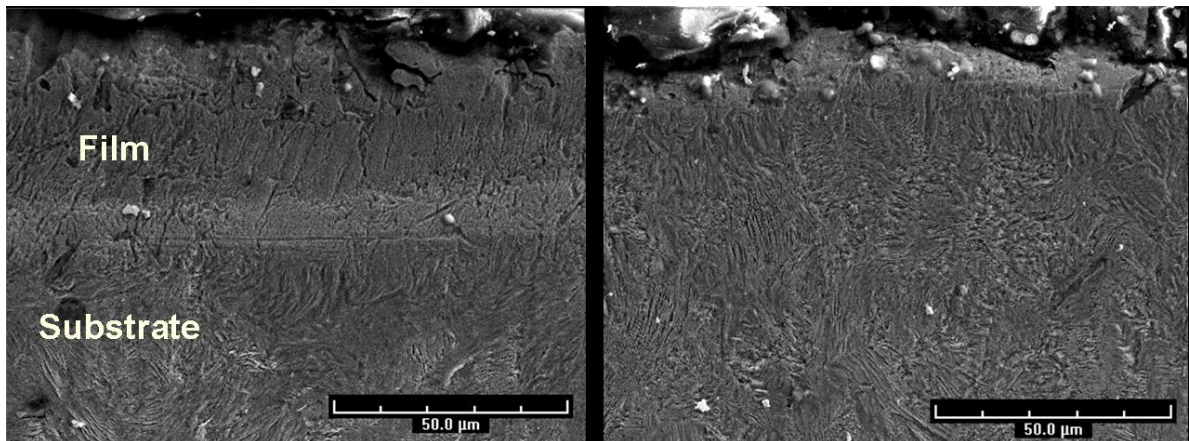
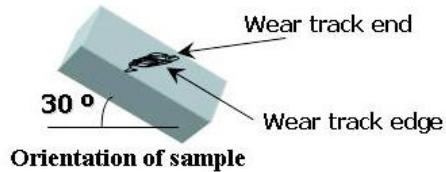
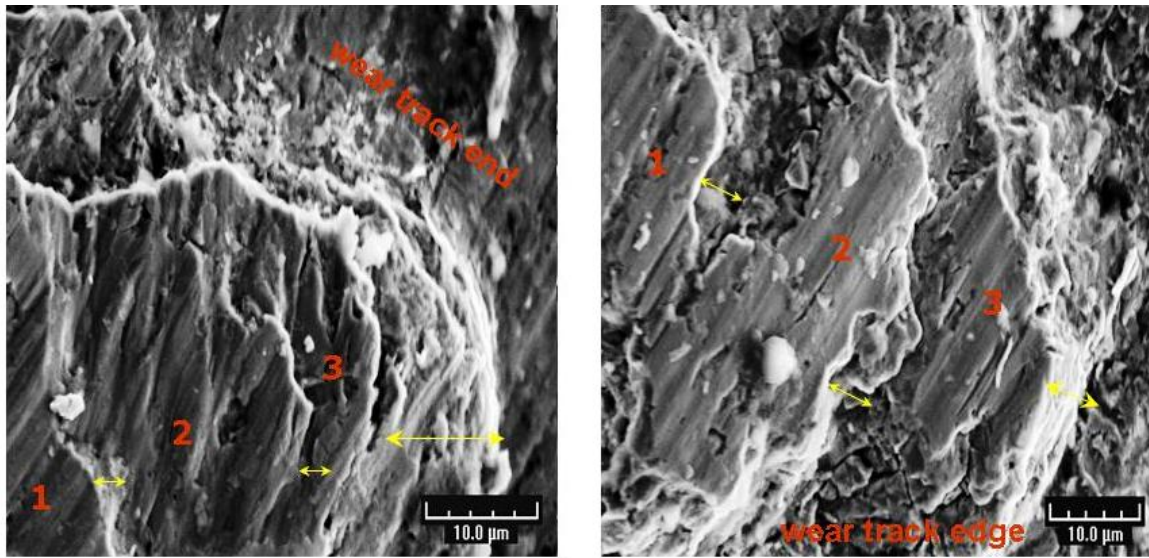


Figure 40: Etched cross-section showing film and substrate (left) and only the substrate (right)



1, 2, 3 represent the three smooth terraces of the tribofilm.

■ Represents the build up of material below each Smooth terrace
 Each time the lubricant is replenished, a new build up and a corresponding smooth terrace forms.

Figure 41: Layered tribofilm structure showing material build up and terrace features

6.2. Frictional Behavior

The friction coefficient vs. time curve for sliding test is shown in Figure 42. It is seen that the friction reaches a constant plateau with the addition of friction modifier based formulation (PBL). This behavior is representative of both sliding and rolling-sliding cases. Notice that there are sudden jumps (static friction peaks) in the smooth curve which are caused due to pause and restart of the test after every 3 hours for changing lubricant. The friction coefficient observed was low implying that the formulation is appropriate for use in gage/flange lubrication. However, the current formulation is unsuitable for the top of the rail application. This is because a minimum

friction level is required for proper traction and braking at the rail/wheel interface. The effects of modifying friction can still be seen otherwise. A selected alteration of certain friction modifying elements in the current formulation can make it potentially feasible for top of the rail application.

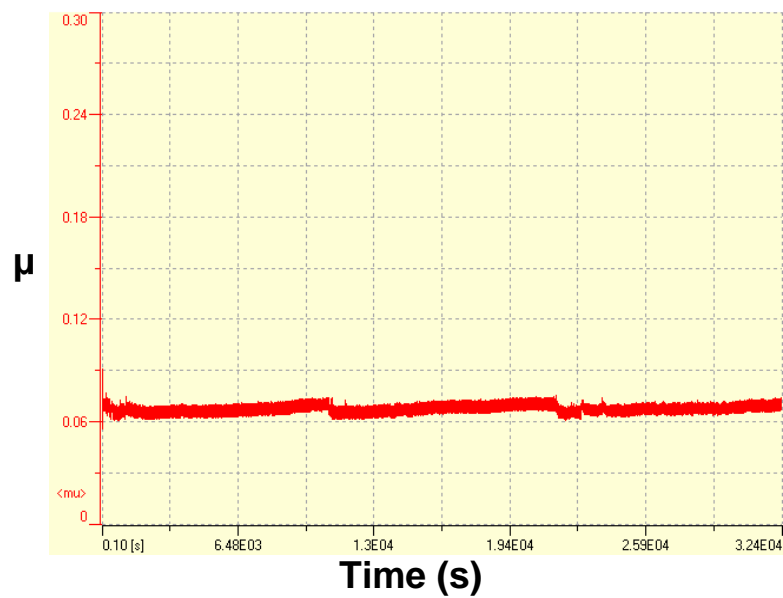


Figure 42: Friction curve during the sliding test at 100 °C for 9 hours

6.3. Hardness of Tribofilm

Figure 43 shows the micro hardness loading and unloading curves for both the film and the substrate. The SEM micrograph shows the areas of indentation. A Vickers indenter with a diamond tip and a constant load of 30 mN was used for conducting the hardness tests. It was found that the film was extremely hard when compared to the

substrate. Hardness values as high as 2700 HV were observed. The film also seemed to be conformal since there was no evident interface demarcation.

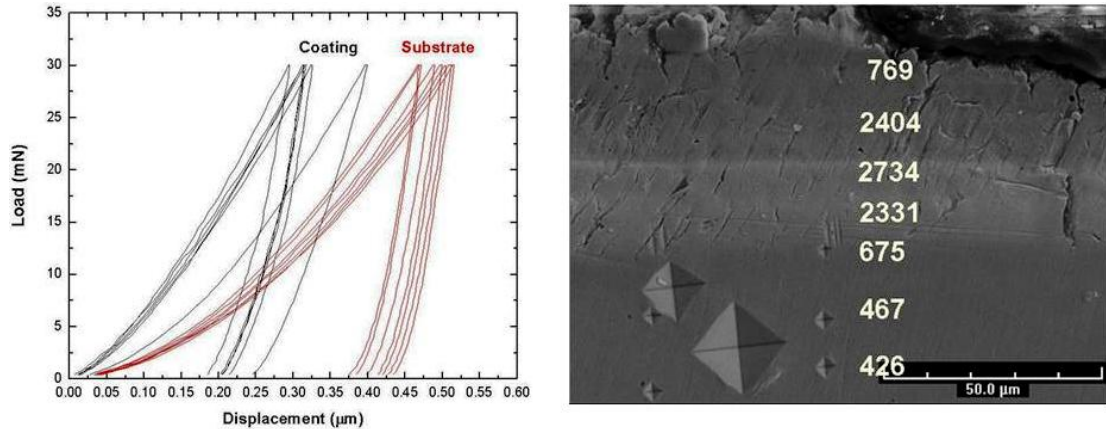


Figure 43: Micro hardness along the cross-section of the film (under 30 mN load)

6.4. Phase Transformation

TEM analysis of a small fragment from the film showed a nanocrystalline structure (Figure 44). This is fundamentally interesting because phase transformation directly affects material properties. Rapid quenching enables high rates of cooling during the sliding process. In fact one of the methods preparing nanocrystalline or amorphous materials is to cool the material at rates $>10^6$ K/s [191]. Particularly during dry sliding, the debris generated usually shows a highly amorphous nature. It is quite possible that the film generated in this experiment exhibits a highly nanocrystalline nature due to the complex non equilibrium dynamics involved. Different nano sized reaction products can

be seen dispersed within the film matrix.

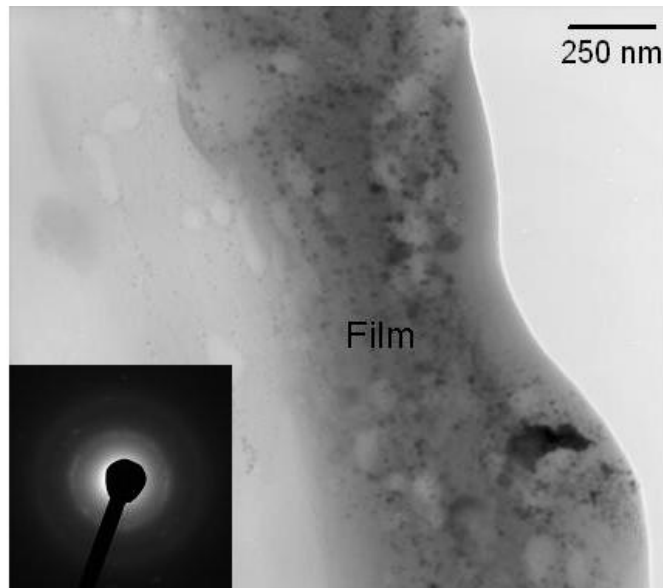


Figure 44: Transmission Electron Micrograph of a fragment of the film showing small particles impregnated in the film. Inset shows selected area diffraction pattern on the film

6.5. Scratch Wear Resistance

Figure 45 summarizes the results of the micro scratch test. The arrow shows the direction of the test (perpendicular to the film). The film showed high resilience to deformation as is seen in the SEM micrograph of the scratch track. A zoomed area on the scratch track at the border of the tribofilm showed that the film suffered no damage while the substrate showed heavy wear. The friction behavior along the arrow (scratch track) shows that the friction was higher on the film when compared to the substrate. This is a result of higher hardness or a higher roughness of the film. However, the

contributions of both these factors cannot be demarcated.

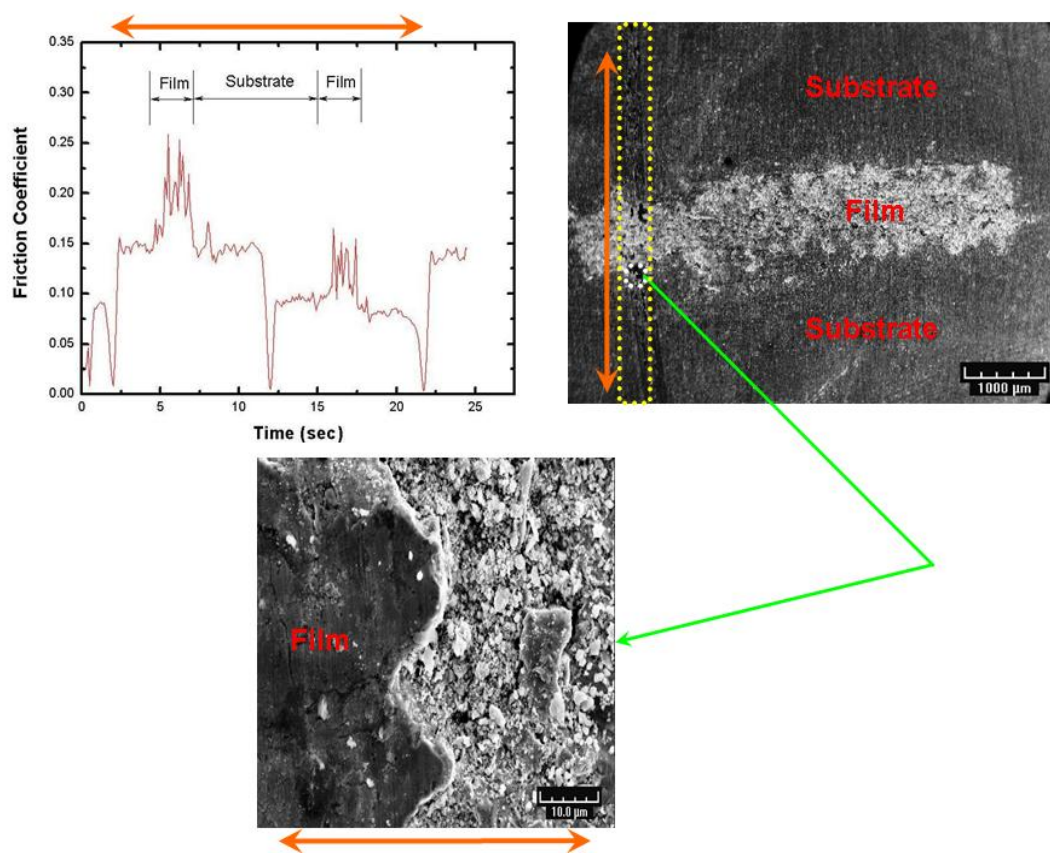


Figure 45: Scratch test on the sliding (100 °C) wear track revealing the wear resistance of the film

6.6. Tribofilm Chemistry

Chemical analysis was conducted on the tribofilm surface. The composition and the possible chemical routes were analyzed. Figure 46 shows the qualitative EDX spectra of the sliding (100 °C) and the rolling–sliding (60 °C) films. The film chemistry

was observed to have typical possible reaction products of Al, Fe, Si and C as expected.

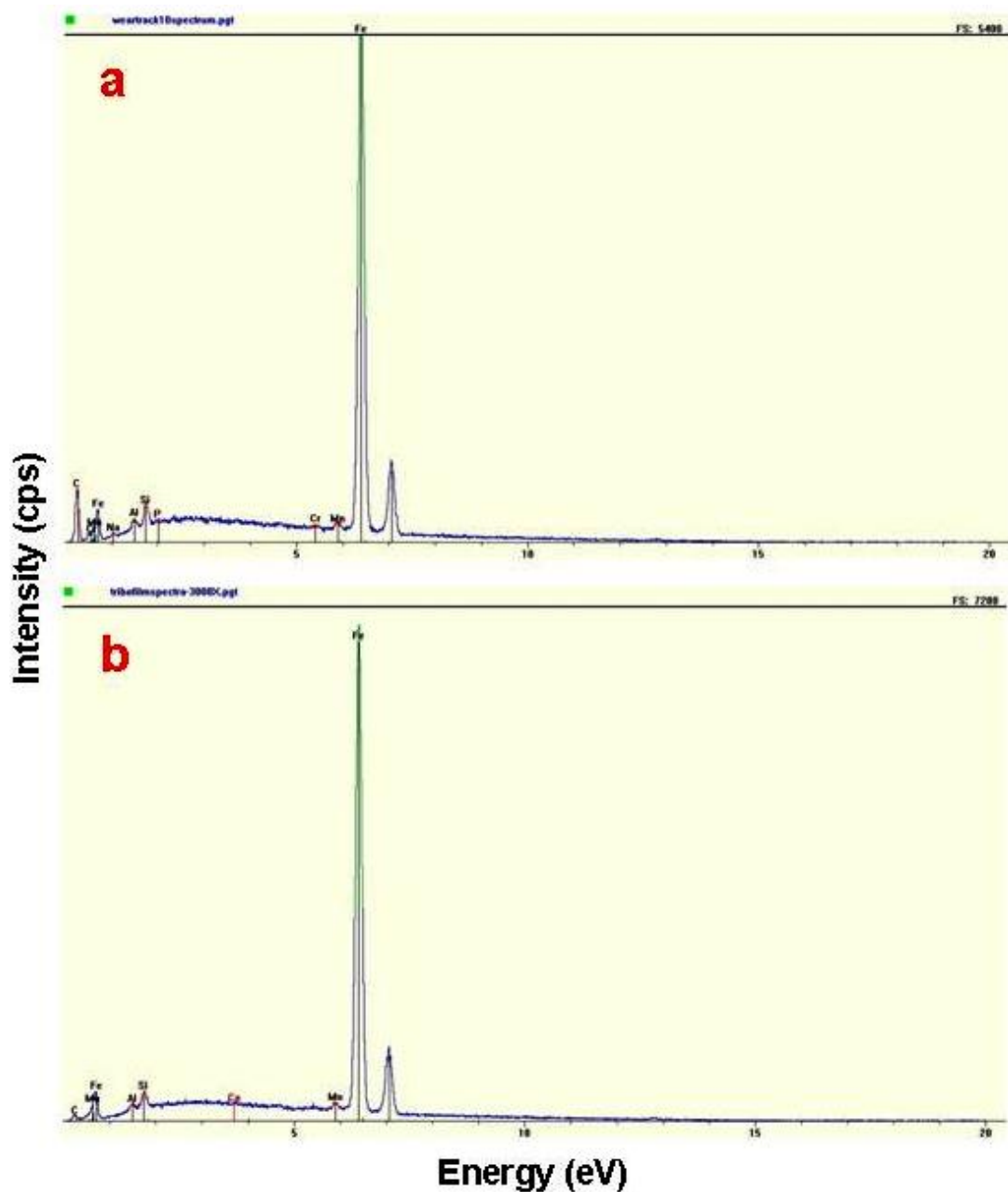


Figure 46: Qualitative energy dispersive X-ray spectra of tribofilms a) sliding tribofilm (100 °C) b) rolling-sliding tribofilm (60 °C)

To confirm the reaction products, XPS analysis was conducted on the tribofilm and the substrate (reference) respectively. An Mg X-ray source was used with a beam diameter of 500 μm . It is important to study the relative changes between the peak intensities at different energy positions in order to deduce the surface chemistry changes. The results are tabulated below for quick reference (Table 6). The corresponding XPS spectra showing different binding energy ranges are shown in Figure 47.

Table 6: Interpretation of XPS data obtained for the tribofilm and the reference substrate

No.	Binding Energy (eV)	Element and valence state	Source compound or reaction product	Remarks
a	26	Ca 3p, -3p	---	---
b	31	W -4f	---	---
c	43	Cr 3p		Reaction product of Cr from the bulk
d	48	Mn 3p		Reaction product of Mn from the bulk
e	56	Fe 3p, -3p		Reaction product. Source of iron is both from bulk and lubricant additive

(Table 6 continued)

No.	Binding Energy (eV)	Element and valence state	Source compound or reaction product	Remarks
f	74.4	Al 2p	Al ₂ O ₃	Aluminum oxide in sapphire phase due to oxidation of the Al particles
g	94.2	Fe 3s	---	Reaction product. Source of iron is both from bulk and lubricant additive
h	103.3	Si 2p	SiO ₂	Reaction product due to oxidation of Si
i	---	---	---	Confidential
j	264	---	---	Unidentified
k	277	---	---	Unidentified
l	286	C 1s	C with N C with Cl C with O	A small shift of about 1 eV shows a possible change in carbon valence state in film and substrate.

(Table 6 continued)

No.	Binding Energy (eV)	Element and valence state	Source compound or reaction product	Remarks
m	349	Ca 2p	---	---
n	398.1	N 1s	---	Contamination due to adsorption of N during nitrogen drying step in sample preparation for XPS
o	532.8	O 1s	SiO ₂	Oxidation of Si. Peak shift of about 0.9 eV observed
p	607.6	---	---	Unidentified
q	694	---	---	Unidentified
r	710.4	Fe 2p	Fe ₃ O ₄	Further oxidation of Fe ₂ O ₃
s	710.9	Fe 2p	Fe ₂ O ₃	Native oxide film on substrate
t	745	O	---	Auger peak
u	990	C	---	Auger peak

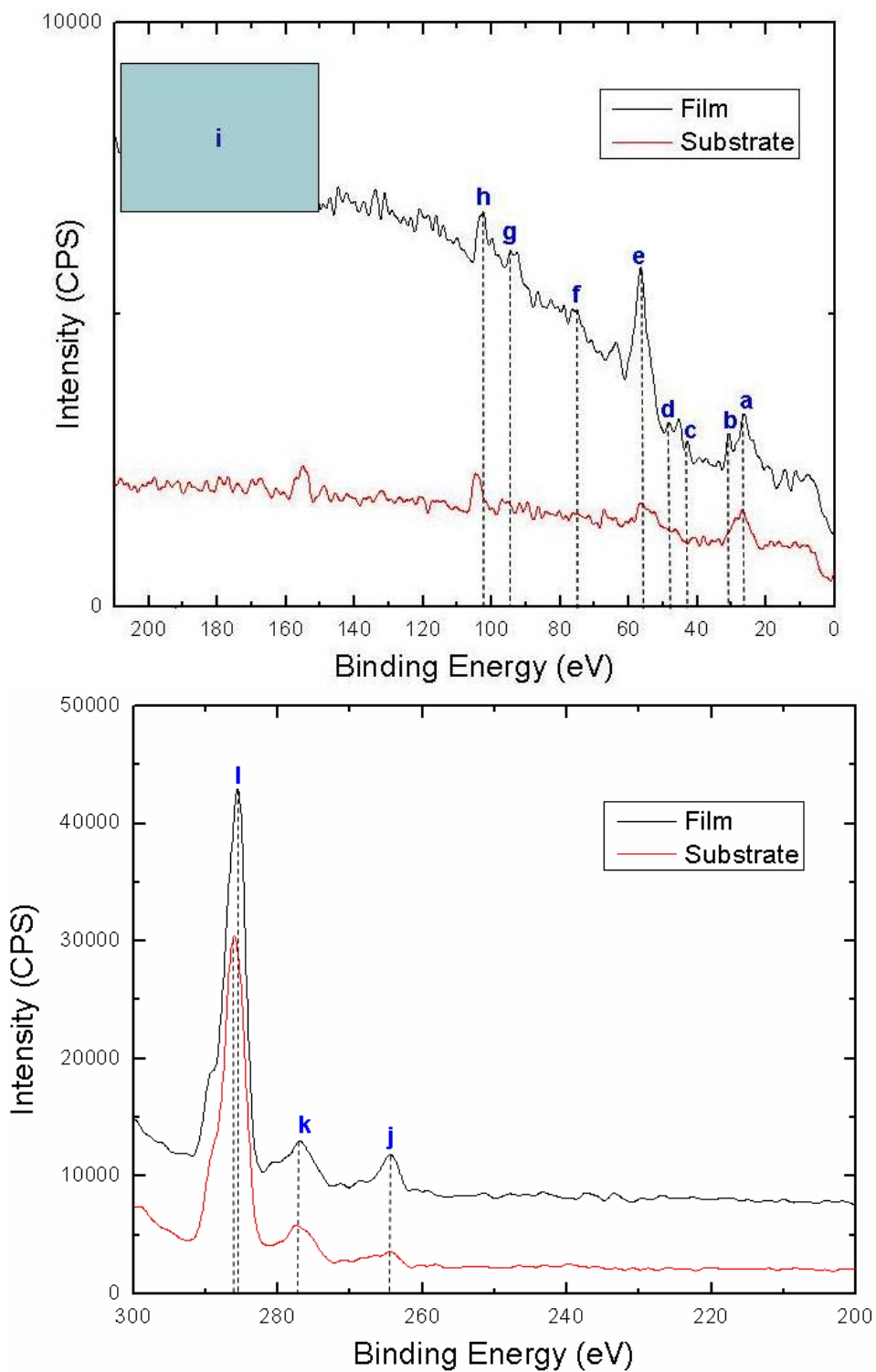
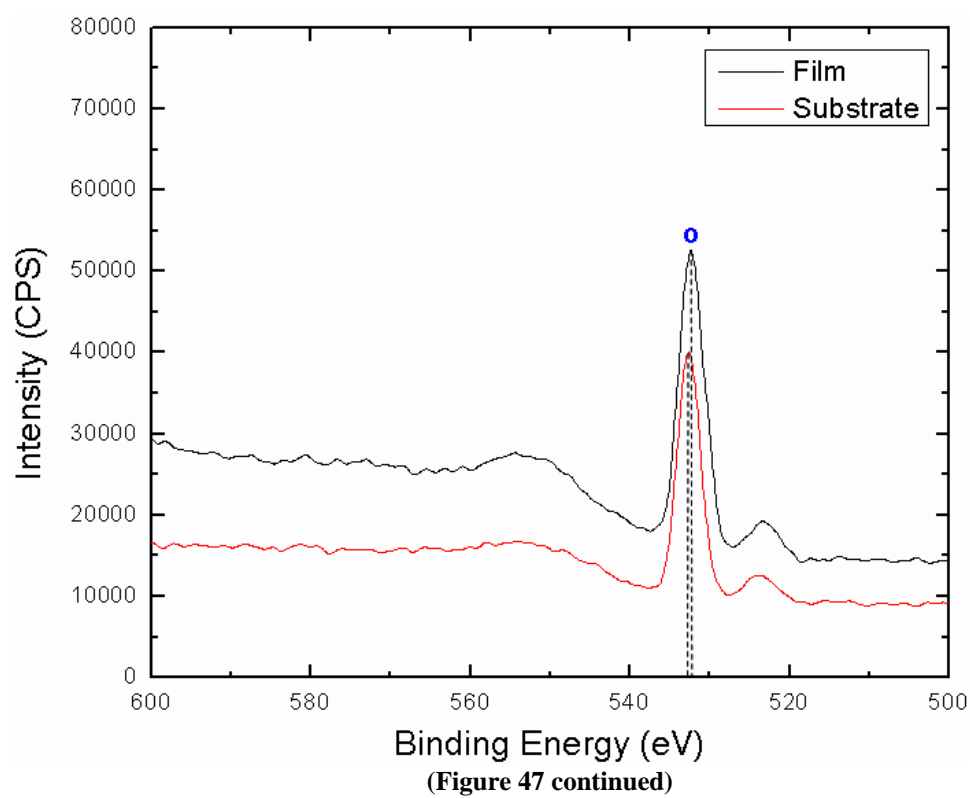
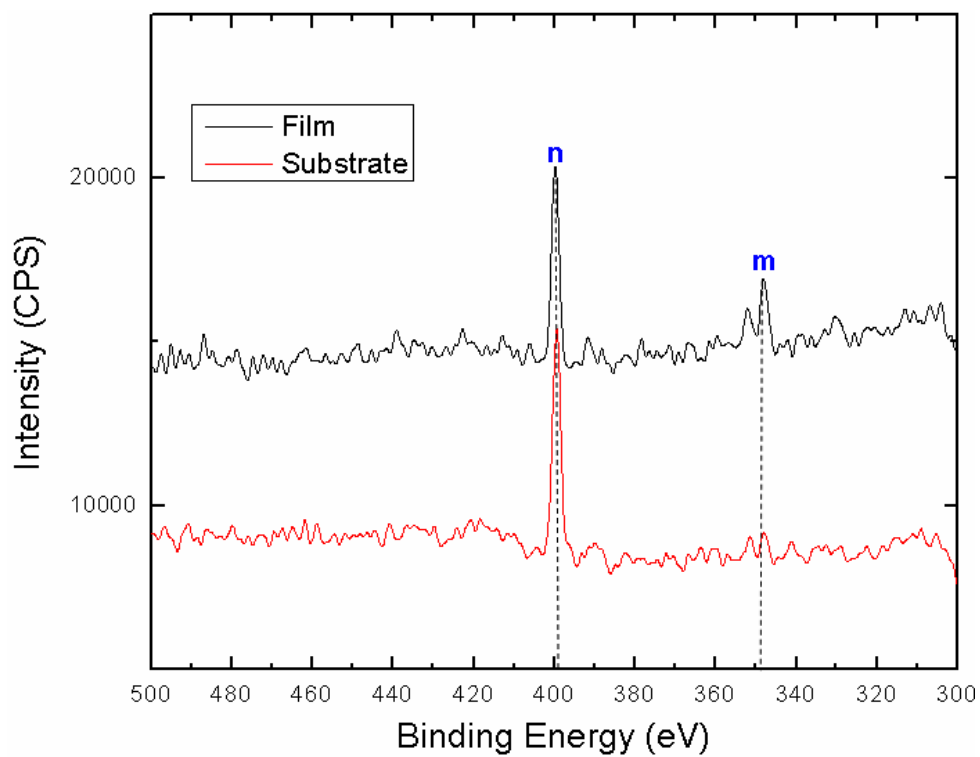
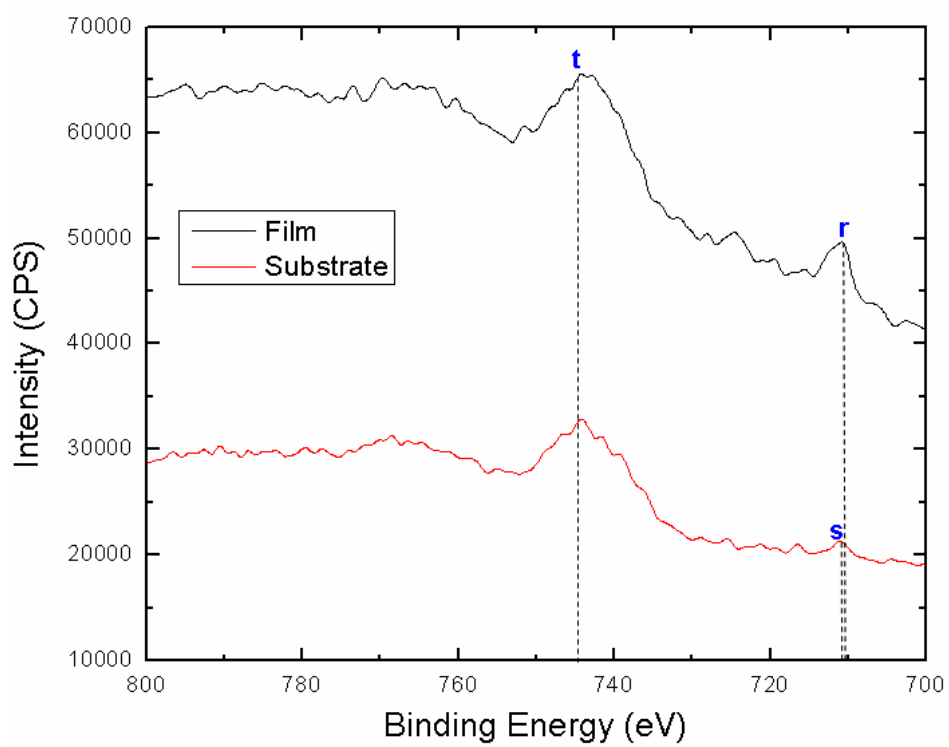
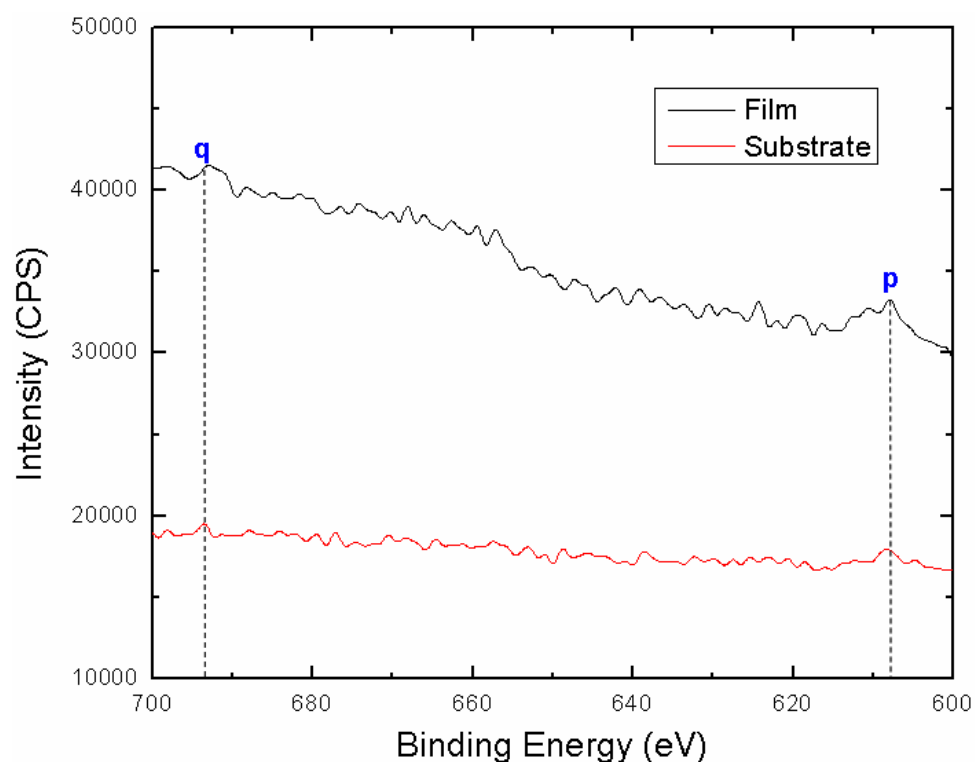
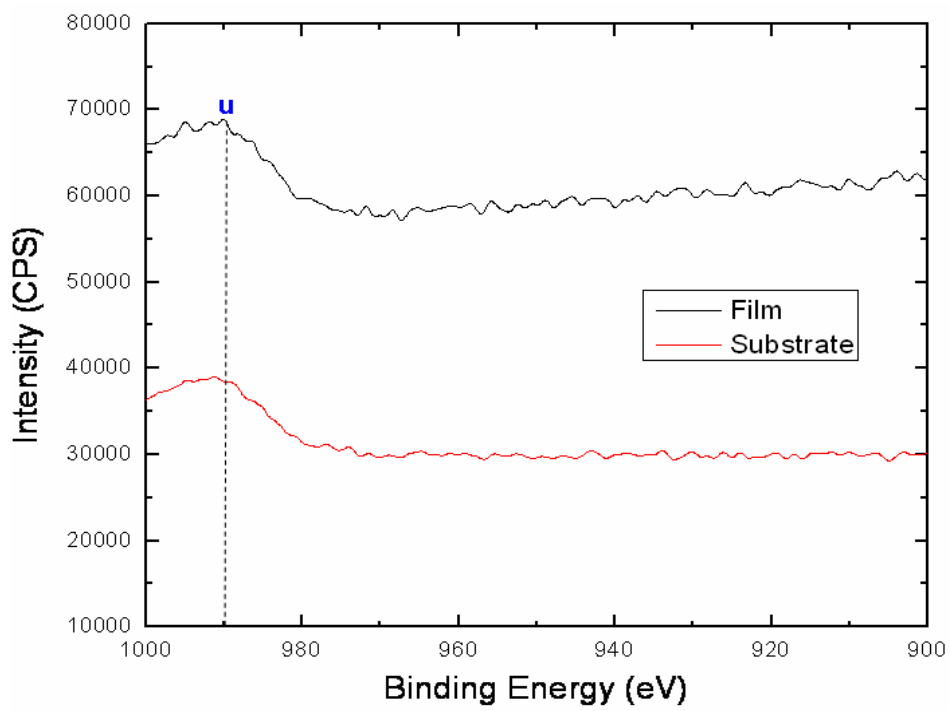
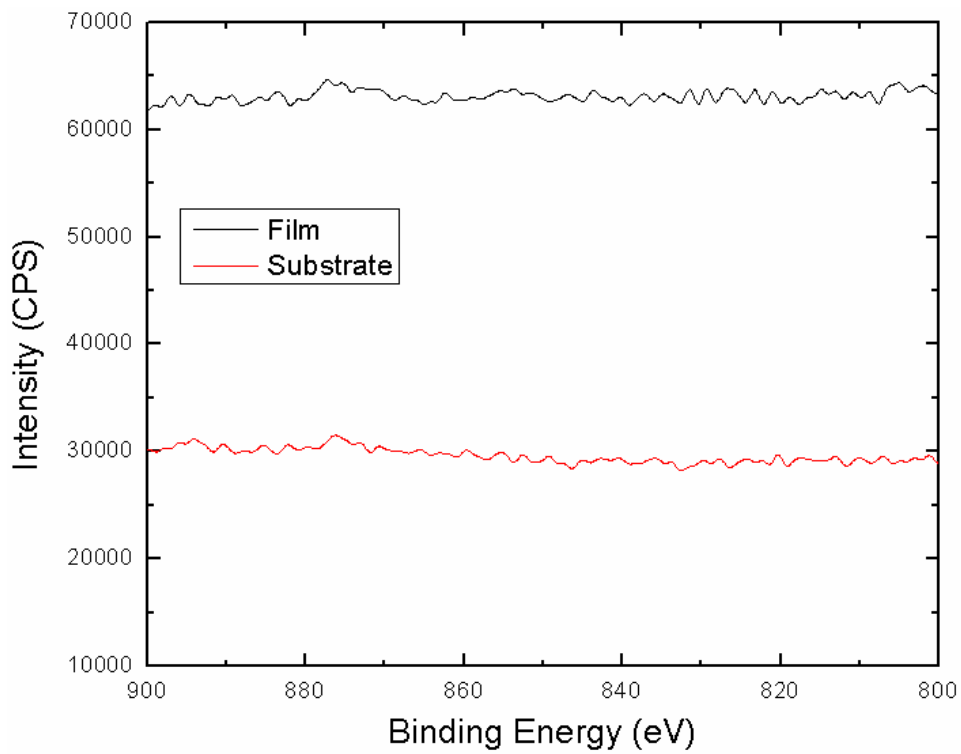


Figure 47: XPS spectra plotted on a range of binding energies (1000 – 0 eV)





(Figure 47 continued)



(Figure 47 continued)

6.7. Self Repairing Effects

Figure 48 shows a chemical map of one of the cross-sectioned samples showing the tribofilm and the substrate. Evidence suggests that a small crack had homogenously got filled with material from the tribofilm showing the property of self-repair. Similar repair on the macro-scale was also observed in other cross-sectioned samples. This supports the earlier hypothesis that the film actually grows and blends into the substrate.

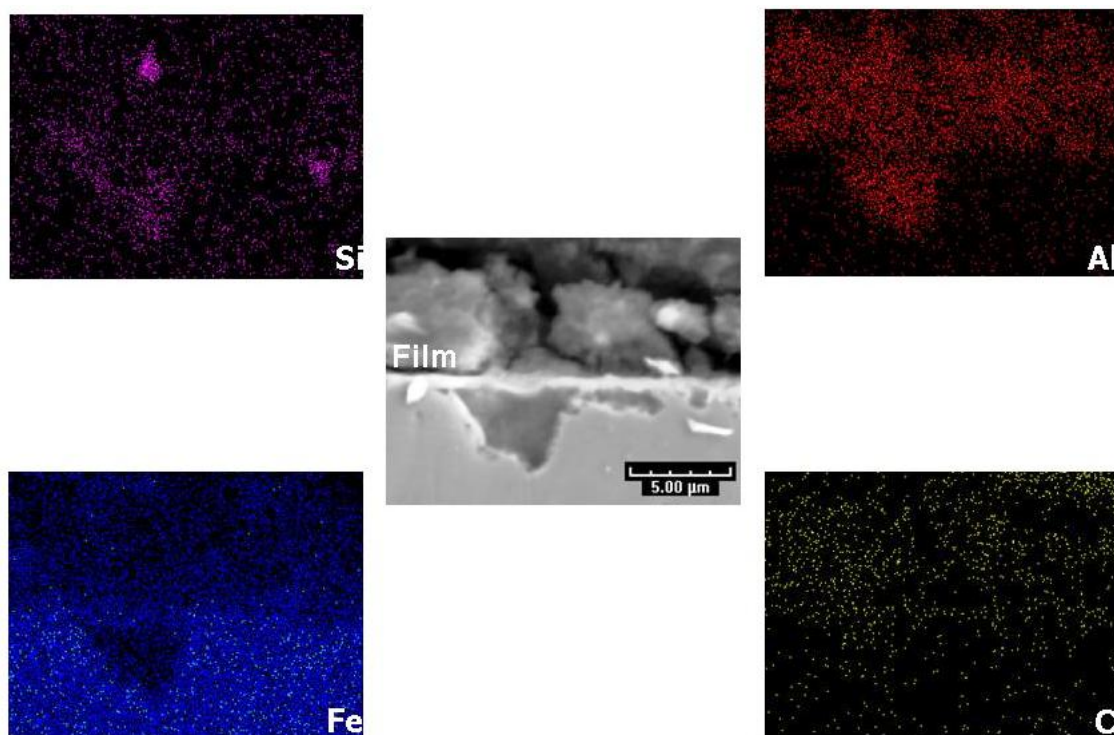


Figure 48: Chemical area map of the sample cross-section showing self-repair

6.8. Proposed Mechanism of Tribofilm Formation

6.8.1. Physical Mechanism

The physical generation mechanism of the tribofilm can be explained as follows:

- 1) As the wear process proceeds, the wear debris and the lubricant additives start reacting chemically under the influence of high energy at the interface generated by way of the chemical mechanism explained later.
- 2) The final products of these reactions start building up material over time which is also continuously being compacted under pressurized movement of the counter face. The synergy of mechanical milling, grinding, and sintering produces the tribofilm.
- 3) This continues until all the final reaction products have formed (equilibrium state reached). Then the continuous sliding motion or kneading motion (in rolling-sliding) creates a smooth “terrace” on this tribochemically built-up material.
- 4) The physical mechanism of tribofilm generation is a gradual build-up of final reaction product material with the subsequent formation of a smooth terrace.
- 5) Every time the lubricant is changed, a new layer forms over the existing tribolayer because of the same mechanism, now operative in the presence of new “lubricant fuel” for the complex physicochemical reactions. In such a manner, a “layered” tribofilm is formed over a period of time.
- 6) It was observed that the different layers exhibited good adhesion and shear strength between each other and the substrate was shown to have minimal wear (Figure 41).
- 7) It is conjectured that the layers would build up until a critical thickness is reached

when the layer's shear strength would be exceeded by the operative lateral forces. But since lubrication is a continuous process, any loss of a layer would be covered up quickly. Ideally, once these tribolayers form, there will always be protective or "sacrificial" layers of tribofilm on the substrate preventing wear and deformation processes.

8) As seen in this experiment, a lubricant change of three times produced a tribofilm showing three distinct tribolayers with evident material build-up and terraces. This indicated good wear resistance and inter-layer cohesion among the tribolayers.

9) It wouldn't be far fetched to say that the physical and chemical processes actually lead to the generation of a nanocomposite, layered high performance tribofilm. A model of the physical mechanism is shown in Figure 49.

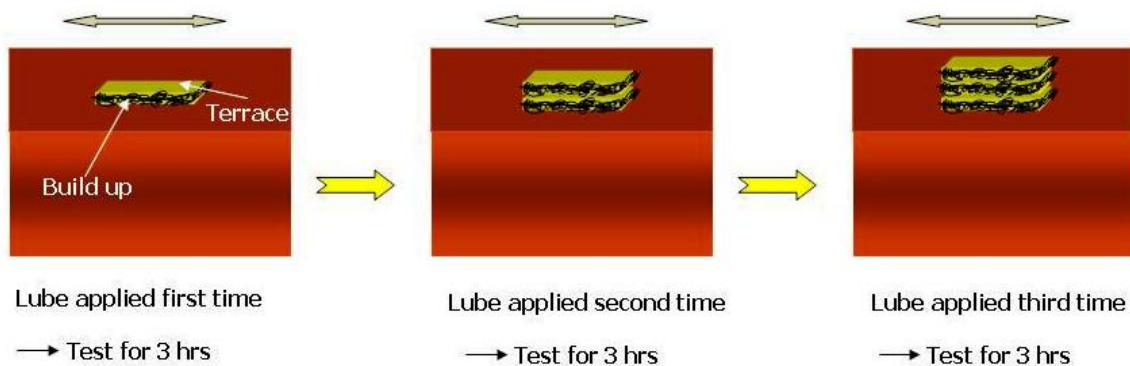


Figure 49: Physical mechanism model of tribofilm formation

6.8.2. Chemical Mechanism

Before arriving at the chemical mechanism, let us understand the significance and impact of nano-sized particles as potential energetic materials. Micro aluminum powder has traditionally been used in power applications ranging from explosives, rocket propellants, and pyrotechnics to utility in thermite reaction mixtures for multiple purposes (e.g. rail welding). In recent years nanometer length-scaled aluminum powder has emerged as a subject of research due to the potential high energy trapped inside these particles [192]. Similarly, other nano-scaled elemental powders have been investigated for potential energy applications. It was reported that spherical Al particles display better combustion properties than Al flakes [193]. Various Al based nano-composite thermite pairs have been explored for use in ordnance applications. These typically include Al/Fe₂O₃, Ni/Al and Al/MoO₃ pairs which are well known thermite mixtures at the micro-scale [194]. The combustion performance of fully dense nano-composite energetic powders prepared by Arrested Reactive Milling (ARM) using the above thermite pairs were compared with performance of other highly exothermic material pairs like B-Ti and B-Zr. Mechanical initiation of the chemical reaction is possible by high-energy milling of these components [195]. B.B. Bokhonov et. al. studied the structural and morphological changes induced due to mechanical activation of nanocrystalline materials. It was found that mechanical activation of a substance led to a change in physical properties. In the case of Al₂O₃, a phase transition was observed [196].

Nano-particles and ultra-fine particles exhibit a very high chemical reactivity, allowing a number of metals to undergo reactions under conditions which were

previously considered infeasible. One of the reasons for this behavior is that their lattices contain a high concentration of dislocations. Also at the nano-scale, the number of surface atoms is comparable to the bulk atoms meaning that the surface area-to-volume ratio is high thus allowing for more reaction initiation points. In fact, the nano particle reactions are initiated in the solid-solid phase and the particles show sintering phenomena as opposed to the liquid-solid reactions at micro-scale [194,197]. J.S.Raut et.al. performed molecular dynamics simulations on nano particle interactions to verify the sintering phenomenon. They concluded that the sintering kinetics decrease as the size of the nano particles increase [198]. A large fraction of the surface atoms of nanoparticles are in a disordered high energy phase [199]. Other reasons for the high reactivity of nano particles, particularly Al are increased ignition sensitivity, faster burn rates, decreased melting temperatures of nano-particles, and increased surface tension and mechanical stress due to the sharp curvature of the nano-spheres [194,200]. For oxidation of Al, if x amount of mass is converted to Al_2O_3 , then the derivative dx/dt is proportional to its reaction rate [197]. The onset of oxidation of Al depends on specific surface area and average particle diameter. It was reported that depending on the above parameters, micro and nano Al particles start oxidizing in different stages based on temperature ranges. First stage oxidation onset indications as low as 130 °C have been recorded [197]. Superfine Al powders having specific surface area of 16 m²/g showed a oxidation initiation temperature of 340 °C (first stage onset) with a second stage intensive oxidation onset of about 540 °C [201].

The critical properties that quantify the reactivity and energy release capacity of nano particles are activation energy and ignition temperature. Nano-scale Al particles ignite well below the melting point of Al (660 °C) based on a solid-solid phase reaction. The temperature increases acutely after the initial ignition creating molten Al and is subsequently followed by a higher heat release due to the solid-liquid reaction. P.Pranda et.al. [197] studied the effect of particle size on reactivity of Al powders. Their results showed that the reaction temperatures decrease with an increase in specific surface area. They report a reaction initiation temperature of 440 °C for a commercial brand of Al nano particles (ALEX® Argonide Corporation) having a specific surface area of 12.0 m²/g. WARP-1 Al nano powder samples (Ceramics and Materials Processing Inc.) with a specific surface area 16.0-26.5 m²/g started reacting at temperatures as low as 200 °C. While the specific surface area of reacted micro Al particles increases slightly due to oxide layer cracking [202], the nano Al particles exhibit an evident decrease due to sintering or annealing [197]. C. E. Aumann et.al. calculated the activation energy for oxidation of nano Al particles of size 24-69 nm as 49 kJ/mol when compared to 165 kJ/mol for Al strip of 0.25 mm thickness [203]. The activation energy of normal Al powder in air is about 215 kJ/cal which is relatively high compared to the nano-scale values [195]. It was reported that in the Al/Ni thermite couple, the activation energy of reaction decreased from 103.6 to 17.4 kJ/mol when the particle size of Al was decreased from 20 μm to 40 nm again emphasizing the importance of increased specific surface area of Al powder in a reactive mixture [194].

J.J.Granier et.al. [204] investigated the ignition behavior of nano-aluminum based thermites. They found that the nano-scale thermite mixture sensitivity to thermal ignition was significantly enhanced when compared with micro-scale thermites. They observed that ignition delay times were reduced by two orders of magnitude (from 10 to 0.01 s) using nano-scale Al in place of micro-scale Al particles in an Al/MoO₃ thermite couple. Mirko Schoenitz et.al. prepared energetic nanocomposite thermite pairs of Al/Fe₂O₃ and Al/MoO₃ using mechanical milling and determined their activation energies and ignition temperatures. Al particles (10 -14 μm) and Fe₂O₃ (325 mesh) were mechanically milled to make the Al/Fe₂O₃ nano-composite materials. They found that the activation energy of this pair was 170±25 kJ/mol while the ignition temperature ranged between 1,100K and 1,249K depending on the heating rates used [195]. Another study proposed a activation energy of 167.5 kJ/mol for the nano-scale Al-Fe₂O₃ thermite reaction [205].

With this background knowledge, we develop a chemical mechanism model for explaining the tribofilm formation. As mentioned before, the custom lubricant (PBL) was formulated using various micro/nano sized particles having sizes varying from 80 nm to a few microns. The main elements were nano Al (80 nm minimum), micro Al (few hundred nanometers to a few microns range), micro Fe (325 mesh) and other additives carefully formulated in to an organic matrix. There was salt contamination in the formulation in the form of NaCl.

A simple geometric calculation of the surface area of the nano Al (80nm) particles was made which gives a specific surface area of 27.7 m²/g which suggests a

high reaction rate. Under the experimental conditions of pressurized sliding and sliding-rolling, these reaction rates are conjectured to be hastened especially with the further reduction of the melting point. We can do a simple interface temperature calculation to get an overall idea of the kinetics of probable chemical reactions. A simple model equation (2) to calculate temperatures between dry sliding metals developed by Bowden and Tabor [25] was used to estimate the approximate interface temperature during this experiment. The temperatures in lubricated conditions are reported to be not too far less compared to the dry condition values [25]. A thermal conductivity of 50 W/m.K was used for the rail steel which translates to 0.119 cal./sec./cm./°K. The other values were substituted from the experimental conditions. A mean coefficient of friction value of 0.07 from the sliding experiment was used for the following calculation.

$$T - T_0 = \frac{\mu W g v}{4aJ} \frac{1}{k_1 + k_2} \quad (2)$$

T = steady state junction temperature (°K)

T₀ = bulk body temperature (°K)

μ = coefficient of friction

W = normal load (gm)

g = constant of gravity (cm/s²)

v = sliding velocity (cm/s)

a = radius of circular contact region (cm)

J = mechanical equivalent of heat (4.186 J/cal.)

k_1 = specific thermal conductivity of counter face material

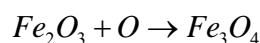
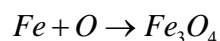
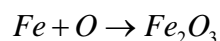
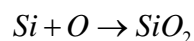
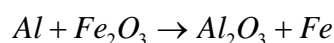
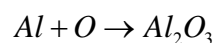
(cal./sec./cm./°K)

k_2 = specific thermal conductivity of substrate material

(cal./sec./cm./°K)

The calculation yields a temperature rise of 614 K (341 °C) and a junction temperature of 987 K (714 °C) for sliding at room temperature. The ignition characteristics of Al nanoparticles depend on parameters like particle diameter and thickness of the passivating outer shell of Al_2O_3 [194,197]. The flash temperature rise (341 °C) is higher than the ignition temperature of 80 nm nano Al particles. These particles are ideally assumed to be uniformly distributed within the lubricant layer, and ignite due to solid-solid phase reactions. Although oxidation would have initiated well below 341 °C, because of the low content of 80 nm particles in the prototype PBL used for this experiment, there may be insufficient energy to further trigger the ignition of the Al particles >80 nm which ignite at higher temperatures. Another reason is that the flash temperatures last only for a few milli-seconds, giving a lower probability of multiple ignitions. As a result, the temperature required to start the nano thermite reaction is not reached. This leads only to local hot spots and localized reactions due to oxidation of a few nano-micro Al particles in the vicinity of each group of the ignited nano Al (80 nm) particles. Hence a scattered tribofilm with local areas of terrace formation takes place as seen in Figure 39. However when a additional temperature of 60-100 °C by external

heating is supplied, there is more likelihood of triggering oxidation reactions of a higher size range of Al particles which could provide sufficient heat to cause more liquid-solid phase reactions and hence enough heat of reaction and temperature (1,087 K) to trigger the nano thermite reaction (Al/Fe₂O₃). Once this highly exothermic reaction is triggered, it can potentially amplify the heat produced which results in nano welding due to melting of Fe particles and also oxidation of Si and Fe. The result is a fully dense tribofilm covering the substrate (Figure 38). A list of probable reactions (unbalanced) is shown below.



The XPS results are in good correlation with the proposed reaction products. Therefore it is seen that a small increase in input energy could trigger a massive energetic reaction. In the actual rail road scenario, the loads and sliding speeds are much higher than those simulated in the lab. This could easily provide the additional

temperature required to trigger the complete reactions. Hence this formulation could be field tested for experimental performance in the future.

The chemical mechanism is summarized as taking the following route:

- 1) The first reaction to be triggered is the oxidation of nano Al (80 nm) particles due to solid-solid phase reaction generating localized heat and mutual sintering.
- 2) Next the nano-micro Al particles get ignited causing melting of Al and subsequent liquid-solid phase reactions producing high heat.
- 3) The nano thermite reaction ($\text{Al}/\text{Fe}_2\text{O}_3$) is triggered once the ignition temperature is reached and the high heat involved in this reaction causes melting of Fe and oxidation of Si and Fe.

CHAPTER VII

CONCLUSIONS AND FUTURE WORK

This thesis research developed a novel methodology to generate a functional tribofilm. The methodology may henceforth be known as *in-situ surface coating engineering*. The surface and mechanical properties of the tribofilm were characterized using state-of-the art techniques. A preliminary model was developed to explain the film formation. Research results led to the following important conclusions and possible future areas of exploration.

7.1. Conclusions

- A functional tribofilm with desired tribological characteristics was generated.
- The tribofilm exhibits good wear resistance with controlled friction. It has potential applications for gage/flange lubrication of railroads.
- The tribofilm developed as a layered structure due to physical build-up of material in consecutive tests exhibiting good interlayer adhesion. The proposed chemical mechanism is a nano particle combustion followed by a nano-thermite reaction providing enormous heat for complex tribochemical interactions. Subsequently there is mechanical sintering of additive particle reaction products and wear debris at the interface.
- The tribofilm presented characteristics of high hardness and self repair ability, and exhibited a distinct nanocrystalline nature.

- The lubricant formulated to generate the tribofilm can be modified by altering the relative concentrations of the additive constituents for possible use in top of the rail lubrication. This would include achieving an acceptable TOR friction coefficient, while still maintaining the high performance properties of the generated tribofilm.
- Potential applications include automotive and heavy machine industries, gas turbines and other high temperature applications involving reciprocating and rotating components requiring lubrication.

7.2. Future Work

- To better the tribo film characteristics by incorporating nano-composites of Al/MoO₃ thermites which have lower activation energy than Al/Fe₂O₃ thermites.
- To develop a model to predict the kinetics of the tribofilm mechanism.
- Nano-mechanical and nano-tribological properties should be investigated experimentally as well as theoretically.
- Explore the generation of tribofilms in other industrial applications.

REFERENCES

- [1] J.B. Hudson, *Surface Science: An Introduction*, New York, John Wiley & Sons, Inc., 1998.
- [2] E. Rabinowicz, *Friction and Wear of Materials*, New York, John Wiley & Sons, Inc., 1995.
- [3] D.G. Castner, B.D. Ratner, *Surface Science* 500 (2002) 28-60.
- [4] D. Tabor, *Journal of Colloid Interface Science* 75 (1980) 240-245.
- [5] J.F. Healy, *Natural History: A Selection*, London, Penguin Books, 1991.
- [6] J. Bostock, H.T. Riley (Eds.), *Pliny the Elder - The Natural History (37 Vol.)*, Vol 31.1 , London, Taylor and Francis, available online at <http://www.perseus.tufts.edu/cgi-bin/ptext?lookup=Plin.+Nat.+toc> (accessed 20-02-2006), Perseus Library.
- [7] J.d. Trevisa, M.C. Seymour, *On the Properties of Things : John Trevisa's Translation of Bartholomaeus Anglicus De Proprietatibus Rerum*, Oxford, Oxford Clarendon Press, 1988.
- [8] N.G. Goodman, *The Ingenious Dr. Franklin: Selected Scientific Letters of Benjamin Franklin*, Philadelphia, University of Pennsylvania Press, 2000.
- [9] A. Pockels, *Nature* 43 (1891) 437-439.
- [10] M.E. Derrick, *Journal of Chemical Education* 59 (1982) 1030-1031.
- [11] D.W. Deamer, A. Kleinzeller, D. Fambrough, *Membrane Permeability, 100 Years Since Ernest Overton*, New York, Academic Press 1999.

- [12] P. Eichman, From the Lipid Bilayer to the Fluid Mosaic: A Brief History of Membrane Models <http://www1.umn.edu/ships/9-2/membrane.htm> (Date accessed: 02-21-2006), SHIPS resource center for Sociology, History and Philosophy in Science Teaching.
- [13] C.W. Scheele, *Chemische Abhandlung von der Luft und dem Feuer*, 1773 (Personal Collection, Pranay Asthana) Also available online at http://www.reiss-sohn.de/frame88_89.php?page=1887 as listed document, access date 04-28-2006
- [14] F. Fontana, *Mem. Mat. Fis. Soc. Ital.* 1 (1777) 679 (Personal Collection, Pranay Asthana).
- [15] T.d. Saussure, *Gilbert's Ann. Phys.* 47 (1814) 113 (Personal Collection, Pranay Asthana).
- [16] A. Dabrowski, *Advances in Colloid and Interface Science* 93 (2001) 135-224.
- [17] L.P. Williams, *Michael Faraday*, London, Chapman & Hall, 1965.
- [18] C. Susskind, *Wireless Technology*, in: Marton, Marton (Eds.), *Advances in Electronics and Electron Physics*, New York, Academic, 1980, pp. 241-260.
- [19] J.W. Gibbs, *The Collected Works of J. Williard Gibbs*, New York, Longmans, 1928.
- [20] J. Rice, *Thermodynamics of Surfaces*, in: Donnan, Haas (Eds.), *Commentary on the Scientific Writings of J. Williard Gibbs*, Yale, 1936, pp. 505-708.
- [21] A. Zangwill, *Physics at Surfaces*, Cambridge, Cambridge University Press, 1988.
- [22] *The Collected Works of Irving Langmuir*, New York, Pergamon Press 1960.

- [23] D. Dowson, History of Tribology, London and Bury St Edmunds, Professional Engineering Publishing Ltd, 1998.
- [24] P. Jost, The Introduction of a New Technology- Report from the Committee on Tribology, London, British Government, 1966.
- [25] F.P. Bowden, D. Tabor, The Friction and Lubrication of Solids, Oxford, Oxford Clarendon Press, 1950.
- [26] G. Amontons, On the Resistance Originating in Machines (in French), Mem. Acad. Roy. (1699) 206-222. (Personal Collection, Pranay Asthana)
- [27] C.A. Coulomb, The Theory of Simple Machines (in French), Mem. Math. Phys. Acad. Sci. 10 (1785) 161-331. (Personal Collection, Pranay Asthana)
- [28] A. Morin, New Friction Experiments Carried out at Metz in 1831-1833 (in French), Mem. Acad. Sci. 4 (1833) 1-128, 591-696. (Personal Collection, Pranay Asthana)
- [29] L. Euler, Mem. Acad. Sci. Berl. 4 (1750) 122-132. (Personal Collection, Pranay Asthana)
- [30] L. Euler, Mem. Acad. Sci. Berl. 4 (1750) 133-148. (Personal Collection, Pranay Asthana)
- [31] L. Euler, Mem. Acad. Sci. Berl. 18 (1762) 265-278. (Personal Collection, Pranay Asthana)
- [32] W.B. Hardy, J.K. Hardy, Phil. Mag. 6th series 38 (1919) 32-48. (Personal Collection, Pranay Asthana)

- [33] G.A. Tomlinson, *Phil. mag.* 7th series 7 (1929) 905-939. (Personal Collection, Pranay Asthana)
- [34] R. Holm, *Wiss. Veroff. Siemens-Werk* 17 (1938) 38-42. (Personal Collection, Pranay Asthana)
- [35] H. Ernst, M. M. E., *Surface Friction Between Metals- A Basic Factor in the Metal Cutting Process*, Cambridge MA, MIT, 1940, 76-101. (Personal Collection, Pranay Asthana)
- [36] O. Reynolds, *Phil. Trans. Royal. Soc.* 177 (1886) 157-234. (Personal Collection, Pranay Asthana)
- [37] J. Vizintin, M. Kalin, K. Dohda, S. Jahanmir (Eds.), *Tribology of Mechanical Systems: A guide to the present and future technologies*, New York, ASME Press, 2004.
- [38] C. Hatchett, *Philosophical Transactions of Royal Society of London* (MDCCCIII- 1803) 43-194.
- [39] Center for Integrated Microchemical Systems, Texas A&M University, <http://www.chem.tamu.edu/cims/facility.html> (access date: 03/08/2006).
- [40] L. De Broglie, *Ann De Physique* 3 (1924) 22-128. (Personal Collection, Pranay Asthana)
- [41] H. Busch, *Ann Physik* 81 (1926) 974-993. (Personal Collection, Pranay Asthana)
- [42] H. Stintzing, *Verfahren und Einrichtung zum automatischen Nachweiss*, German patent No 485155, Germany, 1929. (Personal Collection, Pranay Asthana)
- [43] M. Knoll, *Z. Tech. Phys.* 11 (1935) 467.
- [44] V.K. Zworykin, J. Hiller, R.L. Snyder, *ASTM Bull.* 117 (1942) 15.

- [45] D. McMullan, Cambridge, England, Cambridge University (Ph.D. Dissertation), 1952.
- [46] O.C. Wells, Br. J. Appl. Phys. 11 (1960) 199-201.
- [47] O.C. Wells, J. Electron. Control. 7 (1959) 373-376.
- [48] K.C.A. Smith, C.W. Oatley, Br. J. Appl. Phys. 6 (1955) 391-395.
- [49] R.F.W. Pease, W.C. Nixon, J. Sci. Instr. 42 (1965) 81-84.
- [50] C.W. Oatley, T.E. Everhart, J. Electron. 2 (1957) 568-570.
- [51] T.E. Everhart, R.F.M. Thornley, J. Sci. Instr. 37 (1960) 246-249.
- [52] J.I. Goldstein, Scanning Electron Microscopy and X-Ray Microanalysis, New York, Kluwer Academic/ Plenum Publishers, 2003.
- [53] C.W. Oatley, Scanning Electron Microscope, Cambridge, Cambridge University Press, 1972.
- [54] Microscopy and Imaging center, Texas A&M University, <http://www.tamu.edu/mic/> (access date: 03/08/2006).
- [55] M. Knoll, E. Ruska., Ann Physik 12 (1932) 607-661.
- [56] J.J. Bozzola, L.D. Russell, Electron Microscopy: Principles and Techniques for Biologists, Sudbury, MA, Jones and Bartlett Publishers, 1999.
- [57] G. Binnig, Physical Review Letters. 56 (1986) 9-12.
- [58] Nano-R™ AFM User's manual, revision 1.1, San Francisco, Pacific Nanotechnology Incorporated, 2004.
- [59] R.G. Steinhardt Anal. Chem. 25 (1953) 697-700.

- [60] C. Nordling, *Physical Review Letters*. 105 (1957) (Personal Collection, Pranay Asthana).
- [61] K. Siegbahn, C. Nordling, Sokolowski, *Proc. of Rehovoth Conf Nucl. Str.* North-Holland, Amsterdam, North Holland, 1957. (Personal Collection, Pranay Asthana)
- [62] J.F. Moulder, *Handbook of X-Ray Photoelectron Spectroscopy*, Minneapolis, Physical Electronics, Inc, 1995.
- [63] H.P. Bonzel, C. Klient, *Progress in Surface Science*. 49 (1995) 107-153.
- [64] *Technology of Materials*, <http://www.xraydiffrac.com/> (access date 02-09-2006).
- [65] X-ray Diffraction Laboratory, Department of Chemistry, Texas A&M University, <http://www.chem.tamu.edu/xray/> (access date: 03/08/2006).
- [66] T. Ohmura, *Journal of Japan Society for Heat Treatment* 42 (Dec 2002) 416-421.
- [67] Module 7.3 - Nanoindentation Analysis of Materials: Determination of Hardness and Young's Modulus, Nanotechnology for Undergraduate Education at Binghamton University, http://nue.clt.binghamton.edu/labs1_3.html (access date 02-10-2006).
- [68] C.C. Vi'afara, M.I. Castro, J.M. V'elez, A. Toro, *Wear* 259 (2005) 405-411.
- [69] P.J. Bolton, P. Clayton, *Wear* 93 (1984) 145-165.
- [70] M. Sate, P.M. Anderson, D.A. Rigney, *Wear* 162-164 159-172.
- [71] U. Olofsson, T. Telliskivi, *Wear* 254 (2003) 80-93.
- [72] D. Markov, *Wear* 208 (1997) 91-104.
- [73] M. Tomeoka, N. Kabe, M. Tanimoto, E. Miyauchi, M. Nakata, *Wear* 253 (2002) 124-129.
- [74] M. Ueda, K. Uchino, A. Kobayashi, *Wear* 253 (2002) 107-113.

- [75] W.R. Tyfour, J.H. Beynon, *Tribology International* 27 (1994) 401-412.
- [76] G. Donzella, M. Faccoli, A. Ghidini, A. Mazzu, R. Roberti, *Engineering Fracture Mechanics* 72 (2005) 287-308.
- [77] L. Deters, M. Proksch, *Wear* 258 (2005) 981-991.
- [78] R.I. Carroll, J.H. Beynon, *Wear* 260 (2006) 523-537.
- [79] I. Minami, K. Mimura, *Synthetic Lubrication* 21 (October 2004). (Personal Collection, Pranay Asthana)
- [80] Y. Gerbig, S.I.U. Ahmed, F.A. Gerbig, H. Haefke, *Synthetic Lubrication* 21 (October 2004). (Personal Collection, Pranay Asthana)
- [81] J.M. Zhu, W.M. Liu, *Synthetic Lubrication* 21 (October 2004). (Personal Collection, Pranay Asthana)
- [82] R.F. Beck, Final Report/ US-USSR Track and Metallurgy Information Exchange, National Technical Information Service Report, Pueblo, Colorado, Sept. 1976.
- [83] J. Kalousek, R. Klein, *AREA Bulletin*, Jan 1976, 429-448.
- [84] D.H. Stone, R.K. Steele, The Effect of Mechanical Properties Upon the Performance of Railroad Rails, in: D.H. Stone, G.G. Knupp (Eds.), *Rail Steels- Developments, Processing and Use*, Tallahassee, FL, ASTM, 1978, pp. 21-62.
- [85] P. Waaraa, T. Norrbya, B. Prakasha, *Tribology Letters* 17 (October 2004) 561-568.
- [86] E.J.M. Hiensch, F.J. Franklin, J.C.O. Nielsen, J.W. Ringsberg, G.J. Weeda, A. Kapoor, B. L. Josefson, *Fatigue & Fracture of Engineering Materials & Structures* 26 (2003) 1007-1017.

- [87] J. Eisenmann, Munich, The Rail as Support and Roadway Theoretical Principles and Practical Examples, in: F. Fastenrath (Ed.), Railroad Track Theory and Practice, Berlin, Frederick Ungar Publishing Co, 1981.
- [88] K. Morton, D.F. Cannon, P. Clayton, E.G. Jones, The Assessment of Rail Steels , in: D.H. Stone, G.G. Knupp (Eds.), Rail Steels- Developments, Processing and Use, Tallahassee, FL, ASTM, 1978, pp. 80-98.
- [89] T.S. Eyre, A. Baxter, Metals and Materials (Oct. 1972) 435-439.
- [90] S.L. Grassie, Wear 258 (2005) 1310-1318.
- [91] W. Herbst, Subway Rails, in: F. Fastenrath (Ed.), Railroad Track Theory and Practice, Berlin, Frederick Ungar Publishing Co, 1981.
- [92] J. Kalousek, A.E. Bethune, Rail Wear Under Heavy Traffic Conditions, in: D.H. Stone, G.G. Knupp (Eds.), Rail Steels- Developments, Processing and Use, Tallahassee, FL, ASTM, 1978, pp. 63-79.
- [93] T. Judge, Railway Track and Structures, Smoothing the Way: New Friction Modifiers and New Ways to Apply Them Are Helping Suppliers Keep the Promise to Reduce Fuel Consumption and Wheel and Rail Wear, Feb 2004. (Magazine available online at <http://www.rtands.com/> access date: 04-26-2006)
- [94] D.T. Eadie, J. Kalousek, Railway Age, Railway Age, Spray it on, Let 'em roll' - New Technology in Top-of-rail Friction Management, June 2001.(Magazine available online at <http://www.railwayage.com/> access date: 04-26-2006)
- [95] T. Judge, Railway Age, A smooth ride: lubrication in its various forms not only provides a better ride, but also reduces wheel and rail wear and fuel consumption, Dec

2004. (Magazine available online at <http://www.railwayage.com/> access date: 04-26-2006)

[96] B.A. Baldwin, *Wear* 45 (1977) 345-353.

[97] P. Diatto, R. Riva, L. Tinucci, G. Tripaldi, S. Giacobbe, G. Ponti, *Lubrication Engineering* 58 (2002) 13-17.

[98] C. McFadden, C. Soto, N.D. Spencer, *Tribology International* 30 (1997) 881-888.

[99] S.K. Biswas, *Wear* 245 (2000) 178-189.

[100] G. Heinicke, *Tribochemistry*, Berlin, Academic Verlag, 1984.

[101] K. Komvopoulos, A. Pernama, J. Ma, *Tribology Transactions* 48 (2005) 218-229.

[102] M. Eglin, A. Rossia, N.D. Spencer, *Tribology Letters* 15 (October 2003) 199-209.

[103] J.F. Graham, C. McCague, P.R. Norton, *Tribology Letters* 6 (1999) 149-157.

[104] S.M. Kim, C.Y. Sit, K. Komvopoulos, E.S. Yamaguchi, P.R. Ryason, *Tribology Transactions* 43 (2000) 569-578.

[105] S.H. Roby, E.S. Yamaguchi, P.R. Ryason, *Lubricant Additives for Mineral-Oil-Based Hydraulic Fluids*, in: G.E. Totten, M. Dekker (Eds.), *Handbook of Hydraulic Fluid Technology*, New York, CRC, 2000, pp. 795- 824.

[106] K. Komvopoulos, V. Chiaro, B. Pakter, *Tribology Transactions* 45 (2002) 568-575.

[107] A.J. Gellman, N.D. Spencer, *J. Eng. Tribol.* 216 (2002) 443-49.

[108] R.G. Pearson, *Journal of American Chemical Society* 85 (1963) 3533-37.

- [109] J.M. Martin, C. Grossiord, T. Le Mogne, J. Igarashi, *Wear* 245 (2000) 107–115.
- [110] N.K. Myshkin, *Wear* 245 (2000) 116–124.
- [111] J.H. Petersen, H. Reitz, M.E. Benzon, J.B. Tiger, J. Chevallier, N.J. Mikkelsen, P. Morgen, *Surface and Coatings Technology* 179 (2004) 165–175.
- [112] K. Matsumoto, A. Rossi, N.D. Spencer, *Proceedings of the International Tribology Conference 2000 II, Nagasaki, 2000*, 1287-96.
- [113] M. Eglin, A. Rossi, N.D. Spencer, *Proceedings of the 28th Leeds-Lyon Symposium on Tribology, Vienna, 2002*, 49-54.
- [114] G. Pereira, A. Lachenwitzer, M.A. Nicholls, M. Kasrai, P.R. Norton, G.D. Stasio, *Tribology Letters* 18 (April 2005) 411-427.
- [115] M.A. Nicholls, P.R. Norton, G.M. Bancroft, M. Kasrai, T. Do, B.H. Frazer, G. DeStasio, *Tribology Letters* 17 (2003) 205-216.
- [116] G.W. Canning, M.L. Fuller, G.M. Bancroft, M. Kasrai, J.N. Cutler, G.D. Stasi, B. Gilbert, *Tribology Letters* 6 (1999) 159-169.
- [117] M.A. Nicholls, G.M. Bancroft, P.R. Norton, M. Kasrai, G.D. Stasio, L.M.W. *Tribology Letters* 17 (2003) 245-259
- [118] M.A. Nicholls, T. Do, P.R. Norton, G.M. Bancroft, M. Kasrai, *Tribology Letters* 15 (October 2003) 241 - 248
- [119] L. Shenghua, Y. He, J. Yuansheng, *International Journal of Molecular Science* 5 (2004) 13-34.
- [120] M.N. Najman, M. Kasrai, G.M. Bancroft, *Tribology Letters* 17 (August 2004).
- [121] P.A. Bertrand, *Tribology Letters* 3 (1997) 367-377.

- [122] Böttcher, H. Jost, SAE Technical Paper 912410, 1991.
- [123] A.G. Papay, Lubrication Science 10 (1998) 209-214.
- [124] C. Grossiord, J.M. Martin, T.L. Mognea, T. Palermob, Surface and Coatings Technology 108–109 (1998) 352–359.
- [125] J. Yao, J. Dong, Lubrication Engineering 52 (1996) 553-556.
- [126] R.M. Mortier, S.T. Orszulik (Eds.), Chemistry and Technology of Lubricants, London, Blackie Academic & Professional, 1997.
- [127] M. Najman, M. Kasrai, G.M. Bancroft, R. Davidson, Tribology International 39 (2006) 342-355.
- [128] A. Van de Ven, P.S. Johal, L. Jansen, Lubrication Science 6 (1993) 3–19.
- [129] T.V. Liston, Lubrication Engineering 48 (1992) 389-97.
- [130] M.F. Morizur, O. Teyssset, Lubrication Science 4 (1992) 277–99.
- [131] C. Guerret-Piécourt, C. Grossiord, T.L. Mogne, J.M. Martin, T. Palermo, Surf. Interface Anal. 30 (2000) 646–650.
- [132] Z. Zhang, M. Najman, M. Kasrai, G.M. Bancroft, E.S. Yamaguchi, Tribology Letters 18 (January 2005) 43-51.
- [133] Elco ZDDP's Zinc Dialkyldithiophosphates, Elco Corporation,
http://www.elcocorp.com/Elco_ZDDP_table.pdf (accessed: 03-09-2006)
- [134] M.N. Najman, M. Kasrai, G.M. Bancroft, B.H. Frazer, G.D. Stasio, Tribology Letters 17 (November 2004) 811-822.
- [135] C. Minfray, J.M. Martin, C. Esnouf, T.L. Mogne, R. Kersting, B. Hagenhoff, Thin Solid Films 447–448 (2004) 272–277.

- [136] J.M. Martin, *Tribology Letters* 6 (1999) 1-8.
- [137] M.A. Nicholls, T. Do, P.R. Norton, M. Kasrai, G.M. Bancroft, *Tribology International* 38 (2005) 15–39.
- [138] Z. Yin, M. Kasrai, M. Fuller, G.M. Bancroft, K. Fyfe, K.H. Tan, *Wear* 202 (1997) 172.
- [139] J.J. Dickert, C.N. Rowe, *Journal of Organic Chemistry* 32 (1967) 647–53.
- [140] S.H. Choa, K.C. Ludema, G.E. Potter, B.M. Dekoven, T.A. Morgan, K.K. Kar, *Wear* 177 (1994) 33.
- [141] W.A. Gehrman, SAE Paper No. 921736, 1992.
- [142] R. Sarin, V. Martin, D.K. Tuli, M.M. Rai, A.K. Bhatnagar, *Lubrication Engineering* 53 (1997) 21-30.
- [143] R. Sarin, A.K. Gupta, D.K. Tuli, A.S. Verma, M.M. Rai, A.K. Bhatnagar, *Tribology International* 26 (1993) 389-394.
- [144] G. Pereira, A. Lachenwitzer, M.A. Nicholls, M. Kasrai, P.R. Norton, G.D. Stasio, *Tribology Letters* 18 (April 2005) 411-427.
- [145] M.A. Nicholls, P.R. Norton, G.M. Bancroft, M. Kasrai, *Wear* 257 (2004) 311–328.
- [146] H. Spikes, *Tribology Letters* 17 (2004) 469-489.
- [147] Z. Yin, M. Kasrai, G.M. Bancroft, K.F. Laycock, *Tribology International* 26 (1993) 383-388.
- [148] M.A. Nicholls, P.R. Norton, G.M. Bancroft, M. Kasrai, T. Do, B.H. Frazer, G. DeStasio, *Tribology Letters* 17 (2003) 205-216.

- [149] G. Margaritondo, Introduction to Synchrotron Radiation, New York, Oxford University Press Inc., 1988.
- [150] G.D. Stasio, M. Capozzi, G.F. Lorusso, P.A. Baudat, T.C. Droubay, P. Perfetti, G. Margaritondo, B.P. Tonner, Rev. Sci. Instrum. 69 (1998) 2062-2089 .
- [151] E.S. Yamaguchi, P.R. Ryason, S.W. Yeh, T.P. Hansen, Tribology Transactions 41 (1998) 262-267.
- [152] Y. Yamada, J. Igarashi, K. Inoue, Lubrication Engineering 48 (1992) 511-514.
- [153] F.G. Rounds, ASLE Trans 21 (1978) 91-101.
- [154] S.S.V. Ramakumar, A.M. Rao, S.P. Srivastava, Wear 156 (1992) 101-20.
- [155] P. Kasper, J.M. Martin, C. Blanc, J.M. Georges, ASME Trans 103 (1981) 483-96.
- [156] P.G. Harrison, T. Kikabhai, Wear 116 (1987) 25.
- [157] P.G. Harrison, T. Kikabhai, J. Chem. Soc., Dalton Trans.: Inorg. Chem. (1987) 807-815.
- [158] Z. Zhang, M. Kasrai, G.M. Bancroft, E.S. Yamaguchi, Tribology Letters 15 (2003) 377-384.
- [159] E.S. Yamaguchi, Z. Zhang, M. Kasrai, G.M. Bancroft, Tribology Letters 15 (2003) 385-394.
- [160] K. Inoue, Lubrication Engineering 49 (1993) 263-268.
- [161] V. Normand, J.M. Martin, K. Inoue, Tribology Letters 5 (1998) 224-235.
- [162] K. Varlot, J.M. Martin, C. Grossiord, R. Vargiolu, B. Vacher, K. Inoue, Tribology Letters 6 (1999) 181-189.
- [163] J.H. Adams, Lubrication Engineering 33 (1977) 241-246.

- [164] K. Varlot, M. Kasrai, J.M. Martin, B. Vacher, G.M. Bancroft, E.S. Yamaguchi, P.R. Ryason, *Tribology Letters* 8 (2000) 9–16.
- [165] J.H. Adams, D. Godfrey, *Lubrication Engineering* 37 (1981) 16-21.
- [166] S. Bec, A. Tonck, J.M. Georges, G.W. Roper, *Tribology Letters* 17 (November 2004) 797-809.
- [167] Y. Qiao, W. Liu, S. Qi, Q. Xue, B. Xu, S. Ma, *Wear* 215 (1998) 165-169.
- [168] C. Jacobsen, S. Wirick, G. Flynn, C. Zimba, *Journal of Microscopy* 197 (2000) 173-184.
- [169] Y.R. Jeng, S.J. Hwang, Z.G.H. Fong, J.A. Shieh, *Lubrication Engineering* 58 (2002) 9-15.
- [170] M. Muraki, H. Wada, *Japanese J. Tribol.* 38 (1993) 1348–1359.
- [171] M.I.D. Barros, J. Bouchet, I. Raoult, T.L. Mogne, J.M. Martin, M. Kasrai, Y. Yamada, *Wear* 254 (2003) 863–870.
- [172] A. Blomberg, S. Hogmark, J. Lu, *Tribology International (UK)* 26 (Dec 1993) 369-381.
- [173] S. Sasaki, *Wear* 134 (1989) 185-200.
- [174] M. Woydt, K.H. Habig, *Tribology International* 22 (1989) 75-87.
- [175] E. Breval, J. Breznak, N.H. Macmillan, *Journal of Materials Science* 21 (1986) 931-935.
- [176] J. Breznak, E. Breval, N.H. Macmillan, *Journal of Materials Science* 20 (1985) 4657-4680.
- [177] J. Denape, J. Lamon, *Journal of Materials Science* 25 (1990) 3592-3604.

- [178] A. Blomberg, M. Olsson, J. Bratthill, H. Engström, S. Hogmark, Sliding Wear Behaviour of Al₂O₃, SiC and SiAlON Face Seals, The Japan International Tribology Conference, Nagoya, 1990, 1371.
- [179] A. Blomberg, M. Olsson, S. Hogmark, Characterization of Surface Films on Ceramic Materials Formed During Dry Sliding Contact, The Australia International Tribology Conference, Brisbane, 1990, pp 79.
- [180] J. Takadom, Z. Zsiga, M.B. Rhouma, C. Roques-Carmes, Journal of Materials Science Letters 13 (1994) 474–476.
- [181] P. Larsson, N. Axé'n, S. Hogmark, Wear 236 (1999) 73–80.
- [182] T. Aizawa, A. Mitsuo, S. Yamamoto, T. Sumitomo, S. Muraishi, Wear 259 (2005) 708-718.
- [183] J. Kusaka, K. Takashima, D. Yamane, K. Ikeuchi, Wear 225–229 (1999) 734–742.
- [184] R.S. Gates, S.M. Hsu, STLE Transactions 32 (1989) 357–363.
- [185] H. Tomizawa, T.E. Fischer, ASLE Transactions 30 (1988) 41–46.
- [186] E. Rabinowicz, M. Imai, ASME (1961) Paper No. 61-Lub 17
- [187] H. Ronkainen, J. Koskinen, J. Likonen, S. Varjus, J. Vihersalo, Diamond and Related Materials 3 (1994) 1329-1336.
- [188] B. Podgornik, S. Jacobson, S. Hogmark, Surface & Coatings Technology 165 (2003) 168– 175.
- [189] B. Podgornik, S. Jacobson, S. Hogmark, Proceedings of the 10th NORDTRIB Conference, Stockholm, Royal Institute of Technology, 2002, 141.

- [190] B. Podgornik, S. Jacobson, S. Hogmark, *Surface & Coatings Technology* 191 (2005) 357–366.
- [191] E. Luscher, G. Fritsch, G. Jacucci (Eds.), *Formation of Non-Crystalline Metallic Alloys With and Without Rapid Quenching*, Boston, Martinus Nijhoff Publishers, 1987.
- [192] P. Brousseau, H.E. Dorsett, M.D. Cliff, C.J. Anderson, Detonation properties of explosives containing nanometric aluminum powder, Report from collaborative work between Defence Research & Development Canada - Valcartier (DRDC-V) and Defence Science and Technology Organisation (DSTO)
- [193] B.Z. Eapen, V.K. Hoffmann, M. Schoenitz, E.L. Dreizin, *Combustion Science and Technology* 176 (2004) 1055-1069.
- [194] E.M. Hunt, M.L. Pantoya, *Journal of Applied Physics* 98 (2005) 0349091-8.
- [195] M. Schoenitz, T.S. Ward, E.L. Dreizin, *Proceedings of the Combustion Institute* 30 (2005) 2071-2078.
- [196] B.B. Bokhonov, I.G. Konrtanchuk, V.V. Boldyrev, *Materials Research Bulletin* 30 (1995) 1277-1284.
- [197] P. Pranda, K. Prandova, V. Hlavacek, *Combustion Science and Technology* 156 (2000) 81-96.
- [198] J.S. Raut, R.B. Bhagat, K.A. Fichthorn, *Nanostructured Materials* 10 (1998) 837-851.
- [199] H. Gleiter, *Progress in Materials Science* 33 (1989) 223.

- [200] J.J. Granier, Combustion Characteristics of Al Nanoparticles and Nanocomposite Al+ MoO_3 Thermites, PhD Dissertation, Texas Tech University, 2005, pp 238.
- [201] Y.-S. Kwon, J.-S. Moon, Combustion Science and Technology 176 (2004) 277-288.
- [202] V.G. Scevchenko, V.I. Kononenko, I.N. Latosh, N.V. Lukin, Combustion, Explosion and Shock Waves 635 (1994).
- [203] C.E. Aumann, G.L. Skofronick, J.A. Martin, Journal of Vacuum Science and Technology 13 (1995) 1178.
- [204] J.J. Granier, M.L. Pantoya, Combustion Flame 138 (2004) 373.
- [205] E.I. Maximov, A.G. Merzhanov, V.M. Shkiro, Zhurnal Fizicheskoi Khimii 40 (1966) 467-470.

VITA

Pranay Asthana received his Bachelor of Engineering degree in Mechanical Engineering from Osmania University in Hyderabad, India in May 2004. He entered the Mechanical Engineering program at Texas A&M University in September 2004, and he received his Master of Science degree in May 2006. His main research interests include Surface Science and Tribology applied to a wide gamut of fields. He is also interested in fundamental Materials Science study involving metals, alloys, composites and bio inspired materials. He has been active in the research fraternity and has contributed to Science with many publications and conference presentations. Apart from his many academic and research achievements, Mr. Pranay Asthana has been involved in many extracurricular activities and has assumed many leadership positions and consistently rendered community and volunteer services.

Mr. Pranay Asthana can be reached at the Mechanical Engineering Department, Texas A&M University, College Station, Texas, 77843. His email address is pranayasthana@yahoo.com. His current contact information can be found from his Masters Thesis advisor, Dr. Hong Liang of the Mechanical Engineering Department, Texas A&M University.